On the lipid mediated regulation of the cell adhesion protein vinculin

Vom Fachbereich für Biowissenschaften und Psychologie
der Technischen Universität Carolo-Wilhelmina
zu Braunschweig
zur Erlangung des Grades einer
Doktorin der Naturwissenschaften
(Dr.rer.nat.)
genehmigte
D i s s e r t a t i o n

von
Indra Chandrasekar
aus Tirunelveli, Indien

1. Referentin: Prof. Dr. Brigitte M. Jockusch
2. Referent: PD. Dr. Günter Schwarz
eingereicht am: 31.03.2005
mündliche Prüfung (Disputation) am: 30.06.2005

2005 (Druckjahr)

To my wonderful teachers and to those women in science who inspired me

Partial results from this thesis were published in agreement with the "Gemeinsamen Naturwissenschaftlichen Fakultät" of the Techinical University of Braunschweig represented by the principle investigator of this thesis. The following publication contains scientific results of the thesis presented here.

Publication

Chandrasekar I, Stradal TE, Holt MR, Entschladen F, Jockusch BM, Ziegler WH. Vinculin acts as a sensor in lipid regulation of adhesion-site turnover. (2005) *J.Cell.Sci.***118 (Pt.7)**, 1461 - 1472

Conference contributions

Indra C., T. Stradal, F. Entschladen, B.M. Jockusch and W.H. Ziegler; Lipid-mediated regulation of vinculin affects cell adhesion and migration.
EMBO/FEBS workshop on frontiers in cytoskeleton research, Gosau, Austria.
September, 2003.

I.Chandrasekar., T. Stradal, F. Entschladen, B.M. Jockusch and W.H. Ziegler; Lipid-mediated regulation of vinculin affects cell adhesion and migration.
STS meeting 2003: Signal Transduction- Receptors, Mediators and Genes, Weimar, Germany. November, 2003

I. Chandrasekar, M.R. Holt, T.E.B. Stradal, B.M. Jockusch and W.H. Ziegler;
Vinculin involvement in lipid regulation of adhesion site turnover.
Bioscience 2004- from molecules to organisms. Glasgow, UK. July, 2004

Abbreviations

Arp2/3	Actin related protein 2/3
ARPC	Actin related protein complex
ADF	Actin depolymerizing factor
°C	Grade Celsius
ATCC	"American Type Culture Collection"
BiPro	Birchpollen
BSA	Bovine serum albumin
cDNA	Complementary DNA
C-Terminus	Carboxyterminus
DMEM	Dulbecco´s modified eagle medium
DNA	Desoxyribonucleic acid
dNTP	Desoxyribunucleoside tri phosphate
DTT	Dithiothreitol
E. coli	Escherichia coli
EDTA	Ethylenediaminetetraacetate
ECM	Extracellular matrix
ERM	Ezrin/radixin/moesin
FA	Focal adhesion
FAK	Focal adhesion kinase
FC	Focal contact
F-Actin	Filamentous actin
FCS	Foetal calf serum
GTP	Guanosine tri phosphate
GFP	Green fluorescent protein
GST	Glutathione S-transferase
g, mg, µg	Gram, Milligram, Microgram
HMW	"high molecular weight marker"
HRP	Horse radish peroxidase
IPTG	Isopropyl-β-D-thiogalactoside
Kd	Dissociation constant
kDa	Kilo Dalton
KD	Kinase dead
LD	Lipid binding deficient
ml, µl	Litre, Millilitre, Microlitre
M, mM	Molar, millimolar
MARCKS	Myrsitolated alanine rich C-kinase substrate
µM, nM	Micromolar, nanomolar
Ni-NTA	Nickel-Nitriloaceticacid
N-Terminus	Aminoterminus
PC	Phosphatidylcholine
PH	Pleckstrin homology
PS	Phosphatidylserine
PI	Phosphatidylinositol
PIP5K	Phosphatidylinositol-4-phosphate-5 kinase
PI3K	Phosphatidylinostiol- 3-kinase

PIP2	Phosphatidylinositol-4,5-bisphosphate (PI-4,5-P)
PIP3	Phosphatidylinositol-3,4,5-bisphosphate (PI-3,4,5-P)
PLC	Phospholipase C
PBS	Phosphate-buffered saline
PCR	Polymerase chain reaction
PKC	Protein kinase C
rpm	Rotations per minute
TBST	Tris-buffered saline tween
Tris	Tris-(Hydroxymethyl)-Aminoethane
UV	Ultraviolet
Vh	Vinculin head
Vt	Vinculin tail
wt	Wild type
WASP	Wiskott-Aldrich syndrome protein
WAVE	Wiskott Aldrich Verprolin homologous protein

Summary

Embryogenesis, tissue formation, wound healing and tumor metastasis all require directed cell migration. Migration mechanics depend on the attachment of cells to the underlying matrix which is required for cellular movements and signaling. Focal adhesions are the major cell-matrix connections that aid in adhesion, spreading and cell motility. The extracellular matrix glycoproteins are linked to the actin cytoskeleton via the transmembrane receptors integrins. The cytoplasmic domain of integrins interacts with several cytoskeletal and regulatory proteins that are involved in the assembly of the adhesion complex and help in the functional regulation of the adhesion dynamics. Vinculin is an important structural and elementary component of the adhesion complex which plays a major role in the molecular architecture and regulation of these adhesion sites. Vinculin acts as a molecular scaffold since it interacts with numerous ligands and serves as a connecting link between the membrane and the actin cytoskeleton. Acidic phospholipids like PIP2 are important ligands whose interaction is known to structurally and functionally modulate vinculin.

This work aimed at the analysis of acidic phospholipid mediated regulation of vinculin at the adhesion sites. Design and construction of a lipid binding deficient mutant “vinculin-LD” allowed to characterize the mode of regulation of vinculin at the focal adhesions. Biochemical analyses showed that “vinculin-LD” failed to co-sediment with lipid vesicles while leaving its interaction with important ligands like actin and the vinculin head (Vh) intact. Cell biological analyses of “vinculin-LD” proved that the lipid binding is not required for the focal adhesion targeting as previously suggested. Analysis of the incorporation rates of this mutant by fluorescent recovery after photobleaching also indicated that the vinculin recruitment to focal adhesions is normal. However, cells expressing “vinculin-LD” had a serious delay in cell adhesion and spreading and the motility was grossly impaired on various extracellular matrices. Thus, PIP2 interaction with vinculin is not essential for its adhesion localization but vinculin acts as a lipid sensor greatly influencing the adhesion site dynamics mediated through PIP2.

1. Introduction

1.1. Cell migration in maintenance and control of physiological processes

Directed cell migration is a highly integrated process that accompanies an organism right from conception to death. It plays a central role in development and maintenance of several biological phenomena like embryogenesis, immune response, tissue repair, tumor formation and metastasis. The failure of cell migration or nondirectional cell motility can lead to pathological conditions and congenital defects. Understanding the basic mechanics of cell migration is also considered important in technological applications like cell transplantation or tissue engineering.

1.1.1. Cell migration in embryogenesis

During embryogenesis, cell migration choreographs all the morphogenetic processes ranging from gastrulation to development of the nervous system. Two major types of cell movements can be observed during embryonic development. The first involves mass cell migration with tissue moving in a coordinated manner and cells maintaining their cohesive contacts while moving. This process is known as convergent extension and is particularly seen in amphibians and fish. The second type requires the loss of cell-cell contacts as it involves migration of the individual cell through the extracellular matrix, as seen during epithelial to mesenchymal transition (EMT) and neural crest formation. The TGF-β superfamily, Wnt and FGF signaling have been implicated in these two types of cell movements but different members and signaling pathways have been specifically associated with each of them (Locascio and Nieto, 2001).

1.1.2. Cell migration in homeostasis

Immune response and tissue repair are two homeostatic processes in the body that involve cell migration. Leukocyte migration is the hallmark of immune response, controlled cell movement allows the interaction of the immune cells with the antigen by which they elicit functions like phagocytosis or antibody production (Manzanares and Sanchez-Madrid, 2004). Cells migrating to areas of insult are stimulated by chemokines which act as traffic signals that guide their path and initiate polarization (Sanchez-Madrid and Angel del pozo, 1999).

Tissue repair or wound healing requires the migration of fibroblast or vascular endothelial cells to the areas of injury. This process is also guided by several signaling molecules that promote cell motility and regulate the cytoskeletal machinery to aid in wound closure (Martin and Parkhurst, 2004).

1.1.3. Cell migration in pathobiology

Failure of cells to migrate during embryogenesis can lead to defective implantation in the uterus and cause loss of pregnancy. In later stages, inappropriate migration of cells can result in congenital anomalies in the brain causing epilepsy or mental retardation (Huttenlocher *et al*. 1994, Bielas and Gleeson, 2004).

In adults, cell migration is involved in maintenance of biological processes like immunity and wound healing as stated earlier. Functional impairment of these processes due to defective cell migration can lead to serious pathologies. For example, chronic inflammatory disorders are caused by hyperactivity of the immune system when there is constant influx of inflammatory cells to sensitized areas in the body. Rheumatoid arthritis and Multiple sclerosis are such diseases caused by the disorganized immune system (Johnson *et al*. 2004). For biologists studying cancer, the major challenge is to identify the underlying molecular mechanisms that are involved in tumor metastasis (migration of tumor cells to different areas of the body). The molecules that switch cells to a metastatic state mostly are migration related proteins that either stimulate or propagate the process (Friedl *et al.* 2004, Ridley, 2000).

1.1.4. Molecular mechanics of cell migration

Cell migration is a highly coordinated, dynamic process. Understanding cell migration as a conceptualized cycle requires the knowledge of chemical and physical properties of various components and the thermodynamic, kinetic and mechanical changes during their assembly. The steps involved in the migration cycle and the molecular players and signaling pathways are detailed below.

A) Cell polarization and protrusive machinery

The initial response of a cell to a migratory stimulus is to polarize and obtain a spatial asymmetry which clearly distinguishes the cell front from the rear and indicates the direction of migration. The extended protrusions can be large, broad lamellipodia

containing a branching "dendritic" network of actin filaments or spike like filopodia with a backbone of actin filaments organized into long parallel bundles. The generation of both, lamellipodia and filopodia is driven by actin polymerization (Pollard and Borisy, 2003).

The protrusive machinery involves continuous actin polymerization at the leading edge, and is mediated through the Arp2/3 complex which binds to the sides or tips of a pre existing actin filament and induces the formation of new daughter filaments (Machesky *et al*. 1994). The Arp complex consists of seven subunits – two actin related proteins, Arp2 and Arp3, along with five unique polypeptides, called ARPC1-5 (Robinson *et al.* 2001). Activation of Arp2/3 complex is performed by WASP/WAVE family members (Machesky and Insall, 1998) which are themselves regulated by the Rho family of small GTPases like rho, rac, cdc42 (Ridley, 2001). The actual pushing force is generated not by the elongation of actin filaments but by an "elastic Brownian ratchet" mechanism (Mogliner and Oster, 1996, Pollard and Borisy, 2003) in which the thermal energy bends the nascent actin filaments and the restoring force of the filament to straighten up renders the propulsive force. Several actin binding proteins regulate actin polymerization through various mechanisms, for example, profilin adds polymerization competent actin monomers, capping proteins inhibit filament elongation, ADF/Cofilin severs and depolymerizes actin filaments. Many proteins are involved in the maintenance of the actin filament polymerization like cortactin which stabilizes branches (Weaver *et al.* 2001), or filamin A and α actinin which stabilize the entire network by cross linking actin filaments (Cunnigham *et al.* 1992).

B) Attachment to the extracellular matrix (ECM)

The extended protrusions are stabilized either by attachment to the ECM (via integrins) or to adjacent cells (via transmembrane receptors). At the cytoplasmic face the transmembrane receptors are linked to the actin cytoskeleton. These adhesions serve as traction sites for migration as the cells move forward over them. The integrins play a major role in cell-matrix adhesions and "inside-out" signaling. Upon activation these heterodimeric transmembrane receptors cluster, they undergo conformational changes to interact with the cytoskeletal and adaptor proteins and initiate the formation of an adhesion complex (Zamir and Geiger, 2001). Several enzymes like kinases and

phosphatases are involved in the regulation of the adhesions. Formation of small adhesions (focal complexes) seen in the leading edge which undergo fast turnover are regulated by rac and cdc 42 (Nobes and Hall, 1995). Cells with large integrin clusters tightly adhere and form strong focal adhesions which are present in the cell body and in slow-moving cells. They are regulated by rho mediated actin-myosin contraction (Nobes and Hall, 1995). These cell-matrix contacts both serve as traction sites and mechanosensors that signal from ECM and accordingly alter the cytoskeletal dynamics. The migratory speed is directly proportional to the tractional force exerted by each adhesion and the strength of the adhesion is related to the density of the adhesion receptors in the cell (Lauffenburger and Horwitz, 1996, Galbraith *et al.* 2002).

The formation and dissociation of focal adhesions involves kinetics and differential regulation of the molecular components, a highly complex process that is not completely understood (Zamir and Geiger, 2001). The main aim of this work is to analyse one such structural and regulatory protein – vinculin which is involved in adhesion turn over and will be discussed in greater detail in the following chapters.

C) Cell body translocation, adhesion disassembly and detachment at the cell rear

Translocation of the cell body is believed to occur due to a combination of traction forces generated by adhesions and rho mediated actomyosin contractility (Huttenlocher *et al.* 1995 and Jay *et al.* 1995). Rapid migration requires efficient mechanisms to release adhesions at the cell rear. In fibroblasts, a process called “membrane riping” leads to adhesion release where a major fraction of integrins is left on the substratum when the cell moves forward. Integrins that undergo regulated release can disperse and form endocytic vesicles in the cell body or remain aggregated, move forward along the edge of the cell and form new adhesions (Lauffenburger and Horwitz, 1996). The mechanism by which adhesion dissociation in the cell rear occurs includes a mechanical force arising from signaling pathways and involves regulatory components that influence adhesion turnover. Rho GTPase is strongly implicated in this process. Inactivation of rho by either inhibition or physiologic regulators induce cytoskeletal breakdown and inhibited migration in various cell types (Riento and Ridley, 2003). Several observations also indicate a role for tyrosine phosphorylation in adhesion release (Crowley and Horwitz, 1995). p125 focal adhesion kinase (FAK) and Src tyrosine kinases are involved in focal

adhesion turn over (Carragher and Frame, 2004) and selective inhibition of Src kinase has been shown to decrease focal adhesion disassembly (Webb *et al.* 2004).

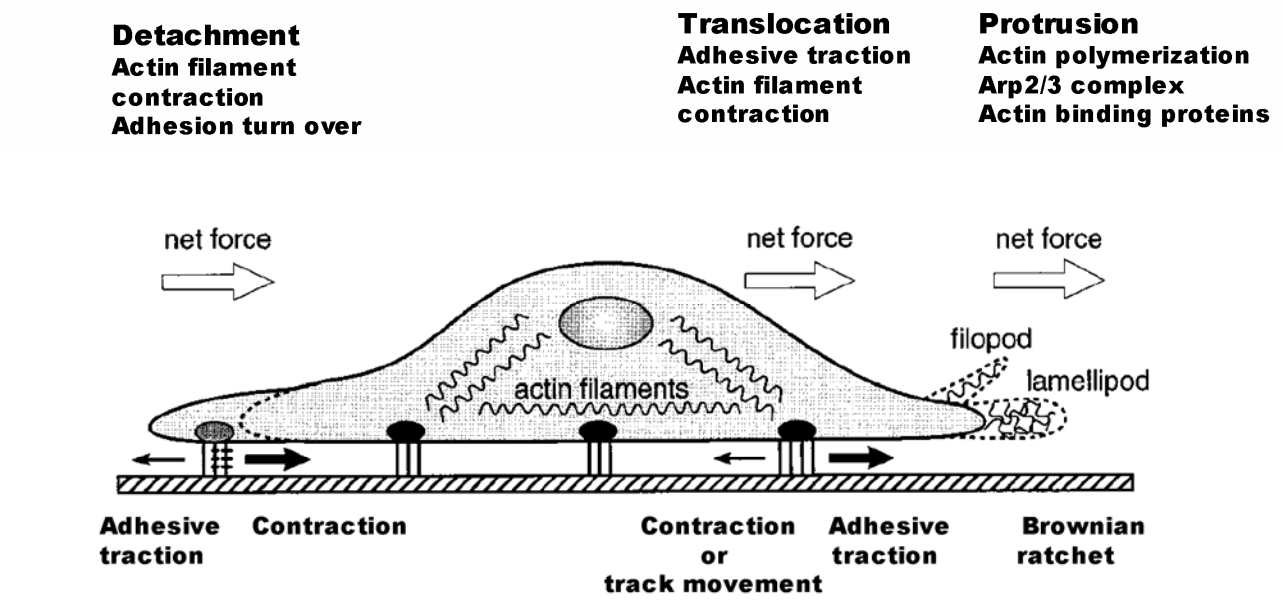

Figure 1.1: Cell migration at a glance
Cell migration involves the interplay of several signaling, cytoskeletal proteins. Initial protrusion is guided by actin polymerization; cell body translocation after adhesion to the ECM is driven by the tractional force generated from the adhesion sites and also through actin filament contraction. Adhesion disassembly and detachment at the cell rear rather involves myosin-mediated actin filament contraction than tractional force (modified after Lauffenburger and Horwitz, 1996).

1.2. Cell adhesion

Cell adhesion is a dynamic process that is crucial for the formation and maintenance of tissues. At these cell contact sites, the extracellular domains of transmembrane adhesion receptors interact with their corresponding ligands in the adjacent cell or in the extra cellular matrix, and the cytoplasmic domain is linked to the cytoskeleton. Linkage of the cytoskeleton to the adjacent cell or to the ECM gives mechanical strength to tissues and serves as anchor points for cytoskeletal movements that mediate changes during tissue development and morphogenesis (Pokutta and Weis, 2002). The proteins involved in cell adhesion mechanisms are typically divided into three classes (1) Cell adhesion

molecules/receptors which are transmembrane glycoproteins that mediate cell-cell or cell-ECM interactions namely integrins, cadherin, immunoglobulin, selectin and proteoglycan (eg: syndecan) superfamilies. (2) ECM proteins that are large glycoproteins including collagens, fibronectins, laminins and proteoglycans that assembles into fibrils. (3) Cytoplasmic plaque/peripheral membrane proteins such as catenins of the cell-cell contact sites and the cytoskeletal proteins like vinculin, talin that form a linkage between the adhesion complex and the actin cytoskeleton (Gumbiner *et al.*1996).

1.2.1. Types of cell adhesions

Cell-cell adhesions can be classified into communicating junctions, such as gap junctions, anchoring junctions, such as desmosomes and adherens junctions, and occluding junctions, such as zonula occludens or tight junctions.

Gap junctions: Gap junctions are intercellular structures allowing for the passive diffusion of the ions and small molecules in aqueous intercellular channels (connexons) between the cytoplasms of the neighbouring cells (Kumar and Gilula, 1996). Most cells of the normal tissues, except skeletal muscle cells communicate via these junctions. The channels are constructed by at least 13 different proteins called connexins.

Desmosomes: Desmosomes are specialised junctional structures that form a tight connection between all the epithelial cells and cardiac myocytes (Schwarz *et al.* 1990). They are linked to cytokeratins, a class of intermediate filaments. Desmosomal structures consist of several transmembrane glycoproteins like desmogleins, desmocollins (cadherin superfamily) and desmoplakins that link the intermediate filaments to the membrane. The cytoplasmic plaque protein associated with desmosomes is plakoglobin (Garrod, 1993).

Adherens junctions: Cadherin-based cell-cell contact is a specialised region of the plasma membrane, where cadherin molecules of the adjacent cells interact in a calcium-dependent manner. Actin filaments are associated with this structure through catenins located at the undercoat of the adherens junction (Geiger and Ginsberg, 1991). Classical cadherins are of three types epithelial (E), placental (P) and neuronal (N). α catenin is the only catenin that forms either direct or indirect linkage to actin cytoskeleton through α-actinin, vinculin, ZO-1, spectrin and a number of other molecules associated to cadherin complex (Yamada and Geiger, 1997). E-cadherin binds to β catenin or to γ catenin (plakoglobin) which, in turn, form the linkage to α catenin.

Tight junctions: In epithelial and endothelial cells, tight junctions are the most apical intercellular junctions that function as selective (semipermeable) diffusion barriers between individual cells. They maintain the different composition of proteins and lipids between the apical and basolateral plasma membrane domains and regulate the growth and differentiation of the cells (Tsukita *et al.* 1999). The proteins involved are integral membrane proteins, such as occludin, claudin and junctional adhesion molecule, JAM and peripheral membrane proteins such as ZO-1, 2, 3 etc.

Cell-matrix adhesions can be classified into focal adhesions, dystroglycan complex and hemidesmosomes.

Focal adhesions: Focal adhesions are the structural connections between the ECM and the actin cytoskeleton. Please refer to chapter 1.2.2 for detailed description.

Hemidesmosomes: Hemidesmosomes are multimeric protein complexes that attach epithelial cells to their underlying matrix, via keratins. They are morphologically similar to desmosomes and localised to the basal surface of some epithelial cell types (Garrod, 1993). Keratin bundles associate to the hemidesmosome plaque via proteins like BP230, BP180 and α6β4 integrin.

Dystroglycan complex: The transmembrane adhesive receptor dystroglycan binds to laminin in the matrix and links it to the actin cytoskeleton. Dystrophin is the cytoplasmic plaque protein that aides in the linkage. Duchennes muscular dystrophy is caused by a mutation in the dystrophin gene (Campbell, 1995).

1.2.2. Molecular model of cell-matrix adhesions

Cells in culture and stationary cells adhere tightly to the underlying substratum through distinct regions of their plasma membrane called cell-matrix junctions, also termed as focal contacts or focal adhesions (FAs). Thirty years back FAs were described as structurally defined cell-matrix contact sites using interference reflection and electron microscopy (Abercrombie *et al.* 1971, Izzard and Lochner, 1980). At these sites the transmembrane receptors, the integrins, interact with extracellular matrix (ECM) proteins e.g. fibronectin, collagens, laminins or vitronectin. On the cytoplasmic face of the focal adhesion, integrins are linked to the actin cytoskeleton through various cytoskeletal and adaptor proteins. Focal adhesions are considered structural connections between the ECM and actin cytoskeleton. A schematic model of these structures is depicted in Figure 1.2.

The focal adhesions of the cultured cells are typically 2-5 μm long and 0.25-0.5 μm wide. The molecular complexity of these adhesion sites is surprisingly large, many of the components are still unknown, and many undergo proteolytic processing and conformational changes which regulates the formation and dissociation of these sites. Classification of these proteins based on their presumed functions categorizes them into following major classes (Zamir and Geiger, 2001).

1.2.3. Players and regulators of cell-matrix adhesions

Cytoskeletal proteins like vinculin, talin, α actinin, paxillin, tensin, parvin/actopaxin, can directly bind, cap, bundle or nucleate actin filaments and/or directly interact with cytoplasmic tails of integrins, thus serving the structural linkage between integrins and stress fibres.

Regulatory proteins include various tyrosine kinases, serine/threonine kinases, tyrosine phosphatases, modulators of small GTPases and other enzymes.

p125 focal adhesion kinase (FAK) and src family tyrosine kinases are activated in FAs and play an important role in their assembly. A number of proteins in the focal adhesion are highly tyrosine phosphorylated and inhibition of tyrosine kinases or serum starvation prevents the assembly of FAs (Burridge *et al*. 1992, Keely *et al*. 2004). Protein kinase C is involved in the regulation of FAK and Src kinases (Nakashima *et al.* 2002). Phosphotidyl inositol kinases like PI3K and PI5K are implicated in the regulation of PIP2 and PIP3 levels in FAs, which will be discussed in detail in later chapters. Small GTPases of the rho family control the turnover of contact sites (Ridley and Hall, 1992, Rottner *et al.* 1999). Modulators of these small GTPases localized in FAs are probably involved in their regulation (e.g. GRAF, ASAP1). Enzymes like calpain proteases are known to regulate FAs by proteolysis of talin, paxillin, FAK, Src and tensin (Carragher *et al*. 1999, Chen *et al*. 2000).

Phosphotidyl inositols play a key role in FA regulation by binding to structural as well as regulatory proteins. PIP2 modulates the activity of many actin regulatory proteins that orchestrate actin polymerization to initiate locomotion. The mechanisms by which PIP2 regulates the actin dynamics are described in Chapter 1.4. Actin cross linking proteins (α actinin, filamin) and membrane linking (vinculin, talin) proteins are also known to be

regulated by PIP2. PIP3 influences the activity of many rho GTPases and their modulators (Yin and Janmey, 2003).

Focal adhesions are sites through which cells respond to the ECM with diverse biochemical and biophysical properties. They also aid in intracellular signaling. The exact composition of a given FA therefore will differentially regulate cell adhesion, migration and proliferation. More knowledge of the composition and functional regulation of these components are required to better understand cell migration, adhesion during development, morphogenesis and maintenance of several biological processes.

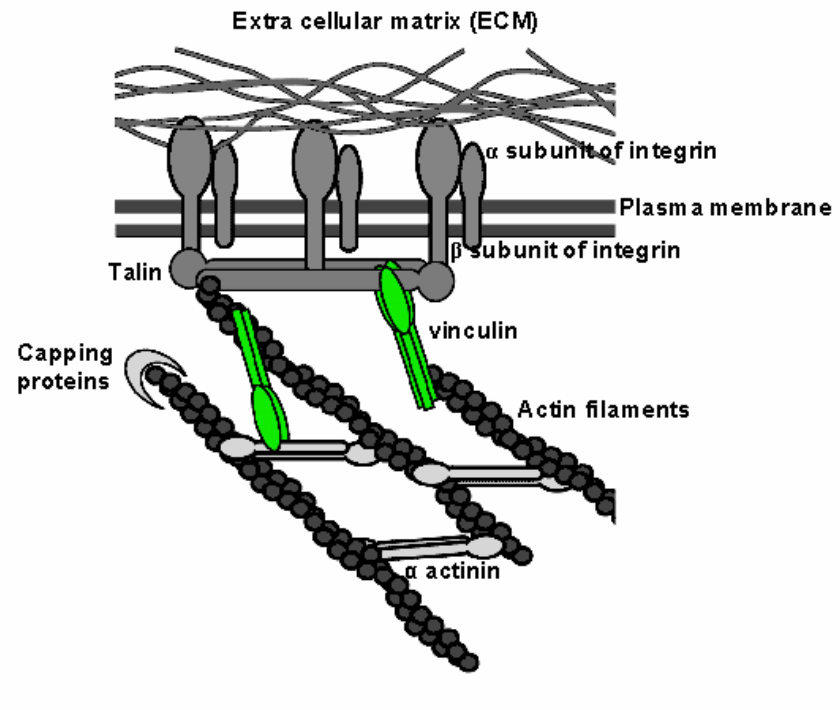

Figure 1.2: Molecular model of a focal adhesion
Simple model of a focal adhesion depicting only a few important structural components. The transmembrane receptor, integrin, is activated by binding to respective ECM protein. Linkage to the actin cytoskeleton is mediated through several cytoskeletal proteins (vinculin, talin, α actinin) which aid in the construction and in maintaining the physical integrity of the focal adhesion (Zamir and Geiger, 2001).

1.3. Vinculin – a structural and regulatory component of focal adhesion

Vinculin ("vinculum" meaning "link" in latin) was first reported as an intracellular protein isolated from chicken gizzard smooth muscle and was shown to be concentrated on the ventral surface of the chicken fibroblasts where they formed focal adhesions to the substratum (Geiger, 1979, Geiger *et al.* 1980). Functionally it was supposed to participate

in the linkage of the termini of the microfilament bundles to the plasma membrane (Geiger *et al.* 1980). It is one of the highly conserved cytoskeletal proteins with more than 95% homology between human and avian species (Weller *et al.* 1990). Vinculin provides a structural and functional link between the cell adhesion receptors (integrins or cadherins) and the actin cytoskeleton (Jockusch and Rudiger, 1996). Vinculin null mice die in early embryogenesis (E8-E10), due to heart and brain defects suggesting its requirement for the complex array of cell contacts and movements that occur during development (Xu *et al.* 1998). Loss of vinculin activity in *C. elegans* leads to defects in muscular activity and lethality at the larval L1 stage (Barstead and Waterston, 1991).

Electron microscopic studies of chicken vinculin show a trilobar "head" 80 Å in diameter from which a long flexible "tail" emanates consisting of four distinct globular masses, connected by a short hinge region (Molony and Burridge, 1985, Winkler *et al.* 1996). The molecular weight of vinculin is 117kDa; it consists of 1066 amino acids (Coutu and Craig, 1988). Biochemical studies show that cleavage by V8 protease within the proline rich hinge region (residues 837-878) generates a 95kDa globular N-terminal head (Vh) and a C-terminal tail (Vt) (Price *et al.* 1989).

1.3.1. Molecular structure of vinculin

Bakolitsa *et al.* have recently elucidated the crystal structure of the full length vinculin molecule (Baklolitsa *et al.* 2004). They describe vinculin as a 'bundle of bundles' with dimensions 100×100×50 Å, made up of five domains with an autoinhibited conformation in which the C-terminal vinculin tail domain is held pincer-like by the vinculin head, and the ligand interactions are regulated both sterically and allosterically.

Domains 1 – 3 (D1 – D3), made up of residues 6 – 717, comprise the vinculin head (VH) observed in the electron microscopic images, which is distinct from the proteolytic fragment 'Vh' which includes D4 and part of the proline rich region. Each domain within VH (D1, D2, and D3) consists of two four helix bundles, which are organized into three tandem pairs, which resemble the N-terminal fragment of α catenin termed as 'vinculin/α catenin repeat' (VCR). In domains D1 and D2 the two four helix bundles pack end-to-end, in D3 the two bundles interact along their sides with a distinct break in helicity in the middle of the central helix. D1 and D3 form a pair of pincers which are locked in position by D2. The pincers hold Vt (domain 5) in the autoinhibited structure (Fig: 1.3).

Domain 4, residues 719 – 835, is a four helix bundle that packs end-to-end with domain 5 (Vt) and is considered to be the 'neck' region with variable conformation observed in the EM images. D4 precedes the proline rich region which is partly disordered (residues 838 – 878) and a 'strap' (residues 878 – 890) that precedes the Vt domain (Fig: 1.3).

The Vt domain, D5 (residues 896 –1066) is held in position by D1 and D3, the conformation of which is essentially identical to that seen in the tail crystal structure described below. The domains D4 and D5 together make the fourth VCR with a large insertion comprising the proline-rich region and the first helix of Vt. Vt makes two contacts with the vinculin head and one with the neck. According to Bakolitsa *et al.* the ligand binding sites on the head, tail and proline-rich regions are structurally distinct, but conformationally and thermodynamically linked. Therefore, activation of vinculin could be achieved by a combinatorial influence of ligands in distinct regions of the molecule, and when the activating potentials exceed the intramolecular binding energy, the molecule is transformed into the activated open state. Izard and colleagues have shown that talin binding induces marked conformational changes in the vinculin head (Domain1), converting the helical bundle structure, and displaces Vt from Vh (Izard *et al.* 2004).

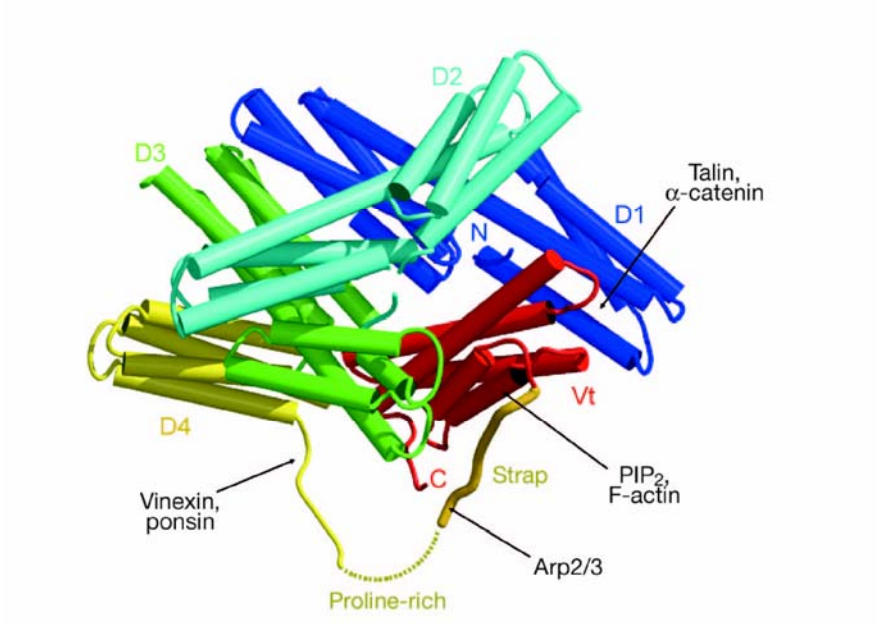

Figure 1.3: Molecular structure of vinculin
Full length vinculin in its autoinhibited state, domains (D1 –D5) are shown in different colors. Major ligand binding sites are indicated (adopted from Bakolitsa *et al.* 2004).

1.3.2. Molecular structure of vinculin tail

The crystal structure of Vt, residues 879 – 1066, was elucidated prior to the full length structure (Bakolitsa *et al.* 1999). The structure comprises a helical bundle, consisting of five helices (H1 to H5), connected by short loops (3-8 residues) and adopts an antiparallel topology (Fig 1.4A). All five helices are markedly amphipathic, with their hydrophobic side chains pointing inside and hydrophilic groups pointing outward. Positive charges cluster in two regions on the surface of the domain, a basic collar surrounding the C-terminal hairpin and a basic ladder that is centered on H3, these basic clusters are identified as the putative acidic phospholipid binding sites (Bakolitsa *et al.* 1999)
(Fig 1.4B). A C-terminal arm following the last helix is divided into three segments, a flexible loop (1047 – 1052), a β clamp (1053- 1061), and a hydrophobic hairpin (1062 – 1066). The hydrophobic hairpin comprising amino acids TPWYQ is implicated in the membrane insertion of the molecule (Bakolitsa *et al.* 1999). The structural model suggests that Vt switches between a soluble helical bundle and a membrane bound unfurled form probably through the binding to acidic phospholipids. This assumption is also supported by the evidence that PIP2 binding increases the susceptibility of Vt to proteases. The authors also considered that vinculin head controls the ligand binding to Vt allosterically by stabilizing the helical bundle and preventing unfurling which was proved later with the description of full length vinculin structure.

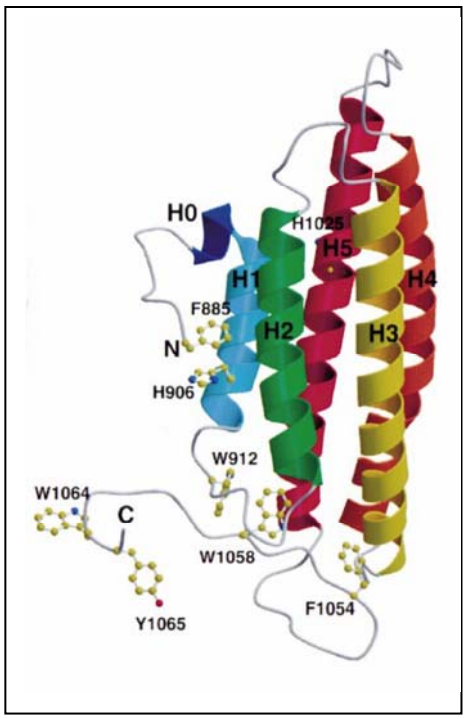

Figure 1.4 A: Structure of vinculin tail
Stereo ribbon representation of Vt. Helices are shown in spectral colors from blue to red and labeled H0–H5. The side chains of all aromatic residues are shown as ball-and-stick and colored by atom type (adopted from Bakolitsa *et al.* 1999).

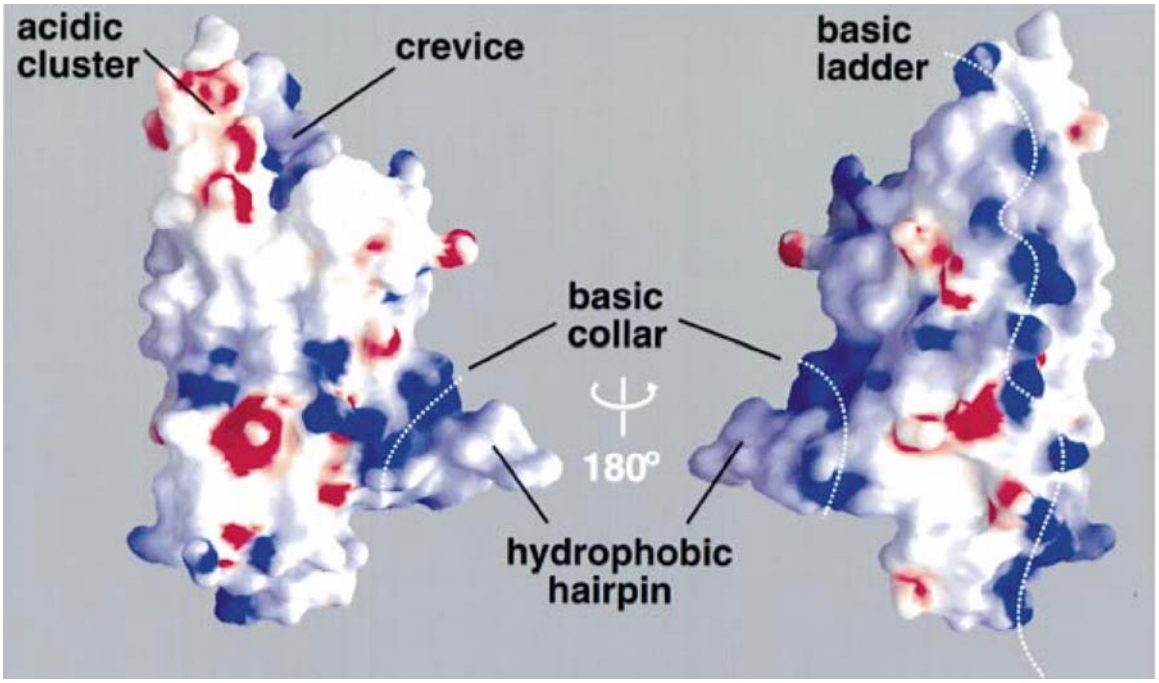

Figure 1.4 B : Molecular surface of vinculin tail
Solvent-accessible surface of Vt, with salient features indicated. The basic ladder includes residues K944, R945, K952, K956, R963, K966, K970, R978, R1008, and R1049. The basic collar includes residues R910, K911, R1039, K1049, R1060, and K1061. The acidic cluster includes residues D1013, E1014, E1015, E1017, and E1021. The hydrophobic hairpin comprises the C-terminal residues 1062–1066 (TPWYQ). The crevice is formed by the H4-H5 turn, the H2-H3 turn, and H0. The coloring is according to electrostatic potential, blue for positive, red for negative (adopted from Bakolitsa *et al.* 1999).

1.3.3. Ligand interactions of vinculin

The ligand binding properties of vinculin are influenced by an intramolecular head-tail interaction (Jockusch and Rudiger, 1996)**.** The vinculin head has binding sites for α actinin, an actin cross linking protein (Kroemker *et al.* 1994), talin, a cytoskeletal protein which can directly bind the β subunit of integrin (Burridge and Mangeat, 1984, Johnson and Craig, 1994), and vinculin tail which mediates the intramolecular interaction (Johnson and Craig, 1994, Miller *et al.* 2001, Weekes *et al.* 1996). In addition to the head domain the vinculin tail can bind to the following proteins**:** paxillin, an adaptor protein (Turner *et al.* 1990, Wood *et al.* 1994), F-actin (Menkel *et al.* 1994, Huttelmaier *et al.* 1997, Jockusch and Isenberg, 1981), Phosphotidylinositol 4,5-bisphosphate (PIP2) (Fukami *et al.* 1994, Johnson *et al.* 1998, Niggli and Gimona, 1993), as well as the lipid

bilayer proper (Bakolitsa *et al.* 1999, Johnson *et al.* 1998), and protein kinase C (Ziegler *et al.* 2002, Weekes *et al.* 1996). The proline rich neck region can bind to VASP (Brindle *et al.* 1996, Reinhard *et al.* 1996), ponsin (Mandai *et al.* 1999), vinexin (Kioka *et al.* 1999) and the Arp2/3 complex (Demali *et al.* 2002) (Figure 1.5). The intramolecular head-tail interaction masks the binding sites for α actinin (Kroemker *et al.* 1994), talin (Johnson and Craig, 1994), actin filaments (Johnson and Craig, 1995), VASP (Huttelmaier *et al.* 1998) and the Arp2/3 complex (Demali *et al.* 2002) and prevents the interaction of these ligands with vinculin in its non activated 'closed' conformation.

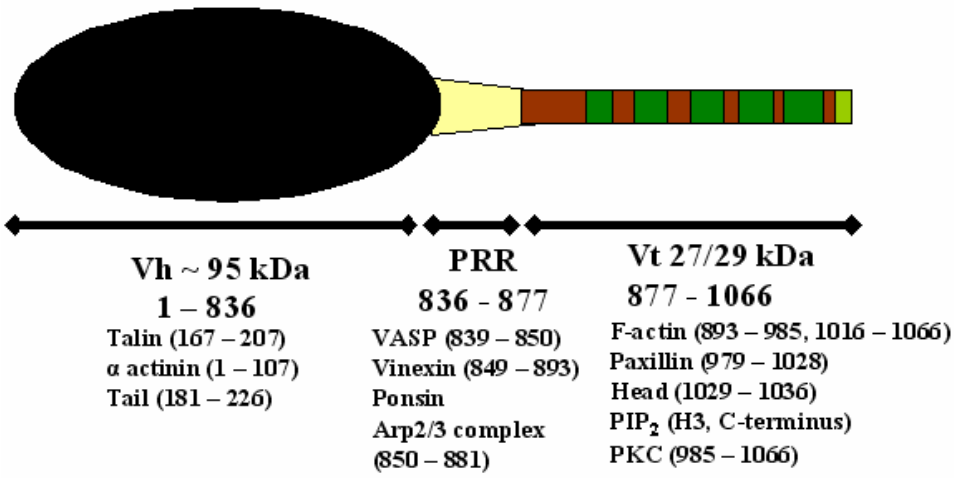

Figure 1.5: Ligand interactions of vinculin
Schematic diagram showing vinculin head (Vh), proline rich neck region (PRR), vinculin tail (Vt) and their respective ligand binding sites (based on Jockusch and Rudiger, 1996, Zamir and Geiger, 2001).

1.3.4. Acidic phospholipid mediated regulation of vinculin

Interaction of the acidic phospholipid, PIP2 with vinculin has been reported earlier (Fukami *et al.* 1994). Influence of PIP2 on vinculin's intramolecular interaction was elaborately studied by several groups. Initially, PIP2 was reported to dissociate the vinculin head-tail interaction, subsequently unmasking its talin-and actin-binding sites (Gilmore and Burridge, 1996). Later, Weeks *et al.* showed that acidic phospholipids inhibit the intramolecular association and expose a cryptic actin binding site and protein kinase C phosphorylation sites in the vinculin tail (Weekes *et al.* 1996). PIP2-mediated

release of the head-tail interaction was therefore considered important for the focal adhesion targeting and assembly of FAs (Gilmore and Burridge, 1996). A conformational change in the vinculin tail due to PIP2 binding was also noticed earlier (Bakolitsa *et al.* 1999) and was considered essential to decrease the affinity between Vh and Vt. The above model has been questioned by the recent findings that indicate the role of talin (Bass *et al.* 1999, DiPaolo *et al.* 2002) and other ligands that influence vinculin activation through their steric and allosteric interactions (Bakolitsa *et al.* 2004). Thus, the role of PIP2 as the sole activator of vinculin seems to be **not** significant any more, though it surely has a pivotal role in the regulation of the molecule in the adhesion sites (this work). Polyphosphoinositides have also been shown to inhibit the interaction of vinculin with actin filaments *in vitro* (Stiemle *et al.* 1999). The authors also suggested that actin and PIP2-binding to vinculin tail is mutually exclusive and the role of PIP2 is to expose talin binding site in Vh, while block the actin binding site in Vt. However, comparison of actin and PIP2-mediated changes in the molecular structure of vinculin indicates that these ligands may provide two alternative pathways to activation (Bakolitsa *et al.* 2004).

1.4. Phosphatidylinositol 4,5-bisphosphate as a signaling molecule

Phosphatidylinositol 4,5-bisphosphate (PIP2) and phosphatidylinositol 3,4,5 bisphosphate (PIP3) represent less than 1% of membrane phospholipids, yet they play a pivotal role in a number of crucial cellular processes. PIP3 is the effector of multiple downstream targets of the phosphotidylinositol 3 kinase (PI3K) pathway. PIP2 acts as the source of two important second messengers in the cell (Berridge *et al.* 1984), diacylglycerol (DAG) and inositol 1,4,5-trisphosphate (IP3). Role of PIP2 in the regulation of the actin cytoskeleton (membrane attachment to the cytoskeleton, phagocytosis) and its involvement in membrane trafficking (endocytosis, exocytosis), cell signaling (protein kinase localization and activation, ARF GTPase regulation) have now been well documented. PIP2 acting as an important regulator of actin dynamics is described in detail below.

PIP2 modulates the activity of many actin regulatory proteins that orchestrate actin polymerization and promotes cell migration. Actin polymerization can be regulated by three different mechanisms of which all are potentially regulated by PIP2. One mechanism involves the Arp2/3 complex, that is known to promote actin nucleation and

filament branching. The complex is stimulated by WASP family proteins that are activated by PIP2 synergistically with other ligands (Rohatgi *et al.* 2000, Rozelle *et al.* 2000). The second mechanism involves uncapping of the plus end of preexisting actin filaments by the dissociation of capping protein, CapZ which is promoted by PIP2 (Heiss and Cooper, 1991, Schafer *et al.* 1996). The third mechanism uses severing of preexisting filaments by gelsolin family proteins or cofilin/actin depolymerizing factor (ADF) to increase the number of actin nuclei. Cofilin/ADF severing activity is inhibited by PIP2 (Ojala *et al.* 2001). Gelsolin has more potent severing activity than Cofilin/ADF. It is activated by Ca2+ to sever and cap filaments. Once bound to actin, gelsolin cannot be dissociated by decreasing the ambient Ca2+ concentration. Phosphoinositides and lysophosphatidic acid are the only known agents that can dissociate gelsolin from the filament ends (Janmey and Stossel, 1987, Meerschaert *et al.*1998).

PIP2 also regulates key molecules involved in actin-membrane linkages. Many actin cross-linking and membrane attachment proteins are regulated by PIP2. Alpha actinin, is activated by PIP2 binding through dissociation of an intramolecular interaction which enables it to bind actin and titin (Young and Gautel, 2000). Filamin, another actin cross linking protein is inhibited by PIP2 (Furuhashi *et al.* 1992). Ezrin/Radixin/Moesin (ERM) proteins, like alpha-actinin, are activated by PIP2. The binding site for actin filaments (Nakamura *et al.* 1999, Barret *et al.* 2000) and transmembrane proteins (Hirao *et al.* 1996, Heiska *et al.* 1998) in the ERM family proteins are exposed by PIP2 interaction. Focal adhesion proteins talin and vinculin are also activated by PIP2. In case of talin, PIP2 binding increases its affinity to the cytoplasmic domain of beta 1 integrins (Martel *et al.* 2001). PIP2 mediated vinculin activation has already been described in the earlier chapters. Thus, PIP2 plays a very significant role as a signaling molecule, in control and maintenance of various cellular processes.

1.4.1. Synthesis and regulation of PIP2 in cells

Phosphatidylinositol 4,5-bisphosphate (PIP2) has been shown to be maintained at relatively constant levels in cells (McLaughlin *et al.* 2002). Growth factor stimulation or cell adhesion to ECM cause rapid changes in cellular PIP2 levels (Auger *et al.* 1989, Weernink *et al.* 2000). Although localized PIP2 production is difficult to quantify, biochemical methods and single cell imaging with PIP2 specific antibodies or with the

PH domain of PLCδ fused to GFP have been successfully employed (Balla *et al.* 2000, Miyazawa *et al.* 1988). However, these methods only detect PIP2 changes on the palsma membrane. The major goal of current research is focused on mechanisms that are involved in PIP2 generation and its regulation. Two major mechanisms by which PIP2 levels are modulated are considered to be either the localized synthesis by phosphoinositide kinases (PIPK) or the release of the electrostatically sequestered PIP2 (McLaughlin *et al.* 2002).

The PIP kinases are divided into three subfamilies type I, II, and III, according to their signaling specificity. The type I and II PIP kinase subfamilies include three isoforms α, β, and γ as well as a number of splice variants classified based on their substrate usage and subcellular targeting (Ishihara *et al.* 1996, Ishihara *et al.* 1998, Itoh *et al.* 2000). Type I PIP kinase activity has been shown to be necessary in actin rearrangements, adhesion, secretion, endocytosis, and ion channel regulation (Arneson *et al.* 1999, Di Paolo *et al.* 2002, Ling *et al.* 2002, Shibasaki *et al.* 1997, Shyng *et al.* 2000). PIPKIγ is specially noted for its isoform and splice variant specific function. It has two known mRNA splice variants, PIPKIγ 635 and PIPKIγ 661, which differ by 26 amino acids in the C-terminus (Ishihara *et al.* 1998). Recent results showed that PIPKIγ 661 targets to FAs and interacts with the FERM domain of talin (Di Paolo *et al.* 2002, Ling *et al.* 2002). This suggests a novel role of PIP kinases as potential regulators of cellular processes like adhesion and migration. In turn, several small G proteins like RhoA, Rac1, and ARF6 are considered as potential regulators of PIP kinases (Doughman *et al.* 2003).

Proteins that sequester PIP2 should satisfy the essential criteria, like-their availability in high concentrations at the membrane associated areas and having high electrostatic affinity for PIP2. MARCKS (Myrsitolated alanine rich C-kinase substrate) is considered to be the best candidate, found attached to the membrane and having high affinity to PIP2 (Mclaughlin *et al.* 2002). Several signals that initiate increase in PIP2 levels could probably modulate these sequestering proteins and trigger the release of PIP2 but more elaborate analyses are needed to understand the molecular mechanism.

1.5. Aims of this work

As pointed out at the beginning of this section, cell adhesion and migration are two basic physiological processes essential for development and maintenance of a living organism. Vinculin is a major structural and elementary component of cell-matrix adhesions, without which the above mentioned cellular processes are non-functional. Thus, the knowledge about the structure, regulation and dissociation of vinculin-containing building blocks at adhesion sites is essential for the understanding of tissue formation. Although the acidic phospholipid-mediated activation of vinculin has already been known for several years as stated earlier, important details regarding its regulation to influence the focal adhesion turnover was not completely solved. The primary goal of this work was to characterize the role of acidic phospholipids as major regulators of the cell adhesion protein vinculin. The problem was approached with a wider perspective in terms of characterizing the effect of acidic phospholipids on vinculin's biochemical properties and its cellular functions. A 'lipid binding deficient' vinculin mutant was designed, and variations in its biochemical properties like acidic phospholipid binding, interactions with important ligands like F-actin and vinculin head domain were analysed and compared to wild type vinculin. The effects of the lipid binding site mutations on the structural and functional regulation of the molecule at the adhesion sites were also addressed by generating cell clones that stably express vinculin wild type and mutants as GFP fusion proteins. Functional processes like cell migration, adhesion, turnover of adhesion sites were the key points studied.

2. Materials and Methods

2.1. Materials

2.1.1. Chemicals and enzymes

All chemicals were of p.A quality and purchased from Sigma (Deisenhofen), Serva (Heidelberg), Merck (Darmstadt), Fluka (Neu-Ulm), Difco (Hamburg), ICN (Eschwege) and Invitrogen (Karlsruhe). All enzymes employed in molecular biology were from the following companies unless otherwise specified, New England Biolabs (Bad Schwalbach), Stratagene (Heidelberg), Boehringer (Mannheim), Appligene (Heidelberg), Invitrogen (Karlsruhe) and Promega (Mannheim).

2.1.2. Cell culture medium and plastic wares

Cell culture media and additives were purchased from Gibco BRL and Sigma.

Plastic wares were obtained from Corning, Eppendorf, Falcon, Greiner and Nunc.

2.1.3. Oligonucleotides

The Oligonucleotides employed in cloning and sequencing reactions were obtained from MWG-Biotech (Ebersberg). The cloning and mutagenesis primers are listed in Table 2.1 and the sequencing primers are listed in Table 2.2 below. The restriction sites present in the primers are also specified.

Table 2.1: Cloning and mutagenesis primers

Number	Name	Purpose	Sequence 5' to 3'
WZ 186	Vt 858SacI sense	Vt wt cloning	AACTGATGAGCTCGCTCCTCCTAAGC
WZ 190	Vt 1066XhoI,SalI reverse	Vt wt cloning	CTCGAGGTCGACTTACTGGTACCAGGG
WZ 121	Vt 1052SalI reverse	Vt Δ1052 cloning	AGGTCGACTCAAGCATCTGTTCGGATTTT
WZ 234	Vh 1EcoRI sense	Vh D1 cloning	GAATTCATGCCAGTGTTTCATAC
WZ 235	Vh 258SalI reverse	Vh D1 cloning	TACAGTCGACCTACCCAGGCATCTT
WZ 100	Vt RK1060/61QQ sense	Vt CT & LD mutagenesis	CTCTGCGCTGGGTCCAACAGACTCCCTGGTATCAGTA
WZ 101	Vt RK1060/61QQ reverse	Vt CT & LD mutagenesis	TACTGATACCAGGGAGTCTGTTGGACCCAGCGCAGAG
WZ 200	Vt KK952/956QQ sense	Vt H-3 & LD mutagenesis	TTCAGTGTGCCCAGGATATCGCCCAGGCCTCTGATGA
WZ 201	Vt KK952/956QQ reverse	Vt H-3 & LD mutagenesis	TCATCAGAGGCCTGGGCGATATCCTGGGCACACTGAA
WZ 202	Vt RK963/966QQ sense	Vt H-3 & LD mutagenesis	CTGATGAGGTGACGCAGTTAGCCCAGGAGGTTGCCAAGC
WZ 203	Vt RK963/966QQ reverse	Vt H-3 & LD mutagenesis	GCTTGGCAACCTCCTGGGCTAACTGCGTCACCTCATCAG
WZ 313	PIP5K 1EcoRI sense	PIP5K KD cloning	GAATTCATGTCGTCAACTGCTG
WZ 314	PIP5K 308stop/SalI reverse	PIP5K KD cloning	GTCGACTTACATGGCTGTGGAG
WZ 188	Vin S842F sense	Vinculin full-length cloning	CCTCAGGAGCCTGACTTCCCGCCTCCTCCACCAGAC
WZ 189	Vin S842F reverse	Vinculin full-length cloning	GTCTGGTGGAGGAGGCGGGAAGTCAGGCTCCTGAGG
WZ 175	Vin G565E sense	Vinculin full-length cloning	CGAGGGGAGGGGGAGAGTCCTCAGGC
WZ 176	Vin G565E reverse	Vinculin full-length cloning	GCCTGAGGACTCTCCCCCTCCCCTCG

Table 2.2: Sequencing primers

Number	Name	Purpose	Sequence 5' to 3'
WZ 179	Vh U0678	Vh sequencing	CAAGGAATAGAAGAAGCTTTG
WZ 180	Vh U0898	Vh sequencing	CTGGAGAGCAGGCCATCAGG
WZ 182	Vh L0321	Vh sequencing	ATGAGGTAATCCCGTGCAGGAAC
WZ 183	Vh L1237	Vh sequencing	CTTCAGCCAAAGCCCCTCGAATCT
WZ 160	Vh U1118	Vh sequencing	GGAGAATGCAGCTCGGAAGCTGGA
WZ 161	Vh U1338	Vh sequencing	CTGACCTCTAAACTAGGAGACTTG
WZ 162	Vh U1558	Vh sequencing	TCGGTCAGGCTGCCATCCGTGGAC
WZ 163	Vh U1778	Vh sequencing	GCAGGAAGCTATGACTCAAGAGGT
WZ 164	Vh U1998	Vh sequencing	ATTCAGGCATCTGTGAAGACAGCC
WZ 165	Vh U2232	Vh sequencing	GTAGCCATGGCCAATATTCAGCCT
WZ 192	Vh U2370	Vh sequencing	GCTGCCTCTGATGAACTG
WZ 193	Vt U2640	Vt sequencing	CCCCCACCACCAGAAGAG
WZ 194	Vt U2860	Vt sequencing	TTCAGTGTGCCAAGGATA
WZ 116	Vt U3052	Vt sequencing	GTGATGAGGAGTCTGAGC
WZ 199	Vt L2621	Vt sequencing	CTGGGTGGAGGGACTTCA
WZ 315	mmPIPkin U223	PIP5K KD sequencing	GCACATCACTACCCAGACTTCAGG
WZ 316	mmPIPkin U528	PIP5K KD sequencing	GCAGTCAGGAGGCATCAACATC
WZ 317	mmPIPkin L387	PIP5K KD sequencing	ATAATAAATTCATCATCGCTGGTC
WZ 318	mmPIPkin L704	PIP5K KD sequencing	ATCGAAATACAGCCCCTCAT

2.1.4. Vectors

The PCR products were directly cloned into the pCR Blunt vector using the Zero Blunt PCR cloning kit (Invitrogen). The prokaryotic expression vector pQE 30 (Qiagen) was employed for recombinant protein expression in *E. coli*; the constructs also had N-terminal coding sequences for the "Flag epitope" for detection in Western blot.

The vinculin head domain (D1) was subcloned into pGex4T-1(Amersham biosciences) for GST fusion protein expression.

For the generation of vinculin full-length GFP fusion constructs, pEGFP-C2 (Clontech) vector was used. Mouse PIP5-kinase α cloned in the myc tagged vector pRK5-Myc was kindly provided by Laura Machesky (University of Birmingham, Birmingham, UK) (Rozelle et al, 2000), the "kinase dead" mouse PIP 5-kinase α was fused to a BiPro tag (Rudiger et al, 1997) and subcloned into pcDNA3 (Invitrogen). Myc tagged L61-Rac in pRK5-Myc was a kind gift from Laura Machesky.

2.1.5. Bacterial cultures and cell lines

The cloning and recombinant protein expression was performed in the *E. coli* strains *XL-1 blue* and *M15 (pREP4)*. The strains had the following genotypic markers.

XL-1 blue supE44 hsdR17 recA1 gyrA46 thi rel A1 lac- F' [pro AB+ lacIq LacZ.M15 Tn10(tetr)]

M15(pREP4) NalS, StrS, RifC, Thi-, Ara+, Gal+, Mtl-, F-, RecA+, Uvr+, Lon+ (Villarejo, 1974)

The strains were grown in 2xYT medium containing the respective antibiotics depending on the vector used.

2xYT medium : 16 g Tryptone (Difco)
10 g Yeast extract (Difco)
10 g NaCl
Made up to 1 litre with H_2O

For agar plates 16 g of Bacto agar was added to 1 litre medium. 150 µg/ml of ampicillin and 30 µg/ml of kanamycin were used in the liquid medium and plates.

The cell lines employed in this study were ATCC strain of C2C12 mouse myoblasts, NIH 3T3 mouse fibroblasts, and B16-F1 mouse melanoma cells
(obtained from Dr. Theresia E. B. Stradal, GBF, Braunschweig).
Mouse embryonic fibroblasts from vinculin null mice MEF-/- and the control fibroblasts MEF+/+ were kindly provided by Prof. Dr. David Critchley (University of Leicester, Leicester, UK).

2.1.6. Antibodies

Antibodies were mainly employed for immuno detection in western blots and *in vivo* imaging of cells by immuno fluorescence.
The antibodies used in immuno blots are listed in Table 2.3, the antibodies and toxins used for immuno fluorescence are listed in Table 2.4 below.

Table 2.3: List of antibodies used in immuno blots

Description	Antigen	Company	Organism	Clonal type	Dilution
Anti Flag (M2)	"Flag epitope"	Sigma	Mouse	Monoclonal	1:10000
Anti GST	GST tag	Sigma	Rabbit	Polyclonal	1:10000
hvin1	Vinculin head	Sigma	Mouse	Monoclonal	1: 1500

The secondary antibodies employed were HRP conjugated Goat anti mouse IgG (1: 5000) and HRP conjugated goat anti rabbit IgG (1: 5000) for detection using enhanced chemiluminescence (ECL).

Table 2.4: List of antibodies and toxins used in immuno fluorescence

Description	Antigen/Source	Company/Institution	Organism	Clonal type	Dilution
hvin1	Vinculin head	Sigma	Mouse	Monoclonal	1: 500
Anti paxillin	Paxillin	BD Biosciences	Mouse	Monoclonal	1: 500
9E10 anti myc	Myc tag	GBF, Braunschweig	Mouse	Monoclonal	Hybridoma supernatant
4A6 anti BiPro	BiPro tag	TU-BS, Cell Biology dept	Mouse	Monoclonal	1: 10
Alexa Fluor^{TM}594 phalloidin	Amanita phalloides	Molecular Probes	-	-	1: 200
Alexa Fluor^{TM}350 phalloidin	Amanita phalloides	Molecular Probes	-	-	1: 200

The secondary antibodies employed were

A12c: Goat anti Mouse IgG (H+L) coupled to Alexa Fluor^{TM} 488, 5 µg/ml in 1% BSA in PBS, 1:400 (Molecular Probes)

A16c: Goat anti Mouse IgG (H+L) coupled to Alexa Fluor^{TM} 350, 5 µg/ml in 1% BSA in PBS, 1:200 (Molecular Probes)

Goat anti mouse IgG conjugated to TRITC (Sigma), 1: 200

2.2. Methods

2.2.1. Molecular biological methods

2.2.1.1. Quantification of DNA

DNA concentrations were determined photometrically. The maximum photometric absorption of RNA and DNA in solution is at 260 nm. The concentration of DNA in a diluted solution is calculated using the molar extinction co-efficient (ε at 260 nm = 50 µg/µl) as given below

OD_{260} × dilution factor × 50 µg/µl = Concentration of DNA µg/µl

2.2.1.2. Restriction endonuclease digestion of DNA

Restriction enzymes were purchased from New England Biolabs and the reaction was set up using the appropriate amount of enzyme in units as recommended by the manufacturer and 2.0-5.0 µg DNA was used for a preparative digestion. The reaction was performed in

the suitable 1× buffer provided by NEB. The reaction mix was usually incubated for 1-2 hrs at 37°C if not otherwise indicated, as recommended by the manufacturer.
For double digestions involving two non-compatible enzymes, temperature inactivation of the primary enzyme was done before subsequent digestion.

2.2.1.3. Ligation

The ligation reaction covalently links the phosphodiester bonds between two fragments of DNA using the ligase enzyme. DNA ligase from T4 Bacteriophage (Boehringer, NEB) was employed in this work to link vector DNA with the insert DNA. Appropriate molar ratios (usually 1:3) between vector and insert DNA were used in a 15 µl reaction with 1 µl ligase and 1× T4 ligation buffer. The reaction mixture was incubated at RT for 1 hour.

2.2.1.4. Transformation in competent cells

The ligated DNA was transformed in chemically competent cells; *E. coli* strain XL1 Blue was used for this purpose. Cells were incubated for 30 minutes on ice with the ligation mixture, heat shock at 42°C was applied for 2 minutes and the cells were regenerated by adding 0.8 ml 2×YT medium and incubated at 37°C for 1 hour. The cells were pelleted down by centrifugation at 6000× g, resuspended in 100 µl medium and plated onto 2×YT agar medium containing appropriate antibiotics.

2.2.1.5. Polymerase chain reaction (PCR)

PCR is a technique employed for rapid *in vitro* amplification of DNA. The amplification is done using the temperature resistant DNA polymerase, free nucleotides, a primer or the starter sequence which specifically binds to the template strand and initiates the amplification. Three major steps involved in the reaction are, the denaturation of the template DNA at high temperatures (95°C), annealing or primer binding to the template strand at 55°C – 60°C and finally an extension step at 72°C for the actual amplification. For exponential increase of amplified DNA the steps are repeated for 25-30 cycles.
DNA polymerase from the thermophilic bacteria like *Thermus aquaticus* (Taq) does not have the 3' to 5' exonuclease or "proof reading" property to prevent mutations. The DNA polymerases from *Pyrococcus furiosus* (Pfu) and *Thermococcus litoralis* (Tli) are used instead.

The standard PCR reaction mixture contained template plasmid DNA (ng concentration), primers specific to the template strand (25 pmol), free nucleotides or dNTP's (2.5 mM), $MgCl_2$ (0.5 – 2.5 mM), 1× PCR buffer and 2.5-5.0 units of DNA polymerase (Taq/Tli/Pfu) in 25 – 50 µl reaction volume.

2.2.1.6. Site directed mutagenesis

The QuikChange™ site directed mutagenesis kit from stratagene was employed to introduce mutations in vinculin.

Oligonucleotide sequences with respective bases exchanged were used in a PCR reaction with the plasmid DNA and PfuTurbo DNA polymerase in 50 µl reaction volume. The PCR products were digested with the restriction enzyme Dpn1 at 37°C for one hour. Dpn1 specifically digests the methylated DNA used as template and retains only the newly synthesized DNA. The reaction mixture was then transformed in XL1 Blue competent cells and plated on to 2×YT agar medium with appropriate antibiotic selection.

2.2.1.7. Preparation of plasmid DNA from bacteria

Plasmid DNA expressed in XL1 Blue cells was prepared by modified alkaline lysis method (Birnboim, 1983). Plasmid mini preparations were performed using the Nucleo Spin plasmid extraction kit from Macherey-Nagel GmbH, Düren, plasmid midi- and maxipreparations were performed using Qiagen columns (Qiagen) according to the manufacturer's recommendations.

2.2.1.8. DNA sequencing reaction

DNA Sequencing reactions were done with the ABI PRISM® Big Dye Reaction Terminator Cycle Sequencing Kit (Applied Biosystems) as per manufacturer's instructions. The sequencing reaction products were precipitated with ethanol and analysed on an ABI PRISM™ TM 310 Genetic Analyzer (Applied Biosystems). ABIPRISM-sequence files were aligned using Seqman (Lasergene software).

2.2.1.9. DNA extraction from agarose gels

DNA was recovered from agarose gel slices with the QIAex Gel Extraction Kit (Qiagen) as per manufacturer's instructions.

2.2.1.10. Cloning strategy – vinculin full length and tail domain constructs

The full length mouse vinculin cDNA amplified from mouse heart cDNA library in pACT (BD Biosciences) and cloned into pEGFP-C2 vector was obtained from Dr. Stefan Hüttelmaier. Sequencing analysis identified several additional mutations in the clone. There were five mutations which resulted in the amino acid replacements in the protein sequence, namely, E16V (Glutamate 16 exchanged to valine), R501Q, E565G, D812G, F842S. The phenylalanine 842 to serine exchange was considered very critical for the protein function since it was in the FP_4 motif involved in the ligand interactions. Comparison of protein sequence alignments of full length mouse vinculin, human vinculin and the cDNA clone eliminated the E16V, R501Q and D812G mutations, since the human vinculin also had the following replacements.

The full length mouse vinculin was subcloned into pCR Blunt vector and site directed mutagenesis was performed to revert back the E565G, F842S mutations. Additionally, a silent mutation of L858 was done to introduce a *Sac*I site for easier subcloning of tail domains (858-1066 AA) into full length vinculin (1-1066 AA). The pCR Blunt vector was modified to remove the *Sac*I site present internally and this vector was employed in further subcloning's with the vinculin tail domains.

The vinculin tail wild type and the mutants (858-1066 AA) were generated by PCR amplification, cloned into the pCRBlunt vector. The pQE 30 vinculin tail wild type clone with the *Sac*I site introduced at L858 was used for the subcloning of mutant tail domains. The pQE30 vinculin tail constructs were employed for the protein expression and purification. The full length vinculin wild type in pCR Blunt vector was digested with *Sac*I and *Sal*I (sequential digestion after heat inactivation) and the vinculin tail mutant inserts were ligated to obtain full length vinculin mutant constructs.

2.2.1.11. Cloning of vinculin head domain (D1)

Vinculin head domain D1 (1-258 AA) was generated by PCR amplification, cloned into the pCRBlunt vector and subcloned into a GST fusion vector pGEX 4T-1 (Amersham Biosciences) using *Eco*RI and *Sal*I restriction cloning sites for prokaryotic expression and purification.

2.2.1.12. Cloning of PIP5K α "kinase dead" mutant

The "kinase dead" mutant of PIP5K α which was a C-terminal deletion construct was generated by PCR amplification using the wild type PIP5K α, cloned into the pCR2.1 vector (Invitrogen) and subcloned using *Eco*RI ad *Sal*I restriction sites, into the pcDNA3 vector fused to a BiPro tag.

2.2.2. Biochemical methods

2.2.2.1. Protein estimation

2.2.2.1.1. Using molar extinction coefficient

Amino acids containing aromatic side chains (i.e., tyrosine, phenylalanine and tryptophan) exhibit strong UV-light absorption and the amino acid cystine absorption do not vary under native conditions. Thus, concentration of protein solutions under native conditions could be derived from their molar extinction coefficient or molar absorptivity as stated below.

Concentration (mg/ml) = Absorbance (OD_{280}) / E_M * Mol.wt

E_M (molar extinction coefficient) =a$E_{M,\ Tyr}$ + b$E_{M,\ Trp}$ + c$E_{M,\ Cys}$

Where a, b, c are the number of tyrosine, trytophan and cystine residues per mole of protein and $E_{residue}$ are the molar extinction of the residue at 280 nm ($E_{M,Tyr}$ = 5690, $E_{M,Trp}$= 1280, $E_{M,Cys}$ = 120).

2.2.2.1.2. Bicinchoninic acid (BCA) assay

The BCA™ Protein Assay kit (Pierce, IL) was used for total protein estimation as per manufacturer's recommendations.

2.2.2.2. Sodiumdodecylsulphate-Polyacrylamide Gel Electrophoresis (SDS-PAGE)

Sodiumdodecylsulphate-Polyacrylamide gel electrophoresis (SDS-PAGE) was performed with a protocol adapted from Laemmli (Laemmli, 1970). SDS-PAGE gels casted contained the separating and stacking regions with varying pH and 1mm spacers were used. 10% separating gels were mostly employed in this work. The protein solutions or cell lysates were diluted in 4× SDS sample buffer, boiled at 95°C for 5 minutes and loaded in the gels. "High molecular weight marker" (HMW) from Sigma was used to determine the molecular weight.

2.2.2.3. Coomassie-Blue-staining of protein gels

Gels were stained using 0.1% Coomassie R-250 Solution in 10% acetic acid and 25% isopropanol. For quick staining the gels were boiled with the staining solution in a microwave and 10 – 15 minutes incubation. Destaining was done using 10% acetic acid and 40% methanol at room temperature.

2.2.2.4. "Semi dry" Western blot

Proteins were transferred from the gels onto a nitrocellulose membrane using the semi - dry blotting apparatus from Biometra. The membrane, gel and whatmann filter papers were equilibrated in the glycine-methanol buffer (25 mM Tris pH 8.5, 150 mM Glycine, 10% Methanol) and the proteins were transferred from the gel (negative electrode) to the membrane (positive electrode) at 100mA per mini gel for 60 – 90 minutes. The efficiency of the transfer was monitored by staining the membranes with PonceauS solution (0.5% PonceauS (Sigma), 40% methanol, 15% acetic acid) and molecular weight marker bands were marked.

Membranes were blocked for 30 minutes to 1 hour at room temperature or at 4°C overnight in blocking buffer (4% dry-milk in TBS-T buffer (20 mM Tris-HCl pH 7.6, 140 mM NaCl, 0.1% Tween 20)). Afterwards, membranes were incubated for 1-1.5 hr at room temperature or at 4°C overnight in TBS-T buffer containing the primary antibody. Membranes were washed thrice for 10 minutes in TBS-T and incubated for 1 hour at room temperature in TBS-T buffer containing the secondary antibody, followed by another 4 washes as described above. Membranes were then incubated for up to 3 minutes with the chemiluminescence substrates in the ECL kit (Amersham Biosciences) and exposed to Hyperfilm ECL (Amersham Biosciences) for 30 seconds – 1 minute. Films were developed manually using the Kodak developer and fixing solutions.

2.2.2.5. CD Spectroscopy

Proteins were diluted to 0.05 – 0.1 µg/µl in phosphate buffer (20 mM NaH_2PO_4 pH 7.2, 0.5 mM EGTA) and measured using a 0.2 cm wide quartz cuvette in a spectropolarimeter (Jasco systems). The spectra was collected for 20 accumulations and used for analysis.

2.2.2.6. Graphic representation of vinculin tail domains

Graphic views of Vt (879-1061) based on PDB entry 1QRK were generated using SwissPDB viewer (http://www.expasy.ch/spdbv) and POVray 3.1 (http://www.povray.org) on a Linux platform (courtesy: Dr. Jochen Kuper)

2.2.2.7. Expression and purification of recombinant proteins

Recombinant proteins fused to "His tag" or "GST tag"was employed in this work whose expression and purification procedures are detailed below.

2.2.2.7.1. Expression of recombinant proteins

The recombinant proteins constructs Vt wild type and mutants in pQE 30 vector (His tag) and vinculin head domain (D1) in pGEX 4T-1 vector (GST tag) were expressed in the M15 strain of *E. coli* (see 2.1.5). The main culture (1-2 L) was prepared by inoculating 20 ml of pre culture in 2× YT medium containing kanamycin/ ampicillin resistance, 30 µg/µl L-Proline, 5 µg/µl Thiamine, 0,2 % Glycerine and incubated in a 37°C shaker (220 rpm). 1mM IPTG was used for protein induction in the culture medium when the OD at 600 nm reaches 0.5. The proteins were allowed to express for 3 hours and the cells were collected by centrifugation at 6500 rpm, 4°C.

2.2.2.7.2. Purification of His tagged protein using Ni-NTA agarose beads

The "His" tagged proteins were purified by affinity purification using Ni-NTA agarose which specifically binds to the 6× Histidine residues in N-terminal protein sequence. The cells collected from one litre of main culture were dissolved in 20 ml of lysis buffer (50 mM NaH_2PO_4 pH 8, 300 mM NaCl, 25 mM Imidazole, 0.5 % Tween 20 with fresh protease inhibitors, β-mercaptoethanol and 1 mg/ml lysozyme). The cells were subjected to ultrasonication for 30 seconds (5×) with 1 minute break in between the cycles. The cell debris was collected by centrifugation at 15000 rpm for 30 minutes at 4°C. 4 ml of Ni-NTA agarose was equilibrated in lysis buffer; the cell lysate supernatant was added to the beads and incubated on ice for 1 hour with periodic shaking. The beads were then subjected to the washing steps, twice in 10 ml of lysis buffer, twice in 10 ml of washing buffer (50 mM NaH_2PO_4 pH 6.0, 300 mM NaCl, 0.5 % Tween 20, 8.7 % Glycerine with fresh protease inhibitors, β-mercaptoethanol). A final washing step with elution buffer without histidine was also performed. The protein bound to Ni-NTA beads were eluted in

5× 1 ml fractions of elution buffer (50mM NaH_2PO_4 pH 6.7, 100mM KCl, 0.5mM EGTA, 25mM EDTA, 0.1% Triton X 100 with freshly added 150mM Histidine, protease inhibitors, β-mercaptoethanol). The fractions were spotted on a nitro cellulose membrane, stained with PonceauS to detect the presence of the protein in the eluate fractions. The fractions were then subjected to desalting procedure using the PD-10 gel filtration columns (Amersham Biosciences). The protein was finally eluted in phosphate buffer (50mM NaH_2PO_4 pH 7.2, 0.2mM EGTA with fresh protease inhibitors, β-mercaptoethanol) from the gel filtration column.

[Note: Protease inhibitors used were AEBSF, 0.2 M in H_2O (1:500), PepstatinA, 1 mM in Ethanol (1:500), Leupeptin, 10 mM in H_2O (1:500), Trasylol, 2.8 mg/ml in H_2O (1:500)]

2.2.2.7.3. Purification of GST fusion protein using glutathione sepharose beads

The GST fusion proteins were purified using the glutathione sepharose beads which have specific binding affinity to Glutathione S-transferase linked to the protein. The cells collected from 1litre of main culture were dissolved in 20 ml of 1× PBS (140mM NaCl, 2.7 mM KCl, 10mM Na_2HPO_4, 1.8mM KH_2PO_4 (pH 7.4) with fresh protease inhibitors, β mercaptoethanol and 1 mg/ml lysozyme). The cells were subjected to ultrasonication for 30 seconds (5×) with 1 minute break in between the cycles. The cell debris was collected by centrifugation at 15000 rpm for 30 minutes at 4°C. Two ml of glutathion sepharose 4 super flow (Amersham Biosciences) was equilibrated in 1× PBS, the cell lysate supernatant was added to the beads and incubated in a shaker at 4°C. The beads were washed thrice with 1× PBS containing fresh protease inhibitors. The protein was eluted in 5× 1 ml fractions of elution buffer (50mM Tris-HCl pH 8.0, 10mM reduced glutathione). The fractions were then processed as described above (2.2.2.7.2).

2.2.2.7.4. Concentration and lyophilization of purified proteins

Protein concentration was estimated by methods described above (2.2.2.1.), the solution was concentrated using the Millipore protein concentrator's with 10kDa molecular weight cut off if necessary or the protein solution was diluted to obtain a final concentration of 1 mg/ml, lyophilized and stored at -80°C.

2.2.2.8. Sucrose-loaded large unilamellar vesicle (SLV) pull down assay

Sucrose-loaded large unilamellar vesicles (SLVs) were generated using a mini-extruder

(Avanti Polar Lipids, Inc.) according to manufacturer's instructions, mixed with Vt protein and sedimented. In brief, vesicles containing phospholipids PC, PS (45%) (Sigma), and PIP_2 (7%) (Merck Biosciences) from bovine brain, in molar ratios 4.8:4.5:0.7, were prepared by solubilizing dried phospholipid films (dried using nitrogen gas) in buffer 1 (600 mM sucrose, 100 mM NaCl, 40 mM Tris-HCl pH 7.5 and 3 mM $MgCl_2$).Vesicles were subjected to repeated freeze-thaw cycles (5 times) and thereafter to extrusion (11 times) using 0.2 μm filters in a mini-extruder. Vesicle suspension was diluted 1:5 in buffer 2 (100 mM NaCl, 40 mM Tris-HCl pH 7.5, 3 mM $MgCl_2$) and vesicles were collected by high-speed centrifugation, 100000×g for 30 minutes in an airfuge (Beckman Instruments). Vesicles were washed again and finally suspended in buffer 2 (1 mg/ml total lipid). Proteins were diluted in buffer 2 (5 μM protein, final concentration), pre-centrifuged at 20000×g for 15 minutes to remove any protein aggregates and incubated with SLVs (0.5 mg/ml final concentration) at 37°C for 15 minutes. After incubation, protein-vesicle mixtures were centrifuged at 20000×g for 15 minutes. Pellet and supernatant fractions were separated and proteins retrieved from supernatants by methanol /chloroform precipitation (Wessel and Flügge, 1984). Pellet and supernatant were subjected to SDS-PAGE and Coomassie stained bands analysed by densitometry (E.A.S.Y. RH apparatus and E.A.S.Y. Image plus Software; Herolab, Inc.). Statistical significance of differences in all data sets (unless stated otherwise) was tested by variance analysis (post hoc Bonferroni/Dunn) using Statview 5.0 ® (SAS Institute, Inc.).

2.2.2.9. "High speed" actin cosedimentation assay

The interaction of Vt variants with actin filaments was tested by high-speed cosedimentation at various molar ratios of actin and vinculin tail. Pre-polymerization of actin was performed by diluting actin in pre-polymerization buffer (20 mM Tris pH 7.4, 100 mM KCl, 2 mM $MgCl_2$ with freshly added 1 mM ATP and 0.2 mM DTT) and one hour incubation at 37°C. Pre-polymerized actin was used at 3μM final concentration in the assay. Varying concentrations of Vt (0.6 – 3 μM) diluted in F-actin buffer (20 mM Tris pH 7.4, 25 mM KCl, 2 mM $MgCl_2$ with freshly added 1 mM ATP and 0.2 mM DTT) were incubated with pre-polymerized actin for one hour in a 37°C shaker. The reaction mixture was centrifuged at 100000×g for one hour in an airfuge (Beckman Instruments).

Pellets and supernatants were analysed by densitometry of Coomassie stained gels as described above (2.2.2.8.).

2.2.2.10. GST pull down assay for vinculin head –vinculin tail interaction

The interaction of Vt variants with the Vinculin head domain (D1, amino acids 1-258) fragment was tested in a GST pulldown assay. GST-Vh (D1) protein bound to glutathione sepharose beads was equilibrated in phosphate buffer (50 mM NaH_2PO_4, 0.2 mM EGTA) and incubated with Vt proteins (6 μM) for 30 minutes at 37°C. Beads were then washed three times with buffer. Pellet fractions were analysed on Coomassie stained SDS-PAGE gels.

2.2.3. Cell biological methods

2.2.3.1. Cultivation of cells

All the cell culture media and additives were purchased from Gibco BRL and Sigma.

The composition of culture medium used to cultivate the different cell lines are listed below.

B16-F1 medium: B16-F1 mouse melanoma cells (ATCC CRL-6323) were grown in DMEM, 4.5 g/l glucose (Invitrogen, Germany) with 10 % FCS (PAA Laboratories, Austria) and 2mM glutamine at 37°C and 7 % CO_2. Penicillin/Streptomycin was used in the medium if needed.

G418 (1 mg/ml) was used in the medium to cultivate the stable cell populations expressing GFP vinculin wild type and mutants.

NIH 3T3 medium: NIH 3T3 murine embryonic fibroblasts (ATCC CRL-1658) were maintained as above but with 10 % FBS (Sigma, Germany).

C2C12 medium: C2C12 mouse myoblasts (ATCC CRL-1772) were cultured in DMEM, 4.5 g/l glucose (PAA Laboratories, Austria) with 10% FCS (PAA Laboratories, Austria) at 37°C and 10 % CO_2.

MEF medium: The vinculin null fibroblasts MEF -/- were grown in DMEM, 4.5 g/l glucose (PAA Laboratories, Austria) with 10 % FCS (PAA Laboratories, Austria), 5 μl β-mercaptoethanol at 37°C and 10 % CO_2. The control fibroblasts MEF+/+ were cultivated as above without β-mercaptoethanol.

2.2.3.2. Transient transfection of cells

Transfections were carried out with SuperFect (Qiagen)for B16-F1 or with FuGENE6 (Roche) for NIH 3T3, C2C12, MEF's according to manufacturers' protocols.

In brief, 1 µg DNA was mixed with 300 mL of DMEM, to which 6 µL of SuperFect were added and vortexed immediately for 10 seconds. The reaction was left for 20 to 40 minutes at room temperature. 1.8 ml of growth medium was added to the reaction mix and the complete mix was added onto cells in a 3.5 cm diameter dish or 0.5 ml to a well in 12 well plates.

47µl DMEM were mixed with 3µl FuGENE6 and 1µg plasmid DNA and incubated for 30 minutes at room temperature. The mixture was added to cells in a 3.5 cm diameter dish with freshly replaced media and incubated at 37°C. The mixture was scaled-up accordingly for 10 cm plates or increased number of cells.

2.2.3.3. Generation of stable B16-F1 populations expressing GFP vinculin constructs using FACS

B16-F1 cells were transfected with GFP vinculin wild type and mutants and the cells were allowed to express the protein for 12 – 16 hours. The cells were then trypsinized and sorted with a fluorescence associated cell sorter (Cytomation Inc, USA). The sorted cells were cultivated in the presence of G418 (1 mg/ml) selection pressure for a week to 10 days. The cells were subjected to a second round of sorting and grown under the selection pressure and several aliquots were frozen for future use.

2.2.3.3.1. Protein expression levels in the B16-F1 stable cell populations

The expression levels of GFP vinculin wild type and variants in different passages (1-5) were analysed in a semi-quantitative Western blot of the cell lysates prepared by lysis of cells in one confluent 10 cm plate with 300-400 µl of 4× SDS sample buffer (2%SDS, 350mM Tris HCl pH 6.8, 10% Glycerin, 8% β-mercaptoethanol, 0.05% Bromophenol blue). The blots were stained using vinculin antibody (hvin) which detects both endogenous vinculin (116kDa) and the exogenous GFP vinculin (~ 141kDa). The blots were subjected to densitometric analysis to determine the total vinculin and ratios between endogenous and recombinant vinculin expression levels.

2.2.3.4. Culture of cells on coverslips for microscopic analysis

For microscopic analyses, cells were seeded onto 12 mm or 15 mm glass cover slips that had been pre treated in a mixture of 60% ethanol and 40% concentrated HCl for 30 minutes to 3 hours in a shaker. Coverslips were then extensively washed in water and allowed to dry separately on Whatman filterpaper overnight and were sterilized by autoclaving or by exposure to UV-light for 45 minutes. Glass coverslips were coated with 50 µg/ml fibronectin (Roche) for 1 to 2 hours at room temperature or overnight at 4°C or 25 µg/ml laminin (Sigma) for 50-60 minutes at room temperature as indicated.

2.2.3.5. Fixation procedures and permeabilization of cells

For immunostaining, cells were fixed with 4% para formaldehyde (PFA) in PBS for 5 – 10 minutes. Cells were then extracted with a mixture of 0.1% Triton X-100 and PFA for 45 seconds for B16-F1 cells and 5-7 minutes for C2C12, NIH 3T3 and MEF's. The cells were thoroughly washed thrice with 1× PBS and stored at 4°C until they were stained.

2.2.3.6. Immunolabelling, fluorescence microscopy and image processing

To avoid non-specific interactions, cells were blocked prior to antibody staining with 1% BSA in PBS for 20 minutes. For antibody staining, coverslips were incubated with 50 µl of primary antibody solution on parafilm for 1-2 hours at room temperature or 45 min at 37°C in a humid chamber, followed by 3 washes in 1× PBS. Staining with secondary antibody with or without addition of fluorescently coupled phalloidin was carried out for 30 – 45 minutes at 37°C in a humid chamber. Coverslips were mounted in 5 µl Mowiol 4-88 (Calbiochem) supplemented with n-propylgalate (2.5 µg/ml) on microscope glass slides, dried and stored in the dark at 4°C until analysis.

Cells were observed on an inverted microscope (Axiovert 135TV, Zeiss) equipped for epifluorescence and phase-contrast microscopy, using 100x NA 1.3 neofluar objective, as well as 63x and 40x.NA 1.3 neofluar objectives, with 1.6 optovar intermediate magnification. Electronic shutters (e.g. Uniblitz Electronic 35mm shutter including driver Model VMMD-1, BFI Optilas) to allow computer-controlled opening of the light paths were attached to the microscope and a filterwheel (e.g. LUDL Electronic Products LTD, SN: 102691 and driver SN: 1029595) to enable two-colour epi-fluorescence in combination with appropriate dichroic beam splitters and emission filters (Chroma Technology Corp., Rockingham, USA). Tungsten lamp (Osram, HLX64625, FCR 12V,

100W) was used for phase contrast optics and mercury lamp (HBO 100W/2, Osram) for epifluorescence. The immersion oil (refraction index of 1.5) was obtained from Zeiss
Data were acquired with a back-illuminated, cooled charge-coupled-device (CCD) camera (Princeton Research Instruments TKB 1000x800, SN: J019820; Controller SN: J0198609) driven by IPLab software (Scanalytics Inc.). Data were stored as 16-bit digital images and analysed on a Power Macintosh G4 using IPLab, Scion Image 1.62 (Scion) or Adobe Photoshop 6.0 software.
Alternatively the cells were examined in a Zeiss Axiovert S100TV microscope using a 100x Plan-Neofluar oil objective (NA 1.3) or 63x Plan-Neofluar oil objective (NA 1.25) and photographed with a TE/CCD-1000 TKB camera (Princeton Scientific Instruments). Images were acquired and processed using MetaMorph software (Universal Imaging Corporation) followed by Adobe Photoshop 6.0 software.

2.2.3.7. Migration assay in 3D collagen matrix

The migratory capacity of the B16-F1 populations expressing GFP-vinculin variants on 3D collagen matrix was analysed by timelapse video microscopy as described (Niggemann *et al*., 1997). In brief, cells were harvested in trypsin-EDTA, and 6 x 10^4 cells in 50 µl medium were mixed with 100 µl of a carbonate-buffered collagen solution (1.67 mg/ml bovine dermal type I collagen, commercially available as vitrogen from Cohesion Technologies, Inc).
The suspension was filled into self-constructed chambers and the collagen was allowed to polymerize at 37°C for 30 minutes. Migration of the cells was recorded for 15 hours in a 1920 fold timelapse mode (one hour equalent to 1920 hours). The paths of 30 randomly selected cells were calculated in 15 minutes step intervals by computer-assisted cell tracking using custom-made software (Niggemann *et al*., 1997) and migratory parameters (number of motile cells, velocity, persistence) were calculated from these data.

2.2.3.8. Live cell imaging of B16-F1 stable populations

The microscope Axiovert 135TV, Zeiss was employed as described in section 2.2.3.6. Due to high probability photo-damage and bleaching by mercury lamps, for the live cell imaging a tungsten lamp was employed for epifluorescence and transmitted illumination. Cells were observed in an open chamber (Warner Instruments, Reading, UK) with a

heater controller (model TC-324B, SN: 1176) at 37°C. Ham's F12 HEPES-buffered medium (Sigma) including complete supplements of the regular growth medium (see 2.2.3.1.) was used for B16-F1 cells. During live imaging, the medium was changed every 30 minutes.

2.2.3.9. Adhesion and Spreading assay

Twelve well plates (Nunc) were coated with either laminin (25 µg/ml) or fibronectin (50 µg/ml) (Sigma) and incubated at room temperature for 1 hour. Alternatively, they were coated with collagen I (1 mg/ml; Cohesion Technologies, Inc.) and allowed to polymerise for 3 hours. B16-F1 cells expressing GFP-vinculin variants were harvested in trypsin-EDTA. 1.5 x 10^4 cells were seeded to each well.

For analysis of adhesion, cells were allowed to attach for 10 minutes at 37°C on laminin and fibronectin or 90 minutes on collagen. Non-adherent was removed by washing wells three times with PBS. Cells were fixed in 4% PFA in PBS. Number of cells in 10 random microscopic fields (450-550 cells) was counted using a Nikon Eclipse TE 300 with a 10x Plan-Fluar objective (NA 0.3).

For analysis of spreading, cells were treated as described above and allowed to attach for 15 minutes at 37°C on laminin or fibronectin. After washing and fixation, cells were stained with TRITC-Phalloidin (Sigma) and mounted on slides. Cells were examined in a Zeiss Axiophot microscope using a 40x Plan Neo-Fluar oil objective (NA 1.3) and photographed with a RTE/CCD – 1300 Y/HS camera (Roper Scientific). Three sub-populations of cells were counted, spread cells with clear peripheral lamellipodia, non-spread cells, which were just attached, and ambiguous cells that fell in neither of the two categories.

2.2.3.10. Fluorescence recovery after photo bleaching (FRAP)

B16-F1 cells were microinjected (InjectMan NI 2; Eppendorf) with constructs encoding GFP-vinculin-wt or the LD mutant. Constructs were allowed to express for 3 hours before mounting coverslips into a chamber containing gassed growth medium. The chamber was placed on a temperature-regulated 37°C microscope stage 15 minutes before viewing. Time-separated confocal 12-bit images were collected using a Zeiss LSM 510 META confocal laser scanning microscope system with a 63x Plan-Apochromat oil

objective (NA 1.4). GFP was excited with the 488 nm line of the Argon laser and reflected and emitted light separated using a 470-500 nm bandpass filter (for interference reflection microscopy) and a 505 nm longpass filter (for viewing GFP emission). Linescans were performed with four-fold averaging per pixel. When bleaching, the 488 nm laser line output was set to 100 % using 50 iterations. Two images (lines) were scanned prior to bleaching to determine the pre-bleach intensity of GFP-vinculin. After bleaching, linescans were collected for 3 minutes and stacked together to form a 2D image using the Lucida Image Analysis package (Kinetic Imaging, Inc.), a so-called kymograph, where the x-axis is distance along the linescan, and the y-axis represents time with t=0 at the top (Courtesy: Dr. Mark R.Holt).

2.2.3.11. Retrograde sliding of focal adhesions

To determine speed of focal adhesion translocation, adhesions in timelapse sequences were manually tracked using the Motion Analysis package (Kinetic Imaging, Inc). The software calculated the speeds after appropriate calibration. Fluorescence recovery in timelapse FRAP sequences was analysed using the Lucida Image Analysis package (Kinetic Imaging, Inc). Since focal adhesions had a tendency to translocate, it was not possible to perform a simple spot analysis. Instead, kymographs were produced along the axis of the adhesion sites and the direction of translocation. Five linescans were then taken along the kymograph time axis taking into account any translocation. The average of this was normalized with respect to the initial fluorescence intensity. Normalized values were subtracted using the first post-bleach intensity, which also resulted in background subtraction.

The data were then inversely plotted to produce a straight-line graph with positive gradient. The x-intercept was used to determine the time constant for fluorescence recovery, i.e., the time taken to recover to a level of 50%. Statistics of data in this paragraph were performed applying an unpaired two-tailed *t* test (with Welch correction) using InStat3 ® (GraphPad Software, Inc.) (Courtesy: Dr. Mark R.Holt).

3. Results

3.1. Design and cloning of various recombinant protein constructs

3.1.1. Cloning of full length vinculin and vinculin tail domains

The structural and functional role of vinculin in the regulation of adhesion sites was studied using recombinant protein constructs. Prokaryotic and eukaryotic expression constructs were employed for biochemical and cellular characterization of the protein. To analyse the involvement of acidic phospholipids (PIP2) in the regulation of vinculin, expression constructs harbouring mutations in the putative lipid binding sites were generated by site directed mutagenesis.

The full length "wild type" vinculin clone comprising the amino acid sequences 1-1066 was derived from a cDNA clone provided by Dr. Stefan Hüttelmaier. Sequencing analysis of this clone identified several mutations which were reverted back by site directed mutagenesis (Refer to chapter 2.2.1.10.). The "wild type" tail domain construct comprising the amino acid sequences 858-1066 was generated by PCR amplication of full length vinculin. (Refer to chapter 2.2.1.10.).

The crystal structure of vinculin tail describes the stretch of arginines and lysines in the basic collar and basic ladder to be the putative PIP2 binding motifs (Bakolista *et al*; 1999). These arginines and lysines were the potential candidates for the target mutations to obtain a lipid binding deficient vinculin mutant. Three different mutant tail domains carrying point mutations in the PIP2 binding motifs were constructed by site directed mutagenesis in the Vt wild type. The mutant carrying point mutations in the C-terminus (basic collar), which had two amino acids exchanged to glutamine (RK 1060/61 to QQ) was named as the **CT** mutant (Vt-CT), another mutant carried the point mutations in the Helix3 (basic ladder), which had four amino acids exchanged to glutamine (KK 952/956 to QQ and RK 963/966 to QQ) was named as the **H-3** mutant (Vt-H-3). The third mutant carried the combination of both CT and H-3 mutations and was named as the **LD** (**L**ipid binding **D**eficient) mutant (Vt-LD) which had totally six amino acids exchanged to glutamine (Figure 3.1). In addition to all the above mutants, a C-terminal deletion construct, similar to one described earlier (Bakolista *et al*; 1999), named as Δ1052, lacking the final 14 amino acids was also constructed to serve as an internal control for

the biochemical characterization of the Vt domains. In the full length "wild type" vinculin construct, the mutant tail domains were exchanged against the wild type domain using appropriate restriction endonuclease digestion, which allowed easier subcloning of the mutants into full length vinculin (also see cloning strategy in chapter 2.2.1.10.)

Vinculin tail (Vt 858-1066) wild type and mutants were cloned in the prokaryotic expression vector pQE 30 for protein expression and employed in the biochemical characterization. Full length vinculin constructs cloned in the GFP fusion vector pEGFP-C2 were used for cellular expression and phenotypic characterization.

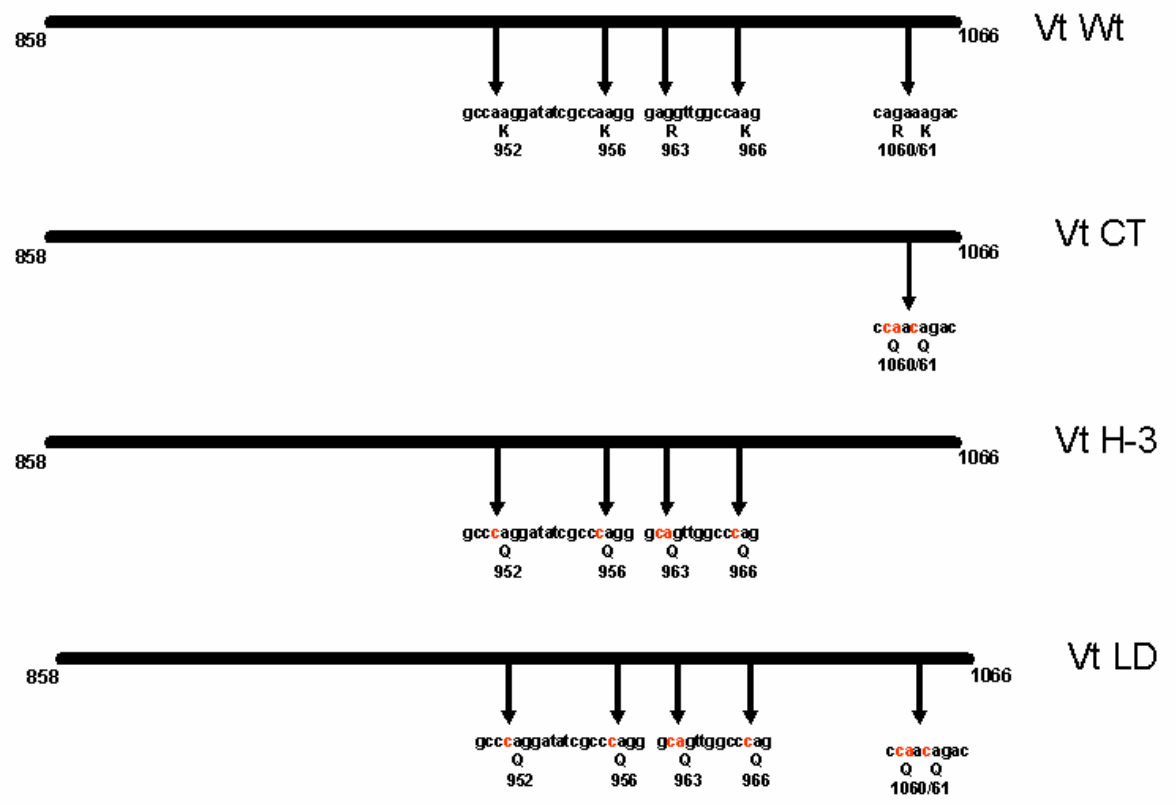

Figure 3.1: Schematic representation of wild type and mutant tail domains.
A) Vt -wt representing the conserved sequences coding for the lysines and arginines (K/R) in the CT and H-3 lipid binding sites.
B) Mutant Vt -CT sequences with lysine and arginine (R1060/K1061) both exchanged to glutamine (Q). Altered sequences are shown in red.
C) Mutant Vt -H-3 sequences with one arginine (R963) and three lysines (K952/K956/K966) exchanged to glutamine (Q). Altered sequences are shown in red.
D) Mutant Vt -LD with the combination of both CT and H-3 mutations. Altered sequences are shown in red.

3.1.2. Cloning of vinculin head domain (D1)

Vinculin head domain (D1), the N-terminal 258 amino acids comprising the vinculin tail and talin binding sites was amplified by PCR and cloned into pGex 4T-1, a GST fusion vector, for protein expression and biochemical analysis (Refer to chapter 2.2.1.11.).

3.1.3. Cloning of mouse PIP 5-kinase α "kinase dead" (KD) mutant

Murine PIP 5-kinase α clone (Rozelle *et al*, 2000) was used to generate the "kinase dead" form of PIP5-kinase α (1-308 amino acids), a C-terminal deletion construct created by PCR amplification, fused to BiPro tag (Rudiger *et al*, 1997) for antibody recognition and subcloned into the eukaryotic expression vector pcDNA3.

3.2. Protein properties and surface model of the mutant vinculin tail domains

Protein properties of the Vt wildtype and mutants were predicted using the Laser gene navigator software. The software calculated the molecular weight, isoelectric point, changes in secondary structure (helical wheel representation) which could help in differentiating the wild type from the mutants. Loss of positively charged residues was implicated by a decrease in pI of the tail domains (Table 3.1.). Graphic views of solvent – accessible surfaces of Vt $_{879\text{-}1061}$ wild type and Vt $_{879\text{-}1061}$ LD indicate the difference in electrostatic potential as a consequence of the amino acid exchanges, basic patches (blue) are changed to acidic (red) or neutral (white) around the basic collar and basic ladder (Figure 3.2.)

Table 3.1: Isoelectric points of vinculin tail domains

Vt Domains	Isoelectric point
Wildtype	8.54
CT	7.90
H-3	7.06
LD	6.54

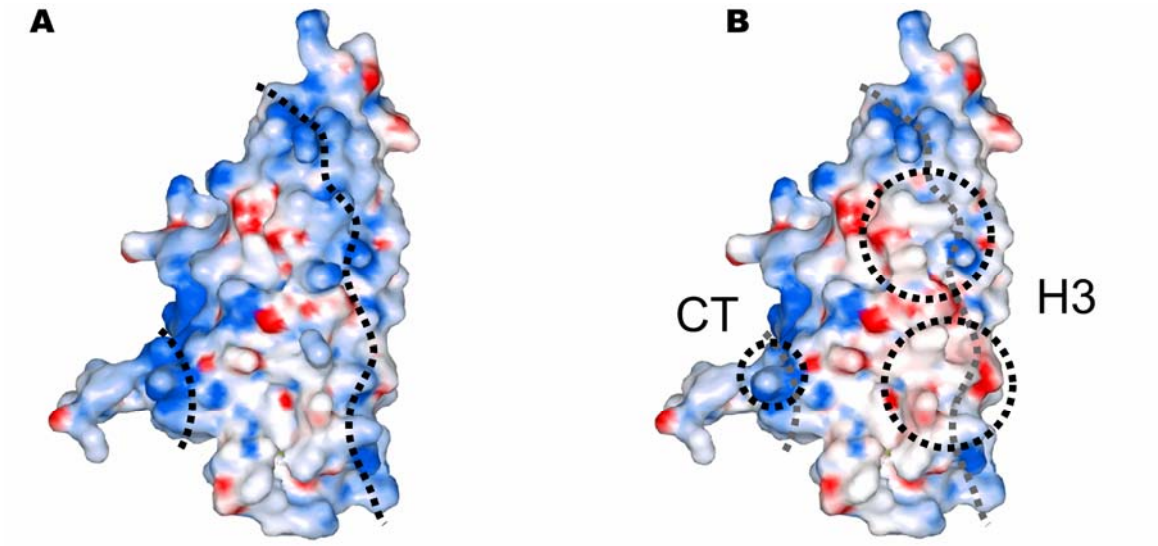

Figure 3.2: Surface models of Vt $_{879\text{-}1061}$ wild type and LD
Solvent-accessible surfaces of Vt $_{879\text{-}1061}$ wild type **(A)** and Vt $_{879\text{-}1061}$ LD **(B).** Coloring reflects the electrostatic potential, basic patches in blue and acidic in red. The two lipid binding sites, basic collar and basic ladder, are indicated by dotted lines. In Vt $_{879\text{-}1061}$ LD **(B)** The areas carrying point mutation of the C-terminus (CT) and helix 3 (H-3) are circled. (Courtesy: Dr. Jochen Kuper)

3.3. Protein expression and purification

Vinculin tail domains (wild type and mutants) were expressed from pQE 30, a prokaryotic expression vector with 6X His tag for recombinant protein expression and affinity purification using Ni-NTA agarose. These constructs also had N-terminal sequences coding for a "Flag epitope" which could be recognized by flag antibody (M2) for easier detection in Western blot. The His tagged fusion proteins were expressed in the M15 strain of *E. coli* and purified using Ni-NTA agarose as described in section 2.2.2.7. The purified proteins were analysed on SDS-PAGE and also by Western blot using a flag antibody (M2).

The vinculin head domain (D1) was expressed from pGEX 4T-1, for expression of a GST fusion protein in the M15 strain of *E. coli* and purified using glutathione-sepharose beads. The purified protein was analysed by SDS-PAGE and Western blot using a GST antibody (also see chapter 2.2.2.7.).

The protein concentration was estimated using the BCA method (Chapter 2.2.2.1.2.) and diluted to a final concentration of 1 mg/ml in phosphate buffer (50mM NaH_2PO_4, 0.2mM EGTA, pH 7.4), lyophilized and stored at -80° C.

Table 3.2: List of vinculin tail domain and vinculin head domain constructs

Construct	Amino acids	Tag	Mol.Wt Calculated (apparent) in kDa
Vt wt	858 – 1066	His, Flag (N-terminal)	25.9 (~30)
Vt CT	858 – 1066	His, Flag (N-terminal)	25.8 (~30)
Vt H-3	858 – 1066	His, Flag (N-terminal)	25.8 (~30)
Vt LD	858 – 1066	His, Flag (N-terminal)	25.8 (~30)
Vt Δ 1052	858 – 1052	His, Flag (N-terminal)	24.0 (~29)
Vh D1	1 - 258	GST	58.8 (~62)

3.4. CD spectroscopic analysis of Vt domains

Circular Dichroism (CD) is observed when an optically active matter absorbs left and right hand polarized light differently, the difference in the absorption is very small corresponding to the ellipticity of 1/100th of a degree which is measured by a CD spectropolarimeter. CD Spectroscopy is a method to analyse the basic secondary structure of a polypeptide chain or protein, since the absorption spectra for each type of secondary structure, (α helix, β pleated, coils) are different. Recombinant proteins are analysed by CD spectroscopy to confirm the proper folding of the protein and that the secondary structure is preserved. CD spectra were processed using the "Spectra Analyzer" and "DicroProt" software (Jasco Systems) which calculates the molar ellipticity and percentage composition of α helices, β sheets and coiled-coils in each molecule.

The CD spectra of Vt wild type and LD in the far UV region showed absorption minima at 208 nm and 226 nm approximately which was typical for protein with an α helical structure. CD spectra of vinculin LD confirmed the maintenance of the secondary structure and proper folding of the protein (Figure 3.3.).

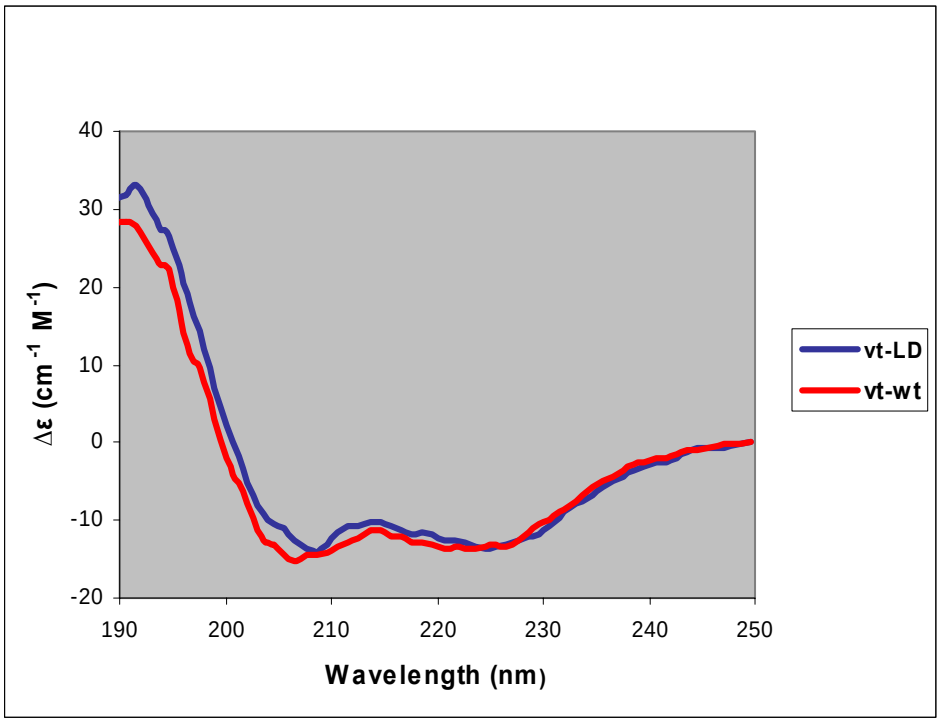

Figure 3.3: CD Spectroscopic analysis of Vt domains

CD Spectra of Vt wild type and Vt LD in the far UV region showing absorption minima at approximately 208 nm and 226 nm

I. Biochemical analyses

3.5. Biochemical characterization of Vt wild type and mutants

The purified vinculin tail domains were subjected to various biochemical analyses to investigate their ability to bind acidic phospholipids, to co-sediment with actin and to confirm intact intramolecular head-tail interaction. All these assays were aimed towards the analysis and comparison of Vt wild type and mutant proteins.

3.5.1. Effect of the Vt mutations on the binding affinity to acidic phospholipids

Binding to acidic phospholipids such as PIP2 is considered a critical step in the activation of cytoplasmic vinculin, leading to its interaction with protein ligands (Hüttelmaier *et al*; 1998) and subsequent targeting of vinculin to focal adhesions (Gilmore and Burridge, 1996). The lipid binding characteristics of Vt wild type and all three mutants were tested in a pull down assay, using sucrose-loaded large unilamellar vesicles (SLVs). Vesicles were generated in a mini-extruder (Avanti polar lipids Inc, USA) and contained

phosphatidylcholine (PC) and acidic phospholipids phosphatidylserine (PS) and PIP2 in the ratio of 4.5: 4.5: 1. This composition was selected to mimic lipid conditions at the inner leaflet of the plasma membrane and also to avoid electrostatic sequestration as a result of highly negatively charged surfaces, which are characteristic for pure PIP2 micelles or PS vesicles. Pure PC vesicles were used as a control. The lipid vesicles were incubated with Vt proteins and sedimented. Vt protein in the pellet (that is bound to vesicles) and in the supernatant (unbound) were detected in Coomassie-stained gels and analysed by densitometry (refer to section 2.2.2.8.). Binding of the Vt wild type to vesicles was compared to Vt-Δ1052, which was earlier reported to display a reduced binding to phospholipids (Bakolitsa *et al*, 1999) and to other mutant tail domains. Vt mutants Vt-Δ1052, Vt-CT and Vt-H3, which all have one lipid binding site altered, showed partial loss of lipid binding (<50% compared to wt) (Figure 3.4.). Mutations of both the lipid binding sites in Vt-LD resulted in residual binding, comparable to the binding obtained for all Vt proteins when using control PC vesicles
(8-10%, white line). The combination of mutations hence abolished the binding of Vt-LD to acidic phospholipids. (Figure 3.4.) Differences in binding were observed in three independent experiments and confirmed by variance analysis ($p<0.05$; Bonferroni/ Dunn, Statview 5.0, 1998).

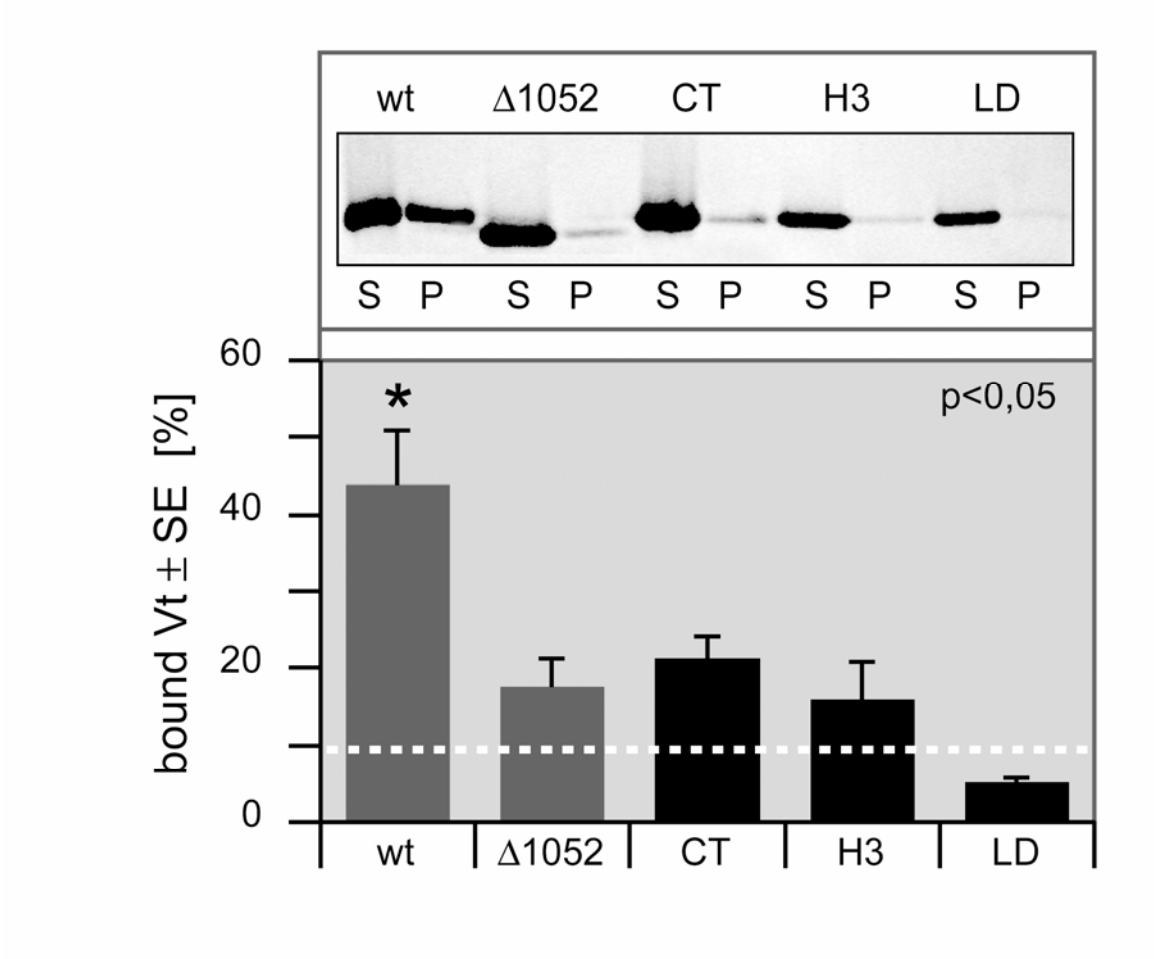

Figure 3.4: SLV pull down assay with Vt wild type and mutants
Top: Coomassie-stained gel with pellet (P) and supernatant (S) fractions of Vt wild type and other mutants.
Bottom: The columns represent the percentage of vesicle-bound Vt protein (mean ± s.e; n=3). Binding of mutant tails to acidic phospholipids is decreased compared to wild type. The white line indicates the binding to control PC vesicles.

3.5.2. Binding to filamentous actin is preserved in the Vt mutant proteins

F-actin is one of the major ligands that bind to the vinculin tail, whose binding is influenced by the intra molecular head-tail interaction and also by the acidic phospholipid PIP2 (Hüttelmaier *et al*, 1998, Johnson and Craig, 1995). In order to analyse the consequence of the mutations in the vinculin tail on its actin binding, the proteins were subjected to a high speed co-sedimentation assay using pre-polymerized actin. Vt proteins were incubated with pre-polymerized actin and sedimented at high speed (100000×g). Pellet and supernatant fractions were subjected to SDS PAGE, stained and analysed by densitometry. The assay was performed using two different molar ratios of

actin:vinculin, 5:1 (Fig 3.5A) and 2:1 (Fig. 3.5B). Cosedimentation of vinculin tail proteins with F-actin at molar ratio of actin: vinculin = 5:1 was > 95% for the wild type and all mutants, suggesting that actin binding is preserved in all the mutants.

At a molar ratio of actin: vinculin = 2:1, the binding of both Vt-H-3 and Vt-LD was decreased by 35% as compared to Vt wild type and Vt-CT. This ratio represents maximal binding capacity of F-actin which is 0.3 – 0.5 moles of vinculin tail per mole of actin. (Johnson et al; 1995) and is not considered physiologically relevant (also refer to chapter 4.2. for details).

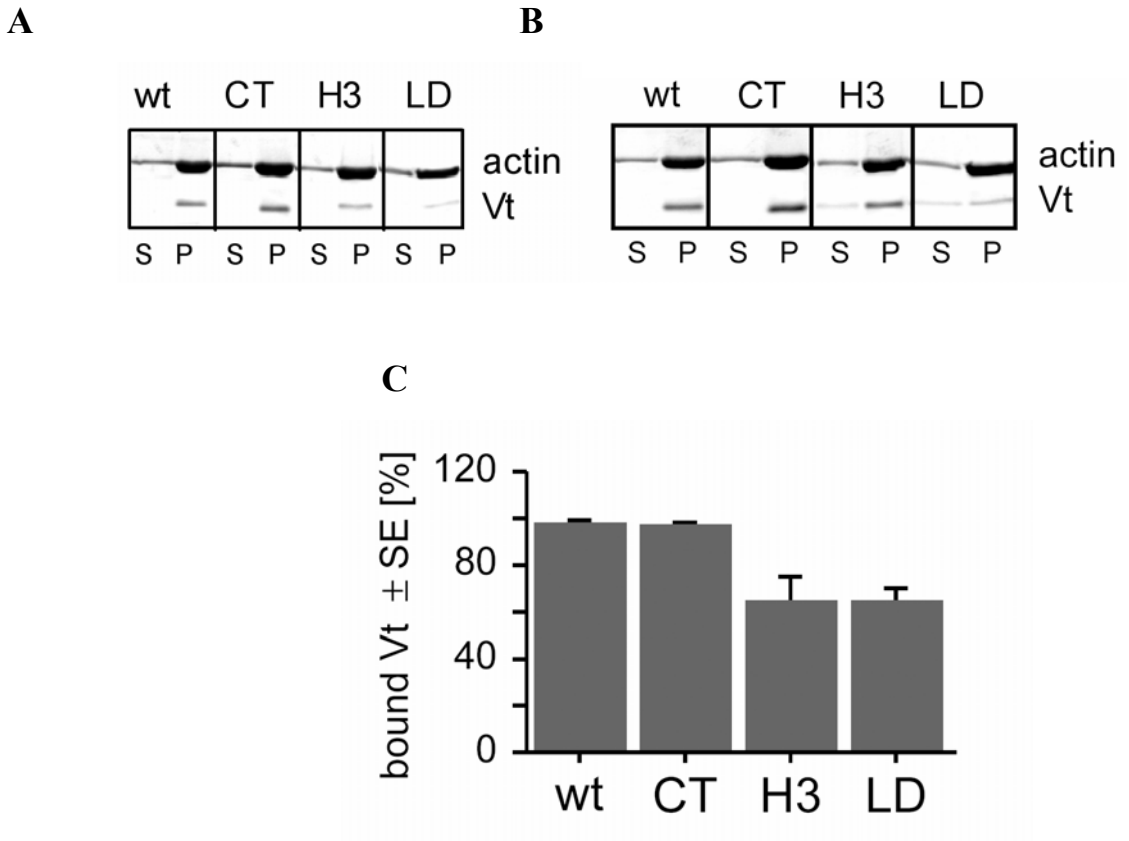

Figure 3.5: Interaction of Vt wild type and mutants with filamentous actin
Pellet (P) and supernatant (S) fractions obtained from cosedimentation assays at (A) 5:1 molar ratio of actin:vinculin, (B) 2:1 molar ratio of actin:vinculin, detected on Coomassie-stained gels. (C) Columns represent the percentage of Vt protein bound to F-actin at molar ratio 2:1 (mean ± s.e; n=3). Vt mutants H-3 and LD show decreased binding at this molar ratio.

3.5.3. Interaction of Vt proteins with GST-Vh (D1)

Intra molecular head – tail interaction in vinculin is critical for activation of the protein (Hüttelmaier *et al*, 1998, Johnson and Craig, 1995). It influences the ligand binding properties by blocking the various binding sites in the head, rod and tail domains. The vinculin tail mutations were designed so as to preserve the head-tail interaction.

Interaction of Vt proteins were determined in a pull down assay using the GST-Vh (D1) fusion protein bound to Glutathione-sepharose beads. The sedimented Vt proteins were densitometrically analysed on a Coomassie-stained gel and the head to tail interaction was found intact for all tested constructs (Figure 3.6).

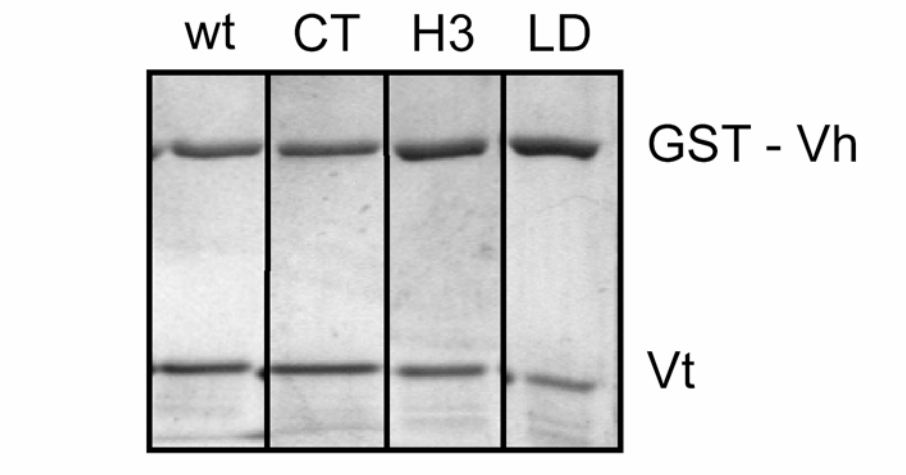

Figure 3.6: GST pull down assay for Vh – Vt interaction
Coomassie-stained gel showing the bound Vt proteins (wt and mutants) to GST Vh (D1) bound to glutathione sepharose beads.

II. Cell biological analyses

3.6. Cellular expression and phenotypic characterization of full length vinculin GFP fusion proteins

Full length vinculin wild type and lipid binding deficient mutants were fused to GFP in the pEGFP-C2 vector and used to analyse the localization in focal adhesions and the effect of the mutations on the functional regulation of vinculin in the adhesion sites during cell migration and adhesion. These experiments were designed to provide deeper insight into the regulation of the protein, mediated through PIP2 at the FAs.

3.6.1. Stable expression of GFP-vinculin constructs in B16-F1 mouse melanoma cells

B16-F1 mouse melanoma cells were chosen for expression of GFP vinculin constructs. Due to their high motility rates on certain extracellular matrices, analyses of cell motility and adhesion turn over were greatly facilitated. B16-F1 cells were transfected with full-length wildtype and mutant GFP-vinculin variants, and populations of cells stably expressing the respective constructs were obtained by a combination of FACS sorting and antibiotic (G418) selection (see chapter 2.2.3.3.). Expression of GFP-vinculin in these populations was stable for more than six passages. These cells were used for a set of experiments to differentiate wt from the mutants based on protein localization, cell adhesion and migration. Protein expression patterns were determined by semiquantitative Western blotting of cell lysates from parental B16-F1 and transfected populations at different passages (1-5). A vinculin antibody (hvin) was used to detect endogenous vinculin and GFP fusion proteins (Figure 3.7.). Comparison of the levels of vinculin as determined by Western blot revealed the ratios of ectopic to endogenous protein varying from 0.3 – 0.45 of total vinculin (Figure 3.7.). Although fusion protein expression was under the control of a CMV promotor which allows overexpression of the protein, absolute amounts of vinculin in transfected cells never exceeded 150% of total vinculin in parental B16-F1 cells, indicating a regulation of endogenous protein levels.

A

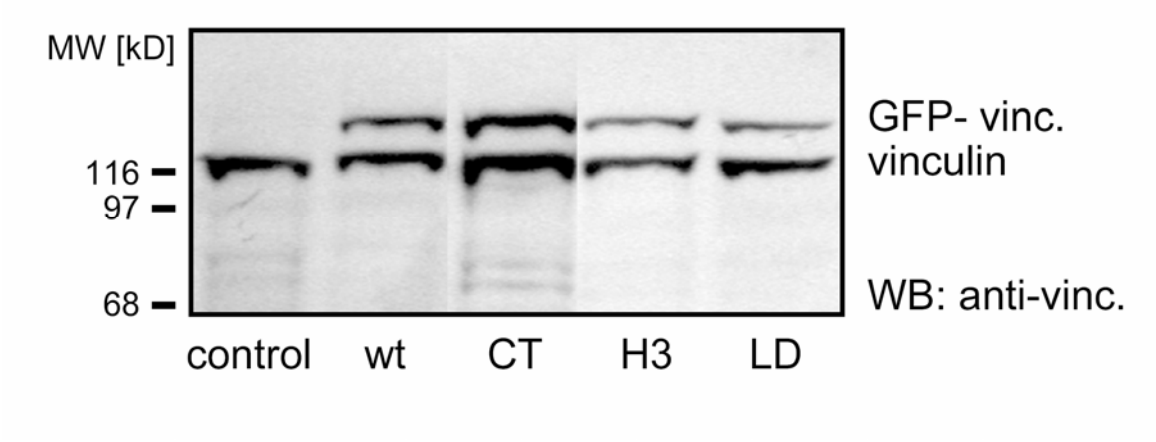

B

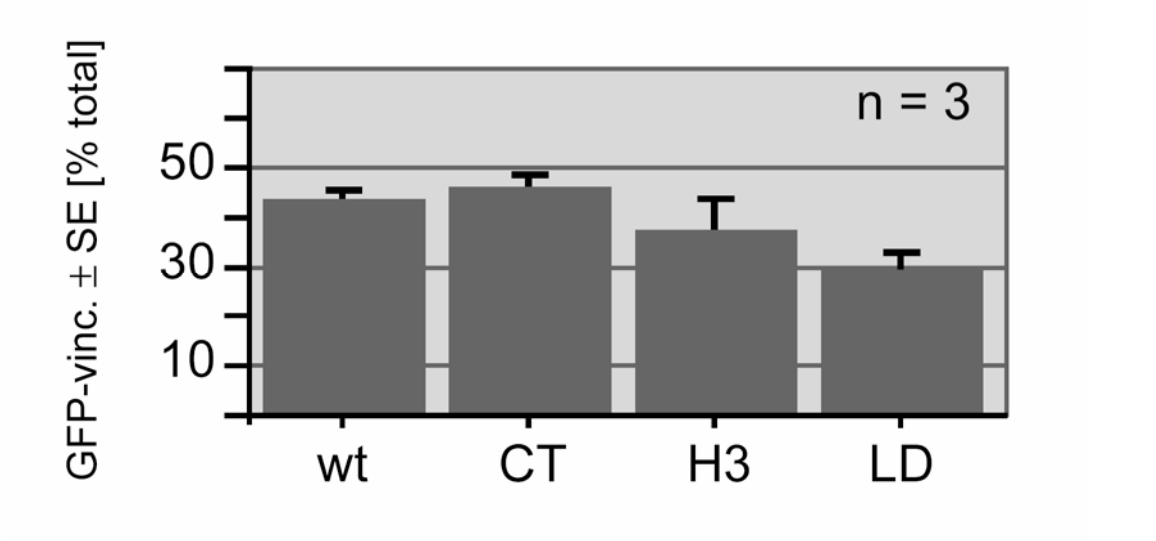

Figure 3.7: Protein expression pattern in B16-F1 stable cell populations
A) Western blot with vinculin antibody (hvin) showing endogenous (117 kDa) and GFP fused vinculin (~141 kDa) from parental cells and cells expressing GFP-vinculin variants. B) Columns represent levels of GFP vinculin in the stable populations expressed as percentage of total vinculin.

3.6.2. Localization of full length GFP vinculin constructs in various cell types

PIP2 mediated activation of vinculin is considered to be important for its ligand interactions and focal adhesion localization (Gilmore and Burridge, 1996). Therefore,

localization studies with GFP vinculin variants were essential to yield more details on the role of PIP2 in activation and adhesion site targeting of vinculin.

The localization studies were carried out in B16-F1 mouse melanoma cells, C2C12 mouse myoblasts and NIH 3T3 mouse fibroblasts. Mouse embryonic fibroblasts from vinculin null mice were also used to study the localization pattern, without endogenous protein background, which could influence the activation of vinculin variants due to formation of tail hetero-oligomers.

B16-F1 cells transfected with GFP vinculin wild type and mutants were seeded onto laminin coated coverslips and fixed after six hours. Cells were then counterstained with paxillin antibody and phalloidin to visualize focal adhesions and actin filaments respectively. Wild type GFP-vinculin as well as all lipid-binding mutants localized to focal adhesions and perfectly colocalized with paxillin and the ends of actin filament bundles. The population of B16-F1 cells expressing GFP-vinculin-LD displayed a high number of cells with abnormally long adhesive extensions, cells contained more pronounced stress fibres and larger focal adhesions as compared to populations expressing other vinculin variants (Figure 3.8.).

C2C12 and NIH 3T3 cells were seeded on fibronectin coated coverslips, transfected with GFP vinculin constructs and fixed after twelve hours. Cells were stained to visualize actin filaments with phalloidin or endogenous vinculin with vinculin antibody. Both GFP vinculin wild type and LD were localized in the focal adhesions. (Figure 3.9.).

Embryonic fibroblasts from vinculin null (MEF-/-) and control mice (MEF+/+) were seeded on glass coverslips, transfected with GFP vinculin constructs and fixed after 12 – 16 hours. There were no differences in the localization of GFP vinculin wt and LD in the vinculin null cells and the control fibroblasts (Figure 3.11.). MEF-/- and MEF+/+ cells were also stained with vinculin antibody to detect the presence of endogenous vinculin (Figure 3.10).

Localization of GFP-vinculin LD at the adhesion sites in the null cells indicated that PIP2 mediated regulation is not essential for focal adhesion targeting of vinculin.

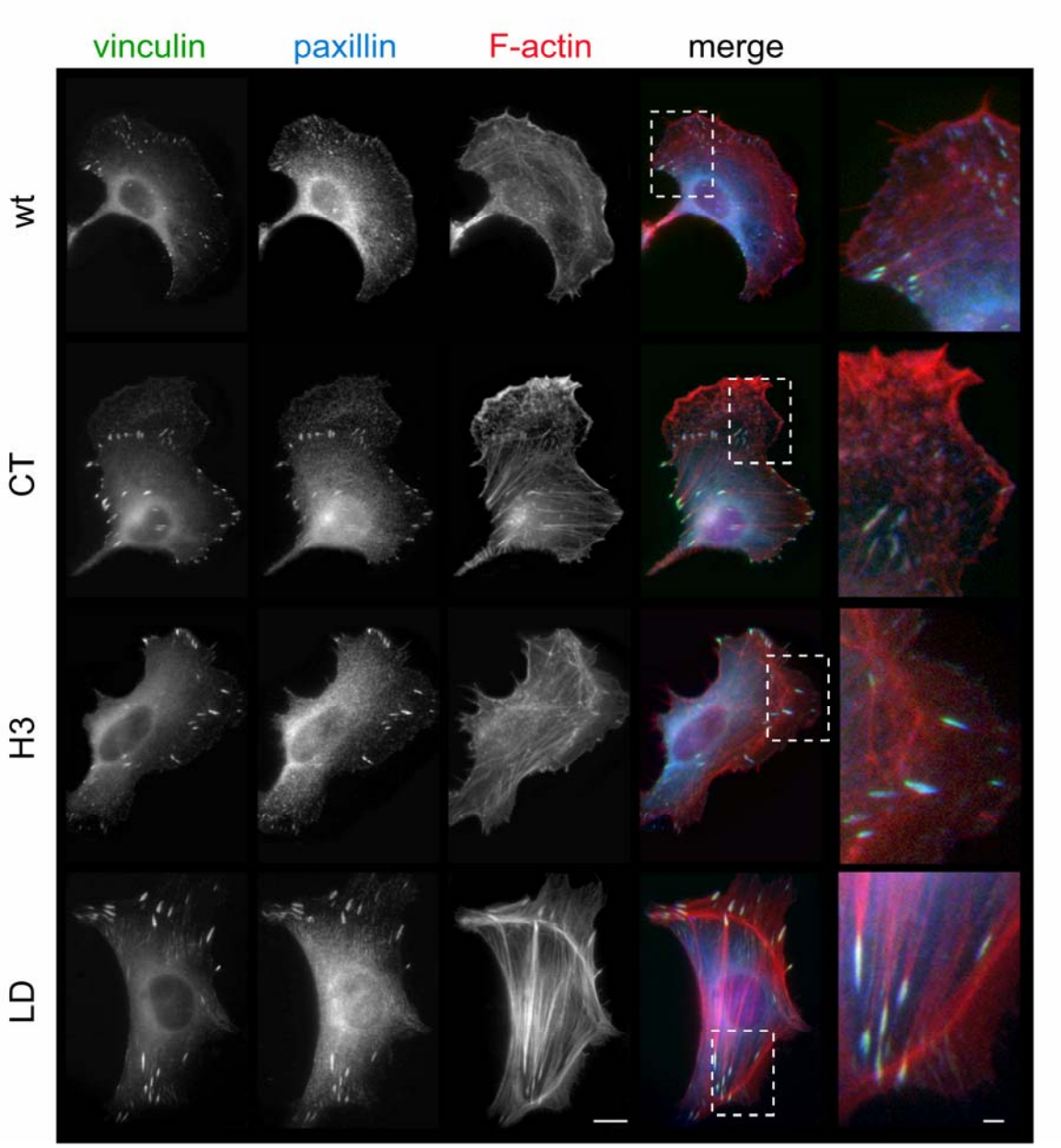

Figure 3.8: Localization of GFP – vinculin variants in B16-F1 cells
B16-F1 cells transfected with GFP-vinculin constructs were seeded on laminin and allowed to attach for six hours. Cells were fixed and stained for paxillin and the actin cytoskeleton. Localization of GFP-vinculin constructs, paxillin and F-actin in exemplary cells are shown individually (grey scale) as well as on merged images of GFP- vinculin (green), paxillin (blue), F-actin (red) and enlargements of the regions indicated. Bars: 10 µm and 2 µm, respectively.

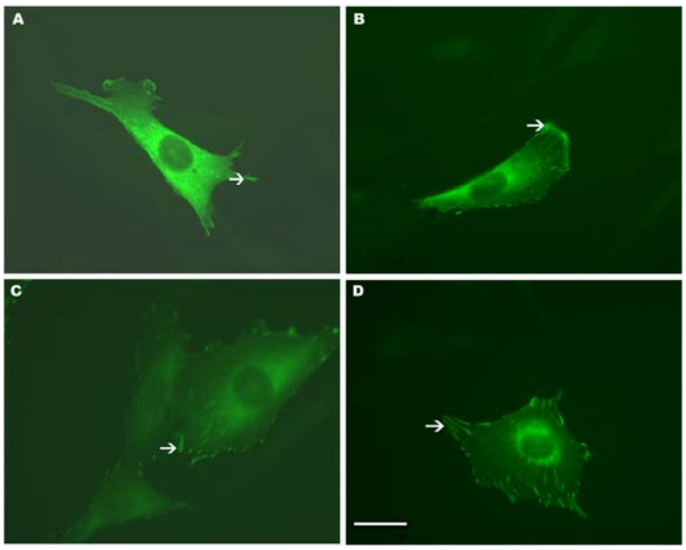

Figure 3.9: Localization of GFP vinculin variants in C2C12 and NIH 3T3 cells
C2C12 and NIH 3T3 cells were seeded on fibronectin and transfected with GFP vinculin constructs. C2C12 cells expressing GFP vinculin wild type (A) and LD-GFP vinculin (B). NIH 3T3 cells expressing wild type GFP vinculin (C) and LD-GFP vinculin (D). Both constructs were localized in focal adhesions (arrow heads). Bar: 10 µm

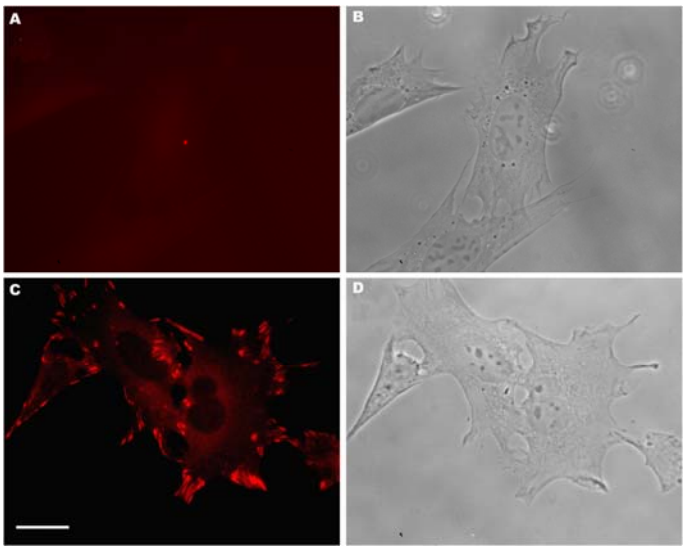

Figure 3.10: Staining for endogenous vinculin in MEF -/- and MEF +/+ cells
MEF -/- vinculin (A and B) and MEF +/+ vinculin (C and D) stained for endogenous vinculin with vinculin antibody and the corresponding phase contrast images. Vinculin null cells (A) lack vinculin staining, while the control cells show endogenous vinculin in focal adhesions (B).Bar: 10 µm

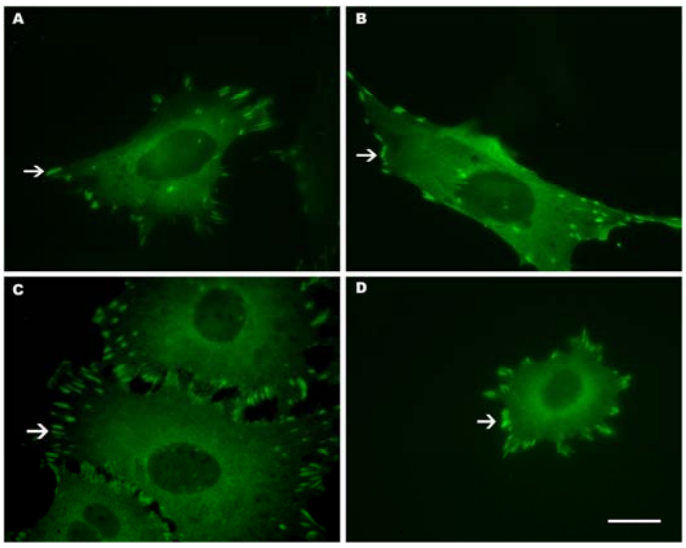

Figure 3.11.: Localization of GFP vinculin variants in vinculin null and control mouse embryonic fibroblasts
MEF -/- vinculin (A and B) expressing GFP vinculin wild type (A) and vinculin LD (B) and MEF +/+ vinculin (C and D) expressing GFP vinculin wild type (C) and vinculin LD (D). Both constructs were targeted to the adhesion sites (arrow heads). Bar: 10 µm

3.6.3. Migration of cells expressing GFP vinculin variants on 3D collagen matrix

The effect of lipid binding site mutations in vinculin on the functional regulation of the protein was analysed during cell motility and adhesion. Spontaneous migration of cells expressing mutant and wild type GFP-vinculin was analysed in a 3D collagen matrix. The cells were mixed with collagen which was allowed to polymerize in a special, self constructed chambers. Migration of cells (n=30) in one field was followed for 15 hours using timelapse video microscopy. (Refer to chapter 2.2.3.7.). The tracking data collected manually were used to calculate the percentage of motile cells and their velocity. After an initial phase of adhesion to the collagen matrix the number of motile cells remained constant and averages (mean ± s.d.) were calculated for each of the populations between 6-15 hours (constant phase). Vinculin LD expressing cells had a five fold reduction in motility (16-20%) when compared to cells expressing wild type and other vinculin constructs (Figure 3.12B Top row). The velocity was determined from the relative movement of motile cells (Figure 3.12B Bottom row). During the constant phase of movement (6-15 hours), the average velocity (mean ± s.d.) of vinculin-LD expressing cells was reduced to 53% as compared to cells expressing exogenous wild type vinculin,

revealing a strong inhibition of cell migration which is characterized by reduction of locomotory activity and also velocity. This effect was observed on a background of endogenous vinculin (70% of total vinculin).Values for vinculin-LD, however, were calculated based on rather short tracks because majority of cells registered did not migrate at all (Figure 3.12A).

A

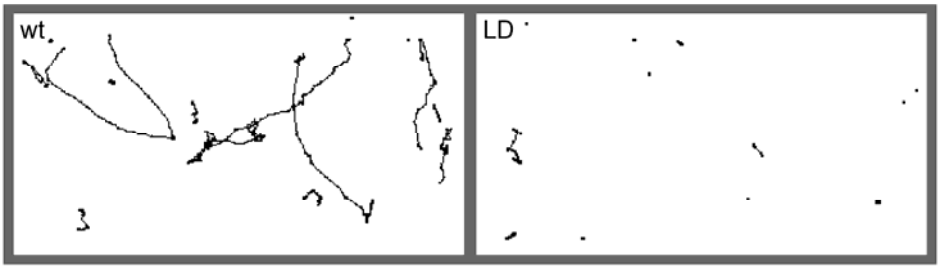

B

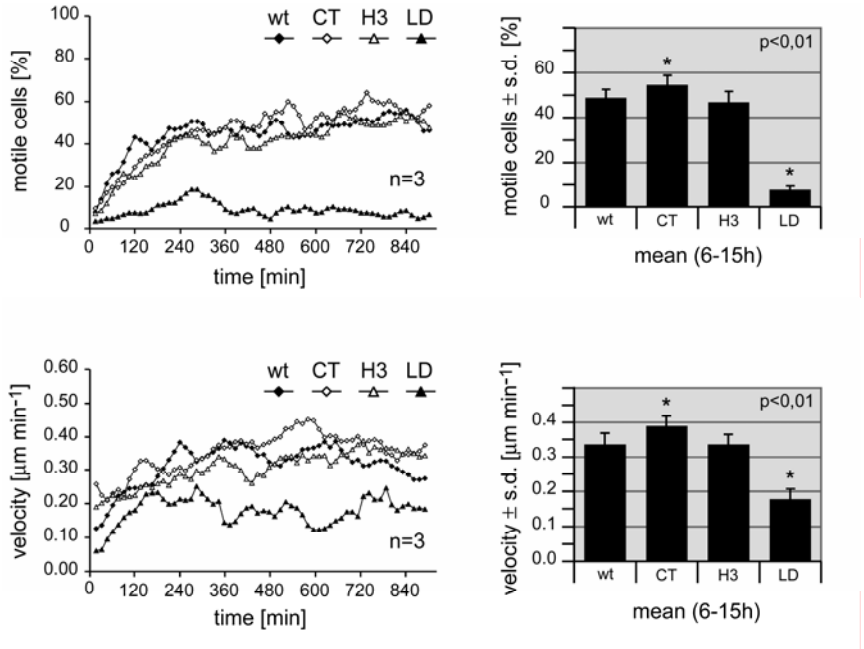

Figure 3.12: Migration assay in 3D collagen matrix
A) Locomotory tracks of cells expressing GFP vinculin wild type and LD (also refer to supplementary movies 3.1 and 3.2)
B) **Top row**: Graph represent the percentage of motile cells tracked from 0-840 hrs and the columns represent the average of motile cells (mean ± s.d.) during the constant phase (6-15 hrs). **Bottom row**: Graph represent the velocity of cells tracked from 0-840 hrs and the columns represent the average velocity of active cells (mean ± s.d.) during the constant phase (6-15 hrs).

3.6.4. Polarization and migration of B16-F1 populations expressing GFP vinculin variants on laminin

Polarization is the initial step preceeding locomotion. The cell develops a leading edge; a region characterized by a high turnover of adhesion sites and increased actin polymerization. The cell body displays mature focal adhesions, stress fibres, and a trailing edge which is considered as region of adhesion dissociation and detachment.

On laminin, B16-F1 cells display a motile phenotype that is characterized by highly polarized cells with wide lamellipodia at their leading front (Ballestrem *et al*., 1998). A large proportion of cells expressing GFP vinculin-wt or vinculin mutants CT and H-3 displayed a motile phenotype after six hours of attachment on laminin. In contrast, the number of cells displaying this phenotype when expressing vinculin-LD was significantly reduced (Figure3.13A). The cells appeared bizarre with long extensions and more pronounced stress fibres. More than 600 cells expressing various vinculin variants were counted and classified into motile, non-motile and ambiguous phenotypes. The number of defective cells in each population was quantified. While 54% of vinculin-wt cells displayed a motile phenotype and only 24% did not, this ratio was inverted in the vinculin-LD cells with 12% polarized and motile cells, while 63% of the cells were spread but not polarized or showed no lamellipodia and these were judged as non-motile (Figure3.13C).

Analysis of migratory capacity of individual cells on laminin using time lapse video microscopy detected the locomotory activity of vinculin-wt expressing cells, while not a single motile vinculin-LD expressing cell was detected in this assay. These differences are illustrated in Figure 3.14, showing selected frames taken from movies of representative cells expressing wt- and LD-vinculin (Refer to supplementary movies 3.3 and 3.4).

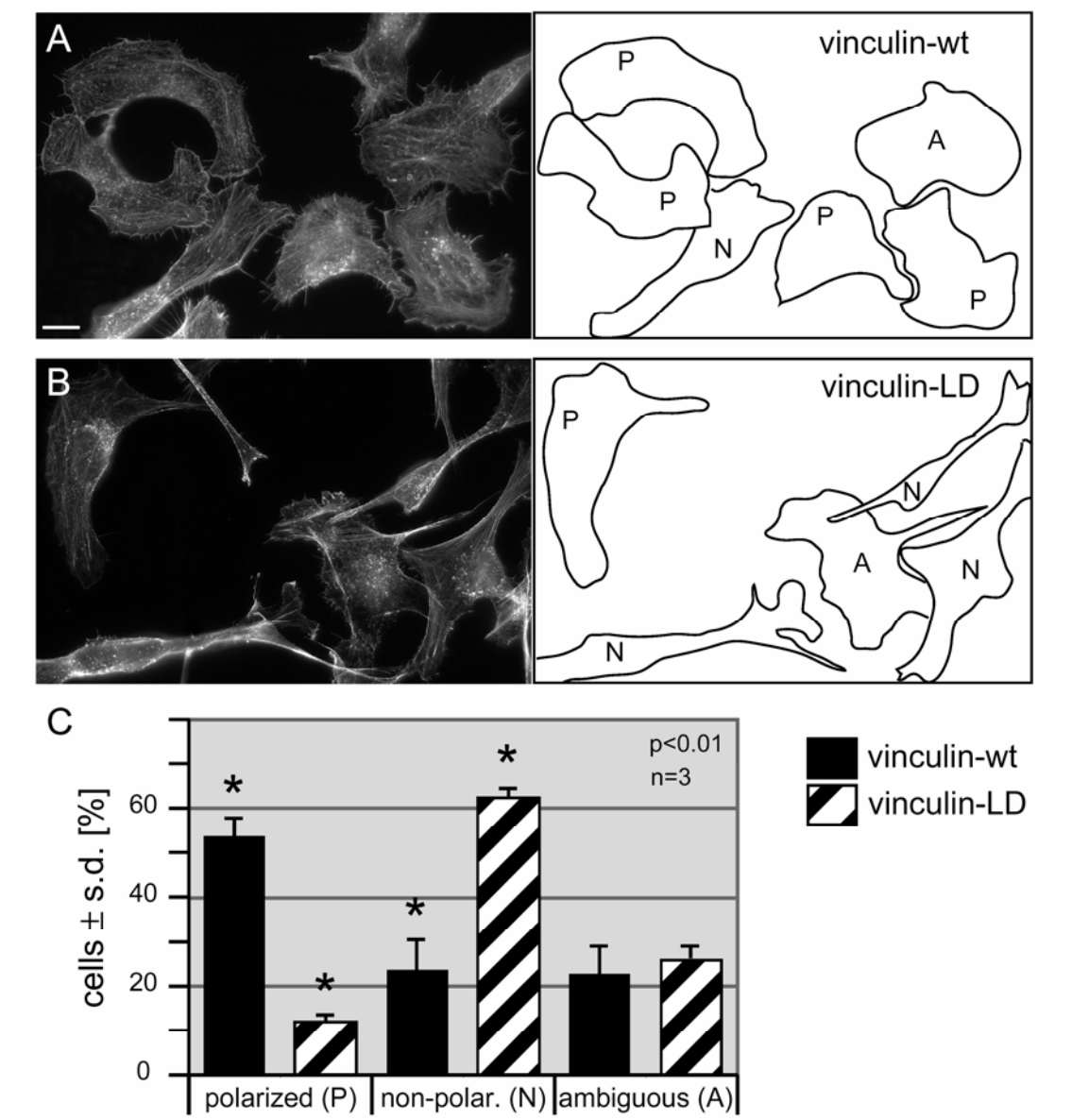

Figure 3.13: Polarization of B16-F1 populations expressing GFP-vinculin constructs on laminin

Representative cells of populations expressing GFP-vinculin constructs wt (A) or LD (B), respectively, are stained for stress fibres with phalloidin (left) and the outlines of cells (right). Classification of cells in categories polarized (P), non-polarized (N) and ambiguous (A) was based on cell shape and the actin cytoskeleton. Bar: 10 µm.

C) Columns represent the percentage of cells in each category taken from >600 cells (n=3) for each vinculin construct.

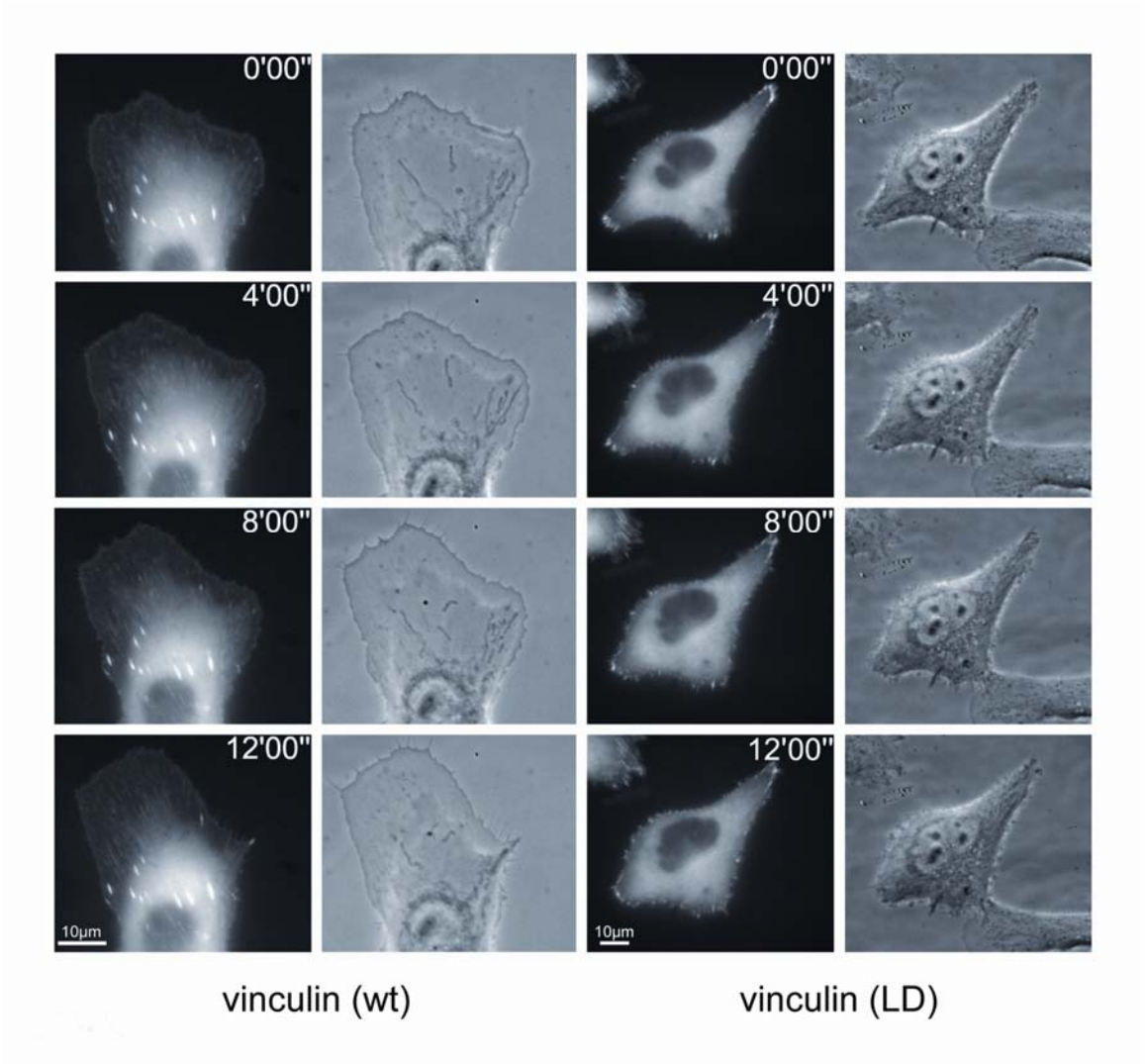

Figure 3.14: Time lapse video microscopy on B16-F1 cells expressing vinculin wt and LD

Selected frames from movies taken in fluorescence and phase-contrast modes, illustrate the locomotory activity of representative cells. Bars: 10 µm.The GFP-vinculin wild type expressing B16-F1 melanoma cell is actively migrating as shown by a protruding lamellipodium, newly appearing adhesions and displacement of the nucleus. The GFP-vinculin-LD expressing cell displays some membrane activity, but no sign of migratory activity (also refer to supplementary movies 3.3 and 3.4).

3.6.5. Adhesion and spreading of B16-F1 stable populations on various extracellular matrices

Adhesion of cells to the extracellular matrix is an important physiological process that initiates adhesion mediated signalling, spreading and cell motility.

The migratory capacity of the cells expressing GFP vinculin LD was observed to be highly reduced in the migration assays described earlier, the graph depicting cell motility on 3D collagen matrix had a lag phase at earlier time points (0- 120 min, Figure 3.12B) which could be associated with a delay in adhesion and spreading. The assays described below were aimed at the analysis of adhesion and spreading of cells expressing GFP vinculin variants on different extra cellular matrices.

B16-F1 cells express receptors for the extracellular matrix proteins laminin (integrins $\alpha1\beta1$/ $\alpha6\beta1$), fibronectin (integrins $\alpha4\beta1$/ $\alpha5\beta1$) and collagen (integrin $\alpha1\beta1$) (Ballestrem *et al*., 1996). Populations of B16-F1 cells expressing GFP-vinculin wild type or mutants were allowed to adhere and spread for various time periods. Comparable degrees of spreading were reached on laminin and fibronectin in 10 minutes after seeding and on collagen after 90 minutes. By that time, more than 80% of cells were spread and displayed peripheral lamellipodia with only a small fraction of polarized cells.

In the adhesion assay, cells that were just attached to the surface were counted after a thorough washing step to remove all non-adherent cells. Cells expressing GFP vinculin LD showed reduced adhesion by 35% on laminin, 25% on fibronectin and 79% on collagen as compared to cells expressing GFP vinculin wild type (Figure 3.15).

In the spreading assay, cells were counted in randomly selected microscopic fields (450 - 550 cells per test) and values were expressed as percentage of spread cells in each stable population (mean ± s.d., n=4-6). GFP vinculin-LD expressing cells displayed a decrease in spreading by 35 – 40% on laminin and 40 – 50% on fibronectin compared to the GFP vinculin-wt population. After 90 minutes of spreading on laminin or fibronectin, differences in the number of adherent and spread cells were decreased to less than 10% (Figure 3.16A and B). These results suggest that vinculin LD expression in these cells leads to a delay in cell adhesion and spreading.

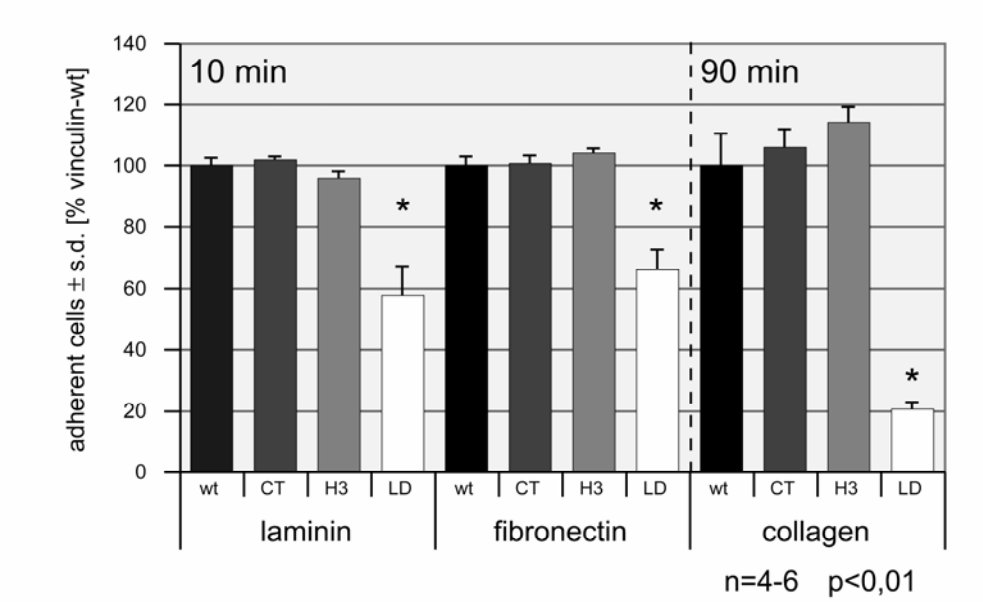

Figure 3.15: Adhesion assay with various extracellular matrices
Columns represent percentage of adherent cells on laminin, fibronectin, collagen (mean ± s.d) in each stable population compared to cells expressing GFP vinculin wild type.

Figure 3.16 A

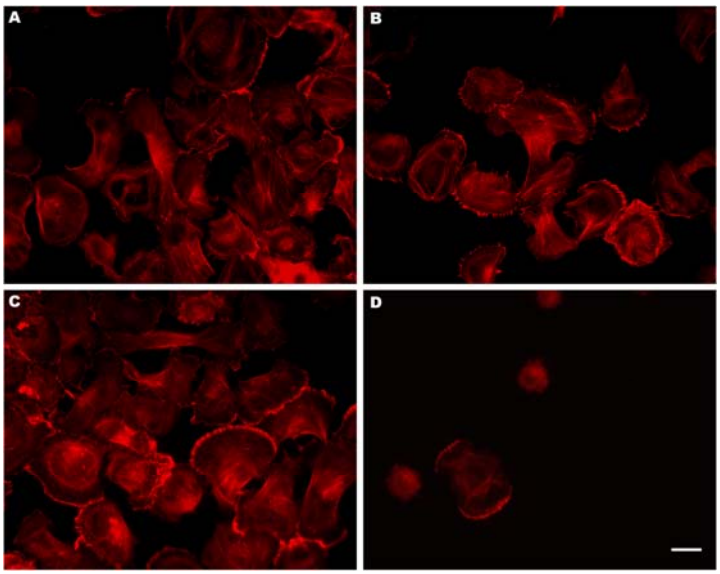

Figure 3.16 B

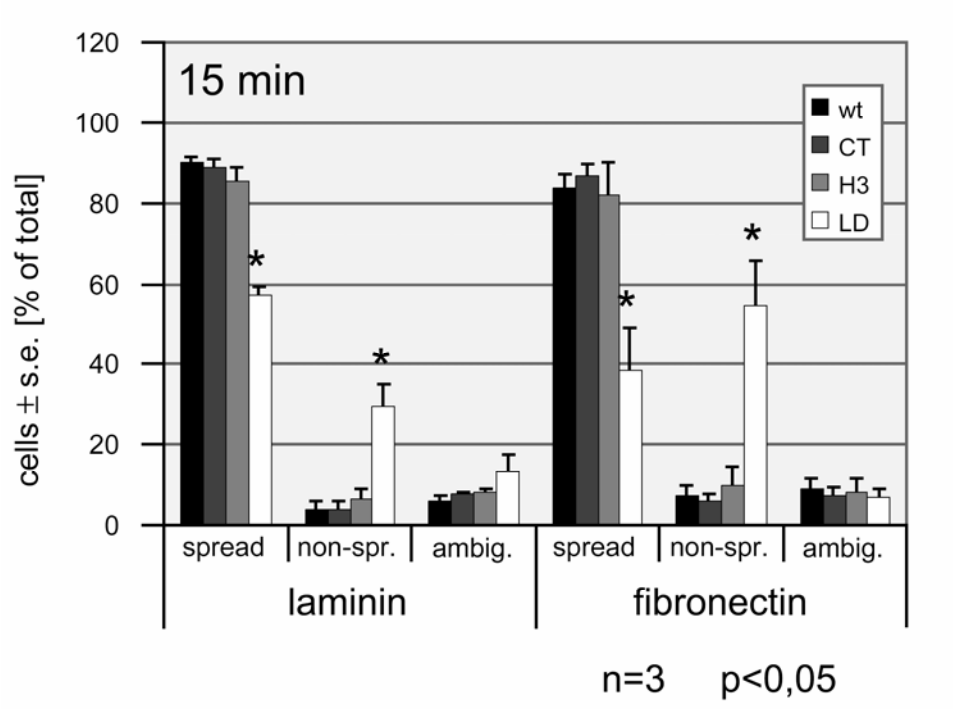

Figure 3.16: Spreading of stable cell populations on various extracellular matrices
A) Spreading assay showing exemplary cells in a selected microscopic field from populations of cells expressing vinculin wt (A), vinculin CT (B), vinculin H-3 (C) and vinculin LD (D) Bar: 10 µm
B) Columns represent stable cells expressing vinculin variants that were spread, nonspread and those classified as ambiguous on laminin or fibronectin.

3.6.6. Rate of incorporation of GFP vinculin variants in individual adhesion sites analysed by fluorescence recovery after photobleaching (FRAP) technique

Localization of vinculin-LD in all cell types including the vinculin null cells could not be distinguished from vinculin wt, but stress fibres as well as number and size of adhesions appeared to be increased in vinculin-LD expressing stable cell populations (Figure 3.8). The exchange rates of vinculin molecules in individual adhesion sites in cells expressing vinculin LD and wt were analysed by fluorescence recovery after photobleaching (FRAP). The technique calculates the rate of re-incorporation of GFP-tagged vinculin variants after bleaching them with 100% laser intensity. Cells expressing GFP vinculin wt and LD were seeded on glass coverslips, mounted on special chambers for live cell imaging and analysed using a laser scanning microscope. Individual adhesions were selected, bleached by increasing the laser intensity and subjected to time lapse video

microscopy. Kymographs from line scans parallel to the length axis of bleached adhesion were generated and the half-time of fluorescence recovery was calculated based on the kymographs (Figure 3.17.) (Refer to chapter 2.2.3.10.). The halftime of fluorescence recovery after photobleaching was about 45 seconds for both wild type and lipid binding deficient vinculin in adhesions that remained stable for more than 10 minutes. In conclusion, lipid-binding deficiency of vinculin-LD does not affect incorporation and exchange rates of the protein in individual adhesion sites.

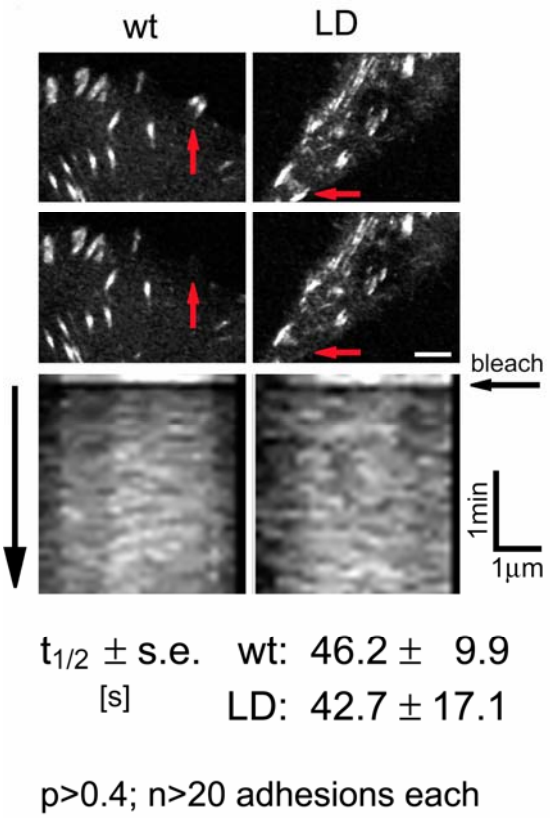

Figure 3.17: Rate of incorporation of GFP vinculin variants in adhesion sites
Cells expressing GFP tagged wt and LD vinculin showing individual adhesion sites before and after bleaching (red arrow) and the representative kymographs from line scans parallel to the length axis of bleached adhesions. Bar: 5 µm

3.6.7. Retrograde sliding of adhesions as a function of overall adhesion site turnover in B16-F1 stable cell populations

The exchange rates of vinculin in individual adhesion sites determined by FRAP analysis clearly indicated that focal adhesion targeting for both wt and LD vinculin are similar. The overall turnover of vinculin molecules in these adhesion sites was assumed to be defective, which might explain the impairment of cell migration. To analyse this hypothesis, live cell imaging assisted by laser scanning microscopy was performed. Individual adhesions were selected and followed for 20 – 30 min and the retrograde sliding of adhesions (translocation of adhesions towards the cell body) was registered. To

estimate the average speed of the sliding adhesions, more than 100 individual sites per vinculin variant were tracked (Figure 3.18). Adhesions containing vinculin LD in B16-F1 cells had a five fold reduction in average speed as compared to vinculin wt expressing cells. The failure of adhesion translocation in vinculin LD expressing cells suggests a prominent stabilization of adhesion sites. The turnover of adhesion sites was also determined by counting the number of adhesions newly formed and dissociated in this period of 20 minutes in cells expressing GFP vinculin variants. From the total number of adhesions analysed, 27% were newly formed and 32% were disassembled in vinculin wt populations, whereas only 9% were formed and 2% disassembled in cells expressing vinculin-LD, indicating the defective turnover. Thus, the impaired cell migration could be attributed to the inability of vinculin LD to sense the acidic phospholipids which gives the signalling information to vinculin for the adhesion turnover.

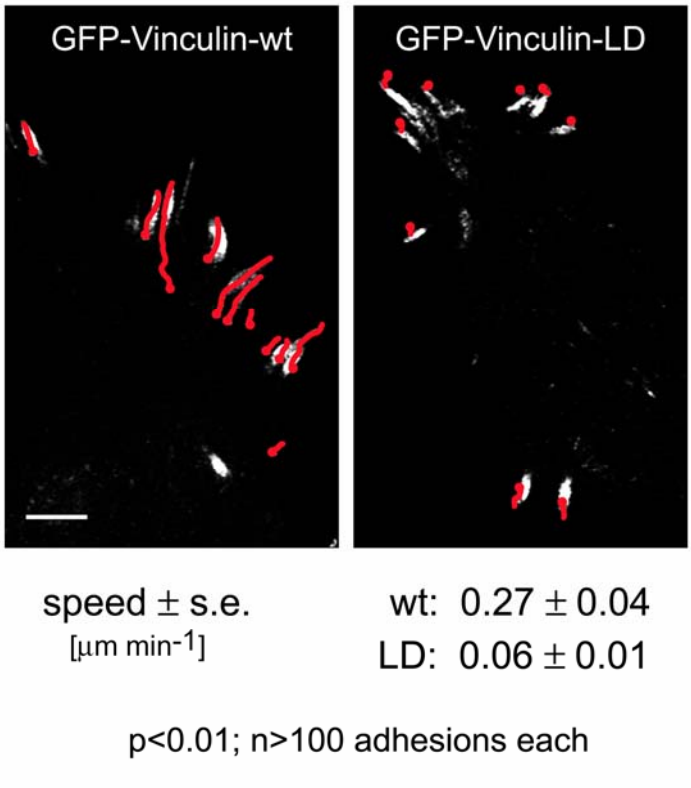

Figure 3.18: Retrograde sliding of adhesions
Cells expressing GFP vinculin-wt or vinculin-LD showing tracks of sliding adhesions during migration, tips of adhesions are marked in red. (t= 0-20 min). Tracks were used to calculate average speed of retrograde movement.
Bar: 5 µm

3.6.8. Effect of PIP5-kinase α on B16-F1 populations expressing GFP vinculin wt and LD due to alterations in the PIP2 levels

Functional impairment of GFP vinculin LD expressing B16-F1 cells suggests the involvement of acidic phospholipids in the focal adhesion turnover, cell migration and adhesion. Alterations in the PIP2 levels in these cells could possibly have different effects on vinculin wt and LD, since the ability of vinculin LD to sense the signals from PIP2 is low. PIP2 levels in these cells were altered by over-expression of murine PIP5-kinase α, the kinase that catalyses the synthesis of PIP2 in cells. PIP5-kinases exist in three isoforms. The γ isoform localizes in focal adhesions and has been reported to bind to talin. PIP5-kinase γ leads to adhesion dissociation since it competes with β-integrin for talin binding.Thus; the γ isoform is not ideally suited for this experiment. Hence, to investigate the effect of changes in PIP2 levels on GFP vinculin wt and LD turnover, murine PIP5-kinase α was preferred over the other isoforms. As an internal control and to mark the effect of kinase activity, a "kinase dead" mutant (KD) of PIP5-kinase α was also expressed in these stable cell populations.

Cells expressing GFP vinculin wt or LD and parental B16-F1 cells were plated on fibronectin coated coverslips, transfected with myc tagged PIP5-kinase α or bipro tagged PIP5-kinase α KD mutant, and were allowed to express the exogenous proteins for 12 hours. Cells were fixed and then stained to visualize actin filaments and PIP5- kinase, active and kinase dead forms. Overexpression of PIP5-kinase α in GFP vinculin wt populations induced re-localization of vinculin from adhesion sites to the perinuclear region within 12 hours after transfection (Figure 3.20). This effect was quite evident also in parental B16-F1 cells. Within 8 hours after transfection, the endogenous vinculin was translocated to the perinuclear region (Figure 3.19). After 12 hours, all transfected cells were rounded and started to detach.

In contrast, cells expressing GFP-vinculin-LD were quite resistant to the PIP5-kinase activity. Out of 60 cells co-expressing vinculin-LD and PIP5-kinase α for 12 hours 41 cells showed vinculin-LD localized to large adhesion sites. In cells co-expressing the GFP vinculin variants and the PIP5-kinase α KD mutant, both GFP vinculin wt and LD were not re-localized indicating the need for an active kinase. These results indicate that

adhesions containing vinculin LD were more resistant to kinase induced elevation of PIP2 levels, probably due to their inefficient binding to acidic phospholipids.

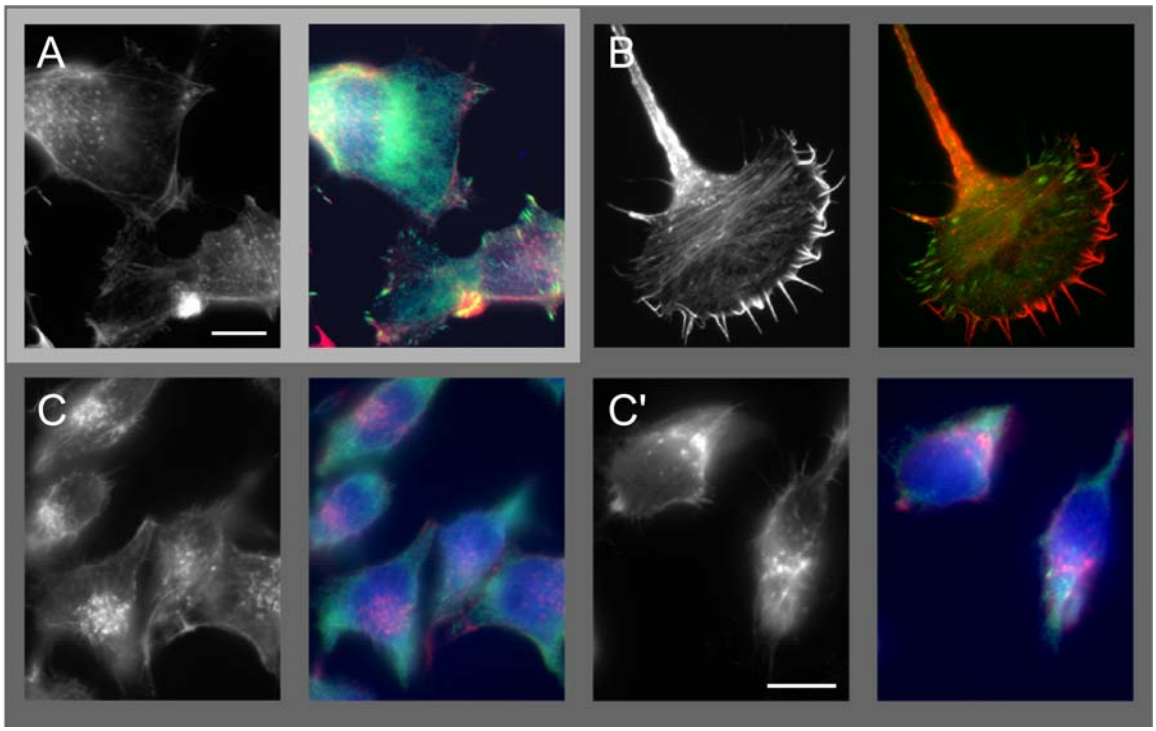

Figure 3.19: PIP 5-kinase α expression in parental B16-F1 cells
A) Cells expressing PIP5-kinase α, fixed after 8 hours, showing the localization of endogenous vinculin (green) in few focal adhesions (lower cell), actin filaments (in grey, or in red in the merged image) and PIP5-kinase (blue)
B) Control B16-F1 cells on laminin fixed after 12 hours and stained for actin filaments (in grey, or in red in the merged image) and endogenous vinculin (green)
C)andC')Cells transfected with PIP5-kinase α, fixed after 12 hours of expression showing re-localization of endogenous vinculin (green) to the perinuclear region, disorganized actin cytoskeleton (in grey, or in red in the merged image) and PIP5-kinase (blue) Bars: 10μm

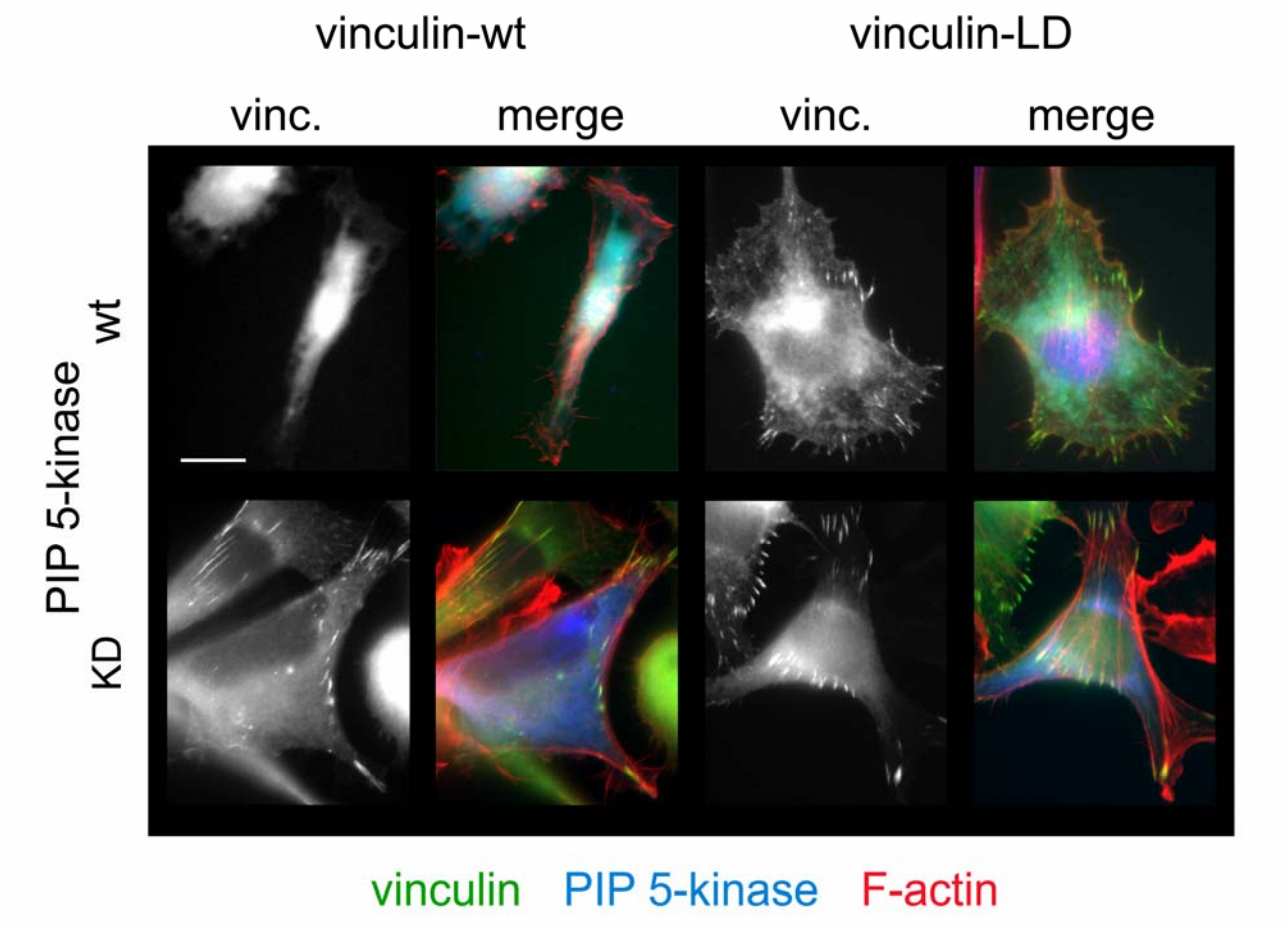

Figure 3.20: PIP5-kinase α expression in stable B16-F1 populations expressing vinculin wt and LD
Representative cells from stable GFP vinculin wt and LD populations co-expressing PIP5-kinase α wt or kinase dead (KD) forms, 12 hours after transfection. Cells were stained to visualize actin filaments (red), PIP5-kinase and the KD mutant (blue). GFP vinculin variants are shown in grey or in green (merged images). GFP vinculin wt was re-localized to perinuclear regions by PIP5-kinase coexpression, while the vinculin LD expressing cells were resistant to the kinase activity (top row). Expression of KD PIP5-kinase α does not affect the localization of either GFP vinculin wt or LD (bottom row). Bar: 10μm

3.6.9. Effect of constitutively active Rac (L61) expression on GFP vinculin wt and LD

Small GTPases of the Rho family (RhoA, Rac1, and Cdc42) are key regulators of cytoskeletal organization and have been implicated in regulation of PIP2 levels in the cells. RhoA and Rac1 stimulate PIP2 synthesis by activating PIP5-kinase isoforms which function downstream of these molecules. Recent findings indicate that synthesis of PIP2

via the three PIP5-kinase isoforms is controlled by RhoA, Rac1 and Cdc42 implicating the regulation of PIP2 levels has a central position in Rho GTPases signaling (Weernink *et al*, 2004). In order to test the effect of Rac on the regulation of PIP5-kinase isoforms, a constitutively active form of Rac (L61) was co-expressed in the B16-F1 vinculin wt or vinculin LD populations.

B16-F1 cells expressing GFP vinculin wt or LD were seeded on fibronectin coated coverslips and transfected with myc tagged L61- Rac. Cells were fixed after 12 hours of expression and stained for actin filaments and Rac (L61). There was no evident re-localization of GFP-vinculin wt or LD from focal adhesions in the B16-F1 stable populations co-expressing L61- Rac. The cells appeared to have a pancake shape phenotype which is typical for Rac over-expression (Figure 3.21).

Rac is known to function upstream of the PIP5-kinase isoforms, However, overexpression of L61- Rac probably was not sufficient to influence the elevation of PIP2 levels in these cells in the absence of other signals.

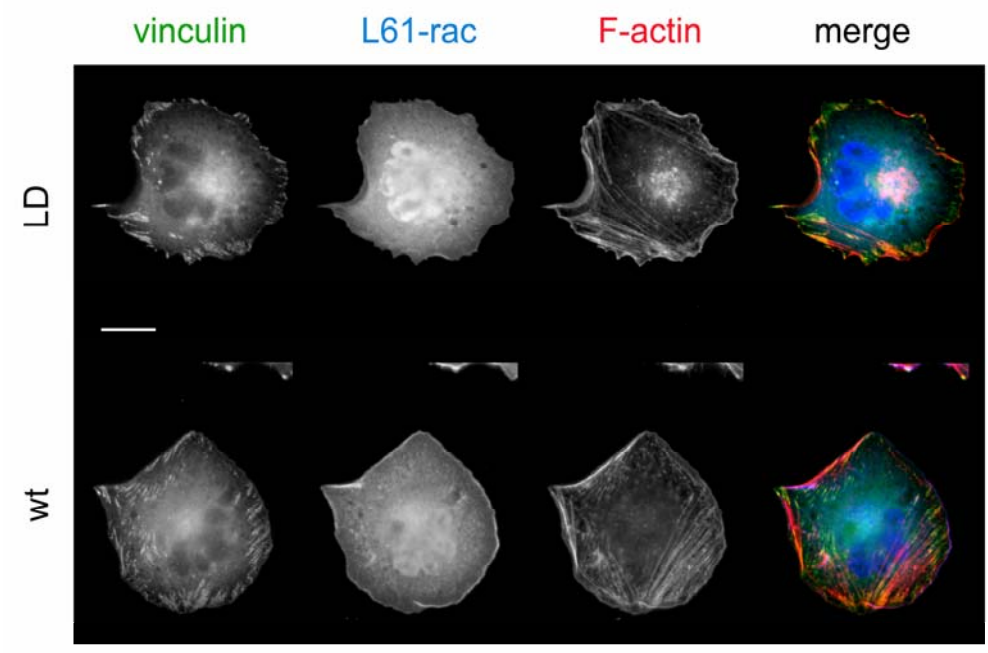

Figure 3.21: L61 Rac expression in B16-F1 cells expressing GFP vinculin wt and LD
Cells expressing GFP vinculin wt and LD (green) transfected with Rac (L61), fixed after 12 hours of expression and stained to visualize Rac (blue), actin filaments (red) representing both vinculin wt and LD in adhesion sites. (Grey and merged pictures)
Bar: 10 µm

4. Discussion

Many cytoskeletal proteins bind to and in some cases are functionally regulated by specific membrane lipids. The molecular basis for such interactions is now beginning to be understood. More insights into the physiological role of these interactions can be obtained with a better knowledge about the molecular structure of specific lipid binding sites (Niggli, 2001). This will aid in the construction of mutant proteins lacking the ability to interact with lipids. Careful analyses of the biochemical properties and cellular expression of these mutant proteins can provide information on the functional regulation of these proteins through lipids. This work focused on the acid phospholipid-mediated regulation of the cell adhesion protein vinculin. Design and construction of a lipid binding site mutant allowed us to characterize the role of lipids in activation and regulation of this protein with more relevance to its functional role in cell adhesion and migration. The following section will discuss the major facts on regulation of vinculin in adhesion sites that were derived from several biochemical and cell biological analyses of the lipid binding deficient mutant "Vinculin-LD".

4.1. "Vinculin-LD" shows decreased binding to acidic phospholipids

Binding of vinculin to acidic phospholipids, more specifically to PIP2, was reported long back (Fukami *et al.* 1994) and was believed to regulate the actin cytoskeleton. Significance of PIP2 interaction with vinculin has already been discussed in the earlier chapters (Refer to chapter 1.3.4). Construction of a lipid binding deficient mutant to further analyse the functional regulation of vinculin by PIP2 was therefore considered essential. The molecular structure of vinculin describes the cluster of basic residues (lysines and arginines) in the basic ladder (helix 2 and helix 3) and the basic collar as lipid binding sites (Bakolitsa *et al.* 1999). Several attempts were made by various research groups to generate a lipid binding deficient mutant and thereafter to analyse its functional consequence on cell adhesion, spreading and migration. In a preliminary report, alanine substitution of the c-terminal basic residues of vinculin abolished binding to 10%PIP2/90%PC vesicles *in vitro* while leaving the focal adhesion targeting unimpaired (Cohen and Craig, 2003). Another C-terminal mutant lacking the terminal 15 amino acids, VtΔC, failed to cosediment with multilamellar vesicles composed of PS, PC

and PIP2 at physiological pH. On lowering the pH, cosedimentation was observed with a midpoint at pH 6.5. Very little cosedimentation occurred with PC vesicles, showing that the mutant retained its specificity for acidic phospholipids (Bakolitsa *et al.*1999). Expression of this mutant in vinculin null MEF cells was unable to restore normal rates of cell spreading and showed mislocalization of the protein to the fibrillar adhesions instead of the peripheral adhesions (Saunders *et al.* 2003). The vinculin tail mutants with alanine substitutions (eg: Vt W1058A, Vt K911A, Vt DM (R910/K911A), Vt TM (R910/K911/K915A), Vt K924A) showed upto 50% reduced binding to the vesicles containing 40%PIP2/60%PC (Bakolitsa *et al.* 2004). In the work presented here, a combination of point mutations in the basic ladder and basic collar in Vt-LD has completely abolished the acidic phospholipids binding (chapter 3.5.1). It includes the point mutation of amino acids K952, R1060, K1061 which were already described in few of the above stated examples to have an effect on the lipid binding capacity. Other mutants including Vt Δ1052, Vt H-3, Vt CT have about 50% reduction in their acidic phospholipid binding indicating the significance of both the binding sites in the lipid interaction.

4.2. Interaction to specific ligands is intact in "Vinculin-LD"

Vinculin is a modular protein having binding sites for numerous cytoskeletal and actin reorganizing proteins (Jockusch and Rüdiger, 1996, Critchley DR, 2000). The lipid binding sites in the C-terminus (basic collar) and the helix 3 (basic ladder) has flanking sequence regions that interact with vinculin tail and actin. Vinculin head-tail interaction is essential to maintain its inactive conformation as described earlier. F-actin is an important ligand which mediates the membrane-cytoskeleton connection. The point mutations at the lipid binding sites were carefully designed to avoid any influence on its ligand interactions. The intramolecular head-tail interaction, tested in a GST pull down assay was found to be intact (Chapter 3.5.3.). Interaction of actin with vinculin has always been controversial and was considered to be mutually exclusive with PIP2 interactions (Steimle *et al.* 1999). The binding capacity between F-actin and vinculin was estimated to be 0.3 – 0.6 moles of vinculin tail per mole of actin (Johnson and Craig, 1995). When a molar ratio of actin:Vt of 2:1 was employed in the actin cosedimentation assay, the concentration of F-actin was exceeding the maximum binding capacity stated

above which could be a possible reason for the 35% decrease in Vt binding (Chapter 3.5.2.). However, the binding affinities for the Vt wt and Vt CT mutant were found to be normal at this molar ratio. Hence, one can conclude that the mutations in the helix 3 lipid binding site may have a slight influence on the "vinculin-LD" interaction with actin at higher molar ratios, but it does not block the interaction.

4.3. The interaction with acidic phospholipids is not crucial for the localization of vinculin

Interaction of PIP2 with vinculin was supposed to release the intramolecular head-tail binding, converting the molecule to the active conformation and permitting various ligand interactions and focal adhesion targeting (Gilmore and Burridge, 1996, Weekes *et al.* 1996). Hence, one might conclude that a vinculin deficient in lipid binding should not localize to the focal adhesions. However "vinculin-LD" expressed in B16-F1 cells perfectly localized to the FA's and co-localized with paxillin, a focal adhesion marker (Chapter 3.6.2). Endogenous vinculin present in the melanoma cells might guide the FA targeting through formation of tail hetero-oligomers (Hüttelmaier *et al.* 1997). However, when expressed in vinculin (–/–) MEF cells (Xu et al., 1998a), vinculin-LD still localized to focal adhesions (Chapter 3.6.2.). Hence, recruitment of vinculin-LD to adhesion sites is apparently independent of phospholipid binding and subsequent activation of the molecule. This confirms that PIP2 interaction with vinculin is not essential for vinculin activation and focal adhesion targeting as previously stated, instead, lipid binding should be considered important in the regulation of adhesion site turnover which will be discussed below

4.4. "Vinculin-LD" acts as a dominant negative mutant and affects cell adhesion and migration

Cell adhesion and migration are two basic cellular processes that require a regulated interplay of actin dynamics and turnover of cell-matrix adhesions (Pollard and Borisy, 2003, Gumbinier *et al.* 1996). Vinculin is a major structural and regulatory component of these adhesions sites, involved in the force coupling and stabilization of nascent FA's after talin binding to integrin (Galbraith *et al.* 2002, Giannone *et al.* 2003). Cell migration was shown to be inhibited in vinculin overexpressing cells and a decrease in vinculin levels promoted cell motility (Rodriguez Fernandez *et al.* 1992, Rodriguez Fernandez *et*

al. 1993). Vinculin deficient mouse embryonic fibroblasts have a defect in cell spreading, but they migrate much faster than control cells (Xu *et al.* 1998a, Xu *et al.* 1998b) due to the failure to stabilize initial adhesions. "Vinculin-LD" expressing mouse melanoma cells display a delay in cell adhesion on various extra cellular matrix components (Chapter 3.6.5). Migration of these cells was also grossly impaired on 3D collagen matrix (Chapter 3.6.3) and on laminin (Chapter 3.6.4).

Cell spreading requires an increased turnover of small, transient adhesion sites in the peripheral lamellipodia which are controlled by the Rac or Rho GTPases (Rottner *et al.* 1999). Activities of non receptor tyrosine kinases like FAK and Src-kinase play an important role in cell spreading (Von Wichert *et al.* 2003). Increased FAK activity has a negative influence on the residence life time of vinculin and paxillin in adhesion sites (Von Wichert *et al.* 2003), leading to enhanced adhesion site turnover. Defective spreading of vinculin null fibroblasts was attributed to high FAK activity in these cells (Xu *et al.* 1998a). B16-F1 cells expressing "Vinculin-LD" also have a delay in cell spreading on laminin and fibronectin (Chapter 3.6.5) which could be attributed to the decreased adhesion site turnover (Chapter 4.5). These results clearly prove that vinculin deficient in lipid binding is unable to functionally regulate actin dynamics and adhesion site turnover and is thus acting as a "dominant negative", seriously affecting cell adhesion, migration and spreading on various extracellular matrices.

4.5. Incorporation of "Vinculin-LD" in adhesion sites is normal

Basal exchange rates of vinculin in individual adhesion sites was similar for both GFP vinculin wt and –LD mutant as judged by the FRAP analysis (Chapter 3.6.6.). This gives an additional proof for the PIP2 independent activation and focal adhesion targeting of vinculin, including the localization studies on various cell types. Thus, the recruitment of vinculin to focal adhesions is independent of acidic phopholipid binding, which is consistent with preliminary reports from other groups, who observed that different lipid binding site mutations in the vinculin tail did not affect its subcellular localization. For example, the alanine substitution mutants had decreased binding affinity to lipid vesicles but their localization to FA's was not altered (Cohen and Craig, 2003). Various vinculin mutants carrying point mutations in the basic collar or the basic ladder were found to

localize perfectly in FA's (Saunders *et al.* 2003). VtΔC, lacking the c-terminal 15 amino acids is the only reported mutant to have slightly altered localization to the fibrillar adhesions rather than to the peripheral adhesions (Saunders *et al.* 2003). However, the analysis of the retrograde sliding of individual adhesions reveals a defect in the over all turnover of the adhesion sites, providing a simple explanation for the observed decrease in cell migration.

4.6. A proposed mechanism for vinculin activation and regulation at the focal adhesions – lessons learnt from "Vinculin-LD"

Interaction of vinculin with actin and the acidic phospholipid PIP2 is mutually exclusive and PIP2 interaction unmasks the talin binding site in the vinculin head while blocking the actin binding site in the vinculin tail (Stiemle *et al.* 1999). In other words, vinculin bound to PIP2 is membrane associated and is not bound directly to actin. Thus, these two ligands provide alternative pathways for vinculin activation and regulation at the adhesion sites (Bakolitsa *et al.* 2004).

In wild type cells, PIP2 acts as an important signaling molecule that regulates adhesion site turnover. Low levels of PIP2 seem to trigger cell adhesion and stabilize nascent focal adhesions. In vinculin-LD expressing cells, the PIP2 level is not monitored correctly, even when endogenous vinculin is still present. An increase in the PIP2 level, as may be the result of external signaling, is immediately recognized by vinculin at these sites in the wild type cells. Consequently, vinculin is dissociating from the actin cytoskeleton which results in enhanced adhesion site turnover. In contrast, "vinculin-LD", localized correctly to intact adhesions, is unable to respond to the release signals and focal adhesion turnover is impaired. This results in a defective interaction between integrins and the actin cytoskeleton, and affects cell spreading. By the same mechanism, the afflicted cells are unable to become polarized and to develop lamellipodia, which leads to their unability to migrate. These events are schematically depicted in Figure 4.1.

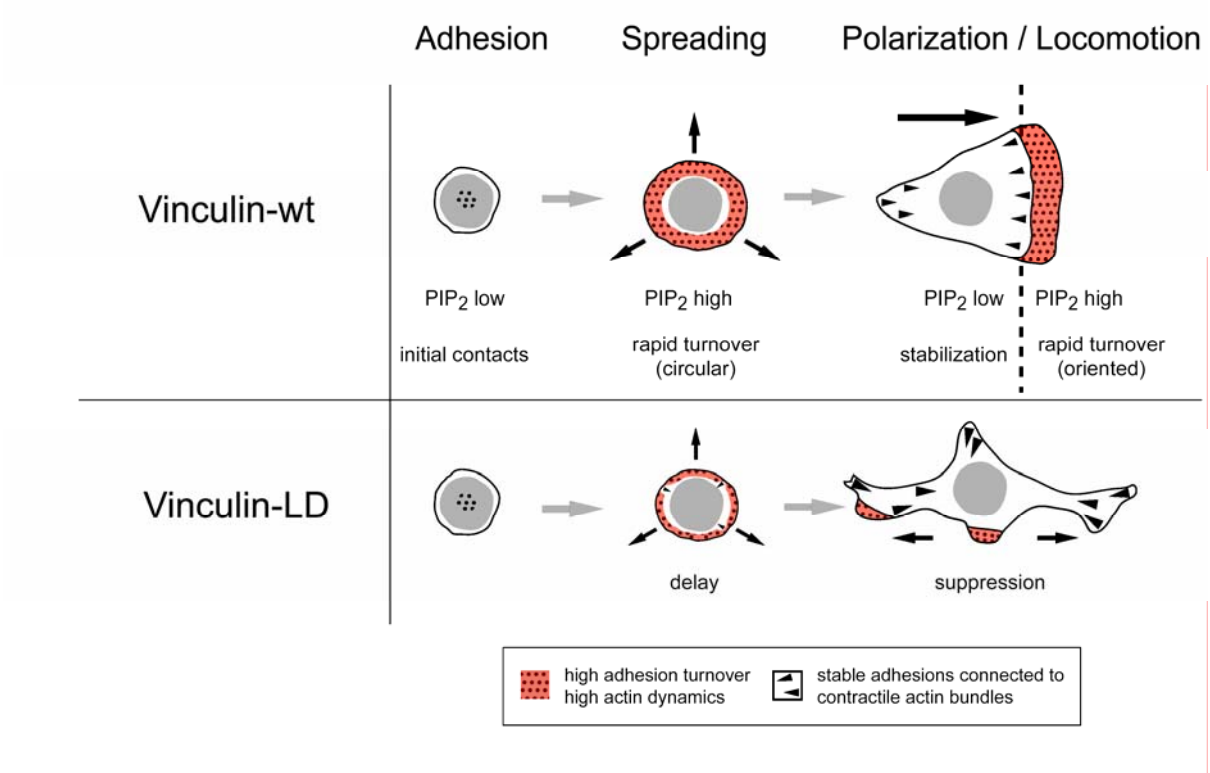

Figure 4.1: Model of vinculin involvement in adhesion site turnover
In motile cells, areas with both high adhesion turnover and high actin dynamics depend on elevated PIP2-levels, which leads to a weakening of the vinculin-actin interaction and subsequent turnover of adhesion sites. In case of vinculin-LD expressing cells adhesion sites are stabilized and efficient progression of lamellipodia is impaired. This leads to a delay in cell spreading and an almost complete inhibition of cell motility.

4.7. Vinculin acts as a sensor in lipid mediated regulation of the adhesion sites

The points discussed above strongly suggest a lipid-dependent regulation of vinculin in the adhesion sites. Increase in cellular PIP2 levels could trigger the release of vinculin from adhesions and this was tested by over expression of murine PIP5-kinase α (Tolias *et al.* 2000). Expression of PIP5-kinase lead to membrane localization of this kinase and to increased PIP2 synthesis (Doughman *et al.* 2003). However, vinculin-LD expressing cells were more resistant to the release signals mediated through increased PIP2 levels when compared to the vinculin wt (Chapter 3.6.8). Vinculin wt very efficiently sensed the elevated PIP2 levels which resulted in adhesion dissociation and cell detachment. In contrast, "vinculin-LD" was unable to sense the change in PIP2 levels due to the

deficiency in lipid binding capacity. Thus, vinculin acts as a sensor that converts the local modulation of PIP2 levels into adhesion site dynamics.

4.8. Future prospects

"Vinculin-LD" could serve as a tool to further analyse the adhesion site dynamics. Molecular players that are involved in the assembly and disassembly of focal adhesions can be evaluated in terms of their interaction with vinculin and PIP2. This could pave the way to an improved understanding of cell adhesion and migration.

In the presence of "vinculin-LD", the analysis of the incorporation rates of various FA markers like talin, paxillin should give more information on the assembly of focal adhesions and on the changes that occur in the early and later stages of maturation, and during disassembly. The influence of PIP2 on the association of vinculin binding partners like protein kinase C and the Arp2/3 complex could also be analysed with "vinculin-LD"expressing cells. For all such studies, the fact that vinculin-LD acts as a dominant negative is advantageous, as the effects of this mutant, as reported here, is seen on top of the endogenous vinculin level.

On the other hand, "vinculin-LD" expression in vinculin null cells and further analyses of the molecular components of the focal adhesions in such cells could aid more insight into the architecture and regulation of such altered adhesion sites.

5. References

Abercrombie, M., Heaysman, J. E. and Pegrum, S. M. (1971). The locomotion of fibroblasts in culture. IV. Electron microscopy of the leading lamella. *Exp Cell Res* **67**, 359-67.

Arneson, L. S., Kunz, J., Anderson, R. A. and Traub, L. M. (1999). Coupled inositide phosphorylation and phospholipase D activation initiates clathrin-coat assembly on lysosomes. *J Biol Chem* **274**, 17794-805.

Auger, K. R., Serunian, L. A., Soltoff, S. P., Libby, P. and Cantley, L. C. (1989). PDGF-dependent tyrosine phosphorylation stimulates production of novel polyphosphoinositides in intact cells. *Cell* **57**, 167-75.

Bakolitsa, C., Cohen, D. M., Bankston, L. A., Bobkov, A. A., Cadwell, G. W., Jennings, L., Critchley, D. R., Craig, S. W. and Liddington, R. C. (2004). Structural basis for vinculin activation at sites of cell adhesion. *Nature* **430**, 583-6.

Bakolitsa, C., de Pereda, J. M., Bagshaw, C. R., Critchley, D. R. and Liddington, R. C. (1999). Crystal structure of the vinculin tail suggests a pathway for activation. *Cell* **99**, 603-13.

Balla, T., Bondeva, T. and Varnai, P. (2000). How accurately can we image inositol lipids in living cells? *Trends Pharmacol Sci* **21**, 238-41.

Ballestrem, C., Wehrle-Haller, B. and Imhof, B. (1998). Actin dynamics in living mammalian cells. *J Cell Sci* **111**, 1649-1658.

Ballestrem, C. G., Uniyal, S., McCormick, J. I., Chau, T., Singh, B. and Chan, B. M. (1996). VLA-beta 1 integrin subunit-specific monoclonal antibodies MB1.1 and MB1.2: binding to epitopes not dependent on thymocyte development or regulated by phorbol ester and divalent cations. *Hybridoma* **15**, 125-32.

Barret, C., Roy, C., Montcourrier, P., Mangeat, P. and Niggli, V. (2000). Mutagenesis of the phosphatidylinositol 4,5-bisphosphate (PIP(2)) binding site in the NH(2)-terminal domain of ezrin correlates with its altered cellular distribution. *J Cell Biol* **151**, 1067-80.

Barstead, R. J. and Waterston, R. H. (1991). Vinculin is essential for muscle function in the nematode. *J Cell Biol* **114**, 715-24.

Bass, M. D., Smith, B. J., Prigent, S. A. and Critchley, D. R. (1999). Talin contains three similar vinculin-binding sites predicted to form an amphipathic helix. *Biochem J* **341 (Pt 2)**, 257-63.

Berridge, M. J. and Irvine, R. F. (1984). Inositol trisphosphate, a novel second messenger in cellular signal transduction. *Nature* **312**, 315-21.

Bielas, S. L. and Gleeson, J. G. (2004). Cytoskeletal-associated proteins in the migration of cortical neurons. *J Neurobiol* **58**, 149-59.

Brindle, N. P., Holt, M. R., Davies, J. E., Price, C. J. and Critchley, D. R. (1996). The focal-adhesion vasodilator-stimulated phosphoprotein (VASP) binds to the proline-rich domain in vinculin. *Biochem J* **318 (Pt 3)**, 753-7.

Burridge, K. and Mangeat, P. (1984). An interaction between vinculin and talin. *Nature* **308**, 744-6.

Burridge, K., Turner, C. E. and Romer, L. H. (1992). Tyrosine phosphorylation of paxillin and pp125FAK accompanies cell adhesion to extracellular matrix: a role in cytoskeletal assembly. *J Cell Biol* **119**, 893-903.

Campbell, K. P. (1995). Adhalin gene mutations and autosomal recessive limb-girdle muscular dystrophy. *Ann Neurol* **38**, 353-4.

Carragher, N. O. and Frame, M. C. (2004). Focal adhesion and actin dynamics: a place where kinases and proteases meet to promote invasion. *Trends Cell Biol* **14**, 241-9.

Carragher, N. O., Levkau, B., Ross, R. and Raines, E. W. (1999). Degraded collagen fragments promote rapid disassembly of smooth muscle focal adhesions that correlates with cleavage of pp125(FAK), paxillin, and talin. *J Cell Biol* **147**, 619-30.

Chen, H., Ishii, A., Wong, W. K., Chen, L. B. and Lo, S. H. (2000). Molecular characterization of human tensin. *Biochem J* **351 Pt 2**, 403-11.

Cohen, D. M. and Craig, S. W. (2003). A cell-free system to investigate the role of inositol phospholipids in vinculin recruitment to focal adhesions. *Mol. Biol. Cell* **14**, 63a.

Coutu, M. D. and Craig, S. W. (1988). cDNA-derived sequence of chicken embryo vinculin. *Proc Natl Acad Sci U S A* **85**, 8535-9.

Critchley, D. R. (2000). Focal adhesions - the cytoskeletal connection. *Curr Opin Cell Biol* **12**, 133-9.

Crowley, E. and Horwitz, A. F. (1995). Tyrosine phosphorylation and cytoskeletal tension regulate the release of fibroblast adhesions. *J Cell Biol* **131**, 525-37.

Cunningham, C. C., Gorlin, J. B., Kwiatkowski, D. J., Hartwig, J. H., Janmey, P. A., Byers, H. R. and Stossel, T. P. (1992). Actin-binding protein requirement for cortical stability and efficient locomotion. *Science* **255**, 325-7.

DeMali, K. A., Barlow, C. A. and Burridge, K. (2002). Recruitment of the Arp2/3 complex to vinculin: coupling membrane protrusion to matrix adhesion. *J Cell Biol* **159**, 881-91.

DiPaolo, G., Pellegrini, L., Letinic, K., Cestra, G., Zoncu, R., Voronov, S., Chang, S., Guo, J., Wenk, M. R. and De Camilli, P. (2002). Recruitment and regulation of phosphatidylinositol phosphate kinase type 1gamma by the FERM domain of talin. *Nature* **420**, 85-9.

Doughman, R. L., Firestone, A. J. and Anderson, R. A. (2003). Phosphatidylinositol phosphate kinases put PI4,5P(2) in its place. *J Membr Biol* **194**, 77-89.

Friedl, P., Hegerfeldt, Y. and Tusch, M. (2004). Collective cell migration in morphogenesis and cancer. *Int J Dev Biol* **48**, 441-9.

Fukami, K., Endo, T., Imamura, M. and Takenawa, T. (1994). alpha-Actinin and vinculin are PIP2-binding proteins involved in signaling by tyrosine kinase. *J. Biol. Chem.* **269**, 1518-1522.

Furuhashi, K., Inagaki, M., Hatano, S., Fukami, K. and Takenawa, T. (1992). Inositol phospholipid-induced suppression of F-actin-gelating activity of smooth muscle filamin. *Biochem Biophys Res Commun* **184**, 1261-5.

Galbraith, C. G., Yamada, K. M. and Sheetz, M. P. (2002). The relationship between force and focal complex development. *J Cell Biol* **159**, 695-705.

Garrod, D. R. (1993). Desmosomes and hemidesmosomes. *Curr Opin Cell Biol* **5**, 30-40.

Geiger, B. (1979). A 130K protein from chicken gizzard: its localization at the termini of microfilament bundles in cultured chicken cells. *Cell* **18**, 193-205.

Geiger, B. and Ginsberg, D. (1991). The cytoplasmic domain of adherens-type junctions. *Cell Motil Cytoskeleton* **20**, 1-6.

Geiger, B., Tokuyasu, K. T., Dutton, A. H. and Singer, S. J. (1980). Vinculin, an intracellular protein localized at specialized sites where microfilament bundles terminate at cell membranes. *Proc Natl Acad Sci U S A* **77**, 4127-31.

Giannone, G., Jiang, G., Sutton, D. H., Critchley, D. R. and Sheetz, M. P. (2003). Talin1 is critical for force-dependent reinforcement of initial integrin-cytoskeleton bonds but not tyrosine kinase activation. *J. Cell Biol.* **163**, 409-419.

Gilmore, A. P. and Burridge, K. (1996). Regulation of vinculin binding to talin and actin by phosphatidyl-inositol-4-5-bisphosphate. *Nature* **381**, 531-5.

Gumbiner, B. M. (1996). Cell adhesion: the molecular basis of tissue architecture and morphogenesis. *Cell* **84**, 345-57.

Heiska, L., Alfthan, K., Gronholm, M., Vilja, P., Vaheri, A. and Carpen, O. (1998). Association of ezrin with intercellular adhesion molecule-1 and -2 (ICAM-1 and ICAM-2). Regulation by phosphatidylinositol 4, 5-bisphosphate. *J Biol Chem* **273**, 21893-900.

Heiss, S. G. and Cooper, J. A. (1991). Regulation of CapZ, an actin capping protein of chicken muscle, by anionic phospholipids. *Biochemistry* **30**, 8753-8.

Hirao, M., Sato, N., Kondo, T., Yonemura, S., Monden, M., Sasaki, T., Takai, Y. and Tsukita, S. (1996). Regulation mechanism of ERM (ezrin/radixin/moesin) protein/plasma membrane association: possible involvement of phosphatidylinositol turnover and Rho-dependent signaling pathway. *J Cell Biol* **135**, 37-51.

Hüttelmaier, S., Bubeck, P., Rudiger, M. and Jockusch, B. M. (1997). Characterization of two F-actin-binding and oligomerization sites in the cell-contact protein vinculin. *Eur J Biochem* **247**, 1136-42.

Hüttelmaier, S., Mayboroda, O., Harbeck, B., Jarchau, T., Jockusch, B. M. and Rudiger, M. (1998). The interaction of the cell-contact proteins VASP and vinculin is regulated by phosphatidylinositol-4,5-bisphosphate. *Curr Biol* **8**, 479-88.

Huttenlocher, A., Sandborg, R. R. and Horwitz, A. F. (1995). Adhesion in cell migration. *Curr Opin Cell Biol* **7**, 697-706.
Huttenlocher, P. R., Taravath, S. and Mojtahedi, S. (1994). Periventricular heterotopia and epilepsy. *Neurology* **44**, 51-5.

Ishihara, H., Shibasaki, Y., Kizuki, N., Katagiri, H., Yazaki, Y., Asano, T. and Oka, Y. (1996). Cloning of cDNAs encoding two isoforms of 68-kDa type I phosphatidylinositol-4-phosphate 5-kinase. *J Biol Chem* **271**, 23611-4.

Ishihara, H., Shibasaki, Y., Kizuki, N., Wada, T., Yazaki, Y., Asano, T. and Oka, Y. (1998). Type I phosphatidylinositol-4-phosphate 5-kinases. Cloning of the third isoform and deletion/substitution analysis of members of this novel lipid kinase family. *J Biol Chem* **273**, 8741-8.

Itoh, T., Ishihara, H., Shibasaki, Y., Oka, Y. and Takenawa, T. (2000). Autophosphorylation of type I phosphatidylinositol phosphate kinase regulates its lipid kinase activity. *J Biol Chem* **275**, 19389-94.

Izard, T., Evans, G., Borgon, R. A., Rush, C. L., Bricogne, G. and Bois, P. R. (2004). Vinculin activation by talin through helical bundle conversion. *Nature* **427**, 171-5.

Izzard, C. S. and Lochner, L. R. (1980). Formation of cell-to-substrate contacts during fibroblast motility: an interference-reflexion study. *J Cell Sci* **42**, 81-116.

Janmey, P. A. and Stossel, T. P. (1987). Modulation of gelsolin function by phosphatidylinositol 4,5-bisphosphate. *Nature* **325**, 362-4.

Jay, P. Y., Pham, P. A., Wong, S. A. and Elson, E. L. (1995). A mechanical function of myosin II in cell motility. *J Cell Sci* **108 (Pt 1)**, 387-93.

Jockusch, B. M. and Isenberg, G. (1981). Interaction of alpha-actinin and vinculin with actin: opposite effects on filament network formation. *Proc Natl Acad Sci U S A* **78**, 3005-9.

Jockusch, B. M. and Rudiger, M. (1996). Crosstalk between cell adhesion molecules: vinculin as a paradigm for regulation by conformation. *Trends Cell Biol* **6**, 311-315.

Johnson, R. P. and Craig, S. W. (1994). An intramolecular association between the head and tail domains of vinculin modulates talin binding. *J Biol Chem* **269**, 12611-9.

Johnson, R. P. and Craig, S. W. (1995). F-actin binding site masked by the intramolecular association of vinculin head and tail domains. *Nature* **373**, 261-4.

Johnson, R. P., Niggli, V., Durrer, P. and Craig, S. W. (1998). A conserved motif in the tail domain of vinculin mediates association with and insertion into acidic phospholipid bilayers. *Biochemistry* **37**, 10211-22.

Johnson, Z., Power, C. A., Weiss, C., Rintelen, F., Ji, H., Ruckle, T., Camps, M., Wells, T. N., Schwarz, M. K., Proudfoot, A. E. et al. (2004). Chemokine inhibition--why, when, where, which and how? *Biochem Soc Trans* **32**, 366-77.

Kioka, N., Sakata, S., Kawauchi, T., Amachi, T., Akiyama, S. K., Okazaki, K., Yaen, C., Yamada, K. M. and Aota, S. (1999). Vinexin: a novel vinculin-binding protein with multiple SH3 domains enhances actin cytoskeletal organization. *J Cell Biol* **144**, 59-69.
Kroemker, M., Rudiger, A. H., Jockusch, B. M. and Rudiger, M. (1994). Intramolecular interactions in vinculin control alpha-actinin binding to the vinculin head. *FEBS Lett* **355**, 259-62.

Kumar, N. M. and Gilula, N. B. (1996). The gap junction communication channel. *Cell* **84**, 381-8.

Laemmli, U. K. (1970). Cleavage of structural proteins during the assembly of the head of bacteriophage T4. *Nature* **227**, 680-5.

Lauffenburger, D. A. and Horwitz, A. F. (1996). Cell migration: a physically integrated molecular process. *Cell* **84**, 359-69.

Ling, K., Doughman, R. L., Firestone, A. J., Bunce, M. W. and Anderson, R. A. (2002). Type I gamma phosphatidylinositol phosphate kinase targets and regulates focal adhesions. *Nature* **420**, 89-93.

Locascio, A. and Nieto, M. A. (2001). Cell movements during vertebrate development: integrated tissue behaviour versus individual cell migration. *Curr Opin Genet Dev* **11**, 464-9.

Machesky, L. M., Atkinson, S. J., Ampe, C., Vandekerckhove, J. and Pollard, T. D. (1994). Purification of a cortical complex containing two unconventional actins from Acanthamoeba by affinity chromatography on profilin-agarose. *J Cell Biol* **127**, 107-15.

Machesky, L. M. and Insall, R. H. (1998). Scar1 and the related Wiskott-Aldrich syndrome protein, WASP, regulate the actin cytoskeleton through the Arp2/3 complex. *Curr Biol* **8**, 1347-56.

Mandai, K., Nakanishi, H., Satoh, A., Takahashi, K., Satoh, K., Nishioka, H., Mizoguchi, A. and Takai, Y. (1999). Ponsin/SH3P12: an l-afadin- and vinculin-binding protein localized at cell-cell and cell-matrix adherens junctions. *J Cell Biol* **144**, 1001-17.

Martel, V., Racaud-Sultan, C., Dupe, S., Marie, C., Paulhe, F., Galmiche, A., Block, M. R. and Albiges-Rizo, C. (2001). Conformation, localization and integrin-binding of talin depend on its interaction with phosphoinositides. *J Biol Chem* **276**, 21217-27.

Martin, P. and Parkhurst, S. M. (2004). Parallels between tissue repair and embryo morphogenesis. *Development* **131**, 3021-34.

McLaughlin, S., Wang, J., Gambhir, A. and Murray, D. (2002). PIP(2) and proteins: interactions, organization, and information flow. *Annu Rev Biophys Biomol Struct* **31**, 151-75.

Meerschaert, K., De Corte, V., De Ville, Y., Vandekerckhove, J. and Gettemans, J. (1998). Gelsolin and functionally similar actin-binding proteins are regulated by lysophosphatidic acid. *Embo J* **17**, 5923-32.

Menkel, A. R., Kroemker, M., Bubeck, P., Ronsiek, M., Nikolai, G. and Jockusch, B. M. (1994). Characterization of an F-actin-binding domain in the cytoskeletal protein vinculin. *J Cell Biol* **126**, 1231-40.

Miller, G. J., Dunn, S. D. and Ball, E. H. (2001). Interaction of the n- and c-terminal domains of vinculin. characterization and mapping studies. *J Biol Chem* **276**, 11729-34.

Miyazawa, A., Umeda, M., Horikoshi, T., Yanagisawa, K., Yoshioka, T. and Inoue, K. (1988). Production and characterization of monoclonal antibodies that bind to phosphatidylinositol 4,5-bisphosphate. *Mol Immunol* **25**, 1025-31.

Mogilner, A. and Oster, G. (1996). Cell motility driven by actin polymerization. *Biophys J* **71**, 3030-45.

Molony, L. and Burridge, K. (1985). Molecular shape and self-association of vinculin and metavinculin. *J Cell Biochem* **29**, 31-6.

Nakamura, F., Huang, L., Pestonjamasp, K., Luna, E. J. and Furthmayr, H. (1999). Regulation of F-actin binding to platelet moesin in vitro by both phosphorylation of threonine 558 and polyphosphatidylinositides. *Mol Biol Cell* **10**, 2669-85.

Nakashima, S. (2002). Protein kinase C alpha (PKC alpha): regulation and biological function. *J Biochem (Tokyo)* **132**, 669-75.

Niggemann, B., Maaser, K., Lu, H., Kroczek, R., Zanker, K. S. and Friedl, P. (1997). Locomotory phenotypes of human tumor cell lines and T lymphocytes in a three-dimensional collagen lattice. *Cancer Lett* **118**, 173-80.

Niggli, V. (2001). Structural properties of lipid-binding sites in cytoskeletal proteins. *Trends Biochem Sci* **26**, 604-11.

Niggli, V. and Gimona, M. (1993). Evidence for a ternary interaction between alpha-actinin, (meta)vinculin and acidic-phospholipid bilayers. *Eur J Biochem* **213**, 1009-15.

Nobes, C. D. and Hall, A. (1995). Rho, rac, and cdc42 GTPases regulate the assembly of multimolecular focal complexes associated with actin stress fibers, lamellipodia, and filopodia. *Cell* **81**, 53-62.

Ojala, P. J., Paavilainen, V. and Lappalainen, P. (2001). Identification of yeast cofilin residues specific for actin monomer and PIP2 binding. *Biochemistry* **40**, 15562-9.

Papagrigoriou, E., Gingras, A. R., Barsukov, I. L., Bate, N., Fillingham, I. J., Patel, B., Frank, R., Ziegler, W. H., Roberts, G. C., Critchley, D. R. et al. (2004). Activation of a vinculin-binding site in the talin rod involves rearrangement of a five-helix bundle. *Embo J* **23**, 2942-2951.

Pokutta, S. and Weis, W. I. (2002). The cytoplasmic face of cell contact sites. *Curr Opin Struct Biol* **12**, 255-62.

Pollard, T. D. and Borisy, G. G. (2003). Cellular motility driven by assembly and disassembly of actin filaments. *Cell* **112**, 453-65.

Price, G. J., Jones, P., Davison, M. D., Patel, B., Bendori, R., Geiger, B. and Critchley, D. R. (1989). Primary sequence and domain structure of chicken vinculin. *Biochem J* **259**, 453-61.

Reinhard, M., Rudiger, M., Jockusch, B. M. and Walter, U. (1996). VASP interaction with vinculin: a recurring theme of interactions with proline-rich motifs. *FEBS Lett* **399**, 103-7.

Ridley, A. (2000). Molecular switches in metastasis. *Nature* **406**, 466-7.

Ridley, A. J. and Hall, A. (1992). The small GTP-binding protein rho regulates the assembly of focal adhesions and actin stress fibers in response to growth factors. *Cell* **70**, 389-99.

Ridley, A. J., Schwartz, M. A., Burridge, K., Firtel, R. A., Ginsberg, M. H., Borisy, G.,
Parsons, J. T. and Horwitz, A. R. (2003). Cell Migration: Integrating Signals from Front to Back. *Science* **302**, 1704-1709.

Riento, K. and Ridley, A. J. (2003). Rocks: multifunctional kinases in cell behaviour. *Nat Rev Mol Cell Biol* **4**, 446-56.

Rodriguez Fernandez, J. L., Geiger, B., Salomon, D. and Ben-Ze'ev, A. (1992). Overexpression of vinculin suppresses cell motility in BALB/c 3T3 cells. *Cell Motil Cytoskeleton* **22**, 127-34.

Rodriguez Fernandez, J. L., Geiger, B., Salomon, D. and Ben-Ze'ev, A. (1993). Suppression of vinculin expression by antisense transfection confers changes in cell morphology, motility, and anchorage-dependent growth of 3T3 cells. *J Cell Biol* **122**, 1285-94.

Rohatgi, R., Ho, H. Y. and Kirschner, M. W. (2000). Mechanism of N-WASP activation by CDC42 and phosphatidylinositol 4, 5-bisphosphate. *J Cell Biol* **150**, 1299-310.

Rottner, K., Hall, A. and Small, J. V. (1999). Interplay between Rac and Rho in the control of substrate contact dynamics. *Curr Biol* **9**, 640-8.

Rozelle, A. L., Machesky, L. M., Yamamoto, M., Driessens, M. H., Insall, R. H., Roth, M. G., Luby-Phelps, K., Marriott, G., Hall, A. and Yin, H. L. (2000). Phosphatidylinositol 4,5-bisphosphate induces actin-based movement of raft-enriched vesicles through WASP-Arp2/3. *Curr Biol* **10**, 311-20.

Rudiger, M., Jockusch, B. M. and Rothkegel, M. (1997). Epitope tag-antibody combination useful for the detection of protein expression in prokaryotic and eukaryotic cells. *Biotechniques* **23**, 96-7.

Sanchez-Madrid, F. and del Pozo, M. A. (1999). Leukocyte polarization in cell migration and immune interactions. *Embo J* **18**, 501-11.

Saunders, R., Jennings, L., Sutton, D. H., Barsukov, I., Holt, M. R., Dunn, G. A., Adamson, E. D. and Critchley, D. R. (2003). Vinculin mutations that decrease PIP2 binding lead to protein mislocalisation and failure to rescue cell spreading defects in vinculin null fibroblasts. *Mol. Biol. Cell* **14**, 63a.

Schafer, D. A., Jennings, P. B. and Cooper, J. A. (1996). Dynamics of capping protein and actin assembly in vitro: uncapping barbed ends by polyphosphoinositides. *J Cell Biol* **135**, 169-79.

Schwarz, M. A., Owaribe, K., Kartenbeck, J. and Franke, W. W. (1990). Desmosomes and hemidesmosomes: constitutive molecular components. *Annu Rev Cell Biol* **6**, 461-91.

Shibasaki, Y., Ishihara, H., Kizuki, N., Asano, T., Oka, Y. and Yazaki, Y. (1997). Massive actin polymerization induced by phosphatidylinositol-4-phosphate 5-kinase in vivo. *J Biol Chem* **272**, 7578-81.

Shyng, S. L., Barbieri, A., Gumusboga, A., Cukras, C., Pike, L., Davis, J. N., Stahl, P. D. and Nichols, C. G. (2000). Modulation of nucleotide sensitivity of ATP-sensitive potassium channels by phosphatidylinositol-4-phosphate 5-kinase. *Proc Natl Acad Sci U S A* **97**, 937-41.

Steimle, P. A., Hoffert, J. D., Adey, N. B. and Craig, S. W. (1999). Polyphosphoinositides inhibit the interaction of vinculin with actin filaments. *J Biol Chem* **274**, 18414-20.

Tolias, K. F., Hartwig, J. H., Ishihara, H., Shibasaki, Y., Cantley, L. C. and Carpenter, C. L. (2000). Type Ialpha phosphatidylinositol-4-phosphate 5-kinase mediates Rac-dependent actin assembly. *Curr Biol* **10**, 153-6.

Tsukita, S., Furuse, M. and Itoh, M. (1999). Structural and signalling molecules come together at tight junctions. *Curr Opin Cell Biol* **11**, 628-33.

Turner, C. E., Glenney, J. R., Jr. and Burridge, K. (1990). Paxillin: a new vinculin-binding protein present in focal adhesions. *J Cell Biol* **111**, 1059-68.

Vicente-Manzanares, M. and Sanchez-Madrid, F. (2004). Role of the cytoskeleton during leukocyte responses. *Nat Rev Immunol* **4**, 110-22.

Villarejo, M. R. and Zabin, I. (1974). Beta-galactosidase from termination and deletion mutant strains. *J Bacteriol* **120**, 466-74.

Von Wichert, G., Haimovich, B., Feng, G. S. and Sheetz, M. P. (2003). Force-dependent integrin-cytoskeleton linkage formation requires downregulation of focal complex dynamics by Shp2. *Embo J* **22**, 5023-5035.

Weaver, A. M., Karginov, A. V., Kinley, A. W., Weed, S. A., Li, Y., Parsons, J. T. and Cooper, J. A. (2001). Cortactin promotes and stabilizes Arp2/3-induced actin filament network formation. *Curr Biol* **11**, 370-4.

Webb, D. J., Donais, K., Whitmore, L. A., Thomas, S. M., Turner, C. E., Parsons, J. T. and Horwitz, A. F. (2004). FAK-Src signalling through paxillin, ERK and MLCK regulates adhesion disassembly. *Nat Cell Biol* **6**, 154-61.

Weekes, J., Barry, S. T. and Critchley, D. R. (1996). Acidic phospholipids inhibit the intramolecular association between the N- and C-terminal regions of vinculin, exposing actin-binding and protein kinase C phosphorylation sites. *Biochem J* **314**, 827-32.

Weernink, P. A., Guo, Y., Zhang, C., Schmidt, M., Von Eichel-Streiber, C. and Jakobs, K. H. (2000). Control of cellular phosphatidylinositol 4,5-bisphosphate levels by adhesion signals and rho GTPases in NIH 3T3 fibroblasts involvement of both phosphatidylinositol-4-phosphate 5-kinase and phospholipase C. *Eur J Biochem* **267**, 5237-46.

Weernink, P. A., Meletiadis, K., Hommeltenberg, S., Hinz, M., Ishihara, H., Schmidt, M. and Jakobs, K. H. (2004). Activation of type I phosphatidylinositol 4-phosphate 5-kinase isoforms by the Rho GTPases, RhoA, Rac1, and Cdc42. *J Biol Chem* **279**, 7840-9.

Weller, P. A., Ogryzko, E. P., Corben, E. B., Zhidkova, N. I., Patel, B., Price, G. J., Spurr, N. K., Koteliansky, V. E. and Critchley, D. R. (1990). Complete sequence of human vinculin and assignment of the gene to chromosome 10. *Proc Natl Acad Sci U S A* **87**, 5667-71.

Wessel, D. and Flugge, U. I. (1984). A method for the quantitative recovery of protein in dilute solution in the presence of detergents and lipids. *Anal Biochem* **138**, 141-3.

Winkler, J., Lunsdorf, H. and Jockusch, B. M. (1996). The ultrastructure of chicken gizzard vinculin as visualized by high-resolution electron microscopy. *J Struct Biol* **116**, 270-7.

Wood, C. K., Turner, C. E., Jackson, P. and Critchley, D. R. (1994). Characterisation of the paxillin-binding site and the C-terminal focal adhesion targeting sequence in vinculin. *J Cell Sci* **107**, 709-17.

Wozniak, M. A., Modzelewska, K., Kwong, L. and Keely, P. J. (2004). Focal adhesion regulation of cell behavior. *Biochim Biophys Acta* **1692**, 103-19.

Xu, W., Baribault, H. and Adamson, E. D. (1998a). Vinculin knockout results in heart and brain defects during embryonic development. *Development* **125**, 327-37.

Xu, W., Coll, J. L. and Adamson, E. D. (1998b). Rescue of the mutant phenotype by reexpression of full-length vinculin in null F9 cells; effects on cell locomotion by domain deleted vinculin. *J Cell Sci* **111 (Pt 11)**, 1535-44.

Yamada, K. M. and Geiger, B. (1997). Molecular interactions in cell adhesion complexes. *Curr Opin Cell Biol* **9**, 76-85.

Yin, H. L. and Janmey, P. A. (2003). Phosphoinositide regulation of the actin cytoskeleton. *Annu Rev Physiol* **65**, 761-89.

Young, P. and Gautel, M. (2000). The interaction of titin and alpha-actinin is controlled by a phospholipid-regulated intramolecular pseudoligand mechanism. *Embo J* **19**, 6331-40.

Zamir, E. and Geiger, B. (2001). Molecular complexity and dynamics of cell-matrix adhesions. *J Cell Sci* **114**, 3583-90.

Ziegler, W. H., Tigges, U., Zieseniss, A. and Jockusch, B. M. (2002). A lipid-regulated docking site on vinculin for protein kinase C. *J Biol Chem* **277**, 7396-404.

6. Appendix

6.1. List of figures

6.2. List of tables

Acknowledgements

I extend my sincere thanks to Prof. Dr. Brigitte M. Jockusch for granting me this great opportunity, to perform my doctoral thesis under her guidance. She has always been very encouraging and supportive to my work. Her concern and care for my personal life in Germany made my stay comfortable and memorable.

I am grateful to Dr. Wolfgang H. Ziegler, for his wonderful supervision, encouragement, support and motivation throughout the study. I enjoyed working with him these three years and I am sure this experience will help me in my future career.

I am thankful to Prof. Dr. Jürgen Wehland, GBF, Braunschweig, for his support throughout this work. My special thanks go to Dr. Theresia E. B. Stradal, for her supervision, guidance, above all, her kind and impressive behavior. I greatly acknowledge the help from Dr. Klemens Rottner with useful discussions and suggestions.

Many thanks to Dr. Frank Entschladen, University of Witten/Herdecke for his kind help and support to this work. I would like to include Ms. Beate Mainusch for her good technical support in this regard.

I am thankful to Dr. Mark R. Holt, KCL, London, for the collaboration, help and support.

I thank Prof. Dr. Günter Schwarz for his kind acceptance to grade the thesis and
Prof. Dr. R.R. Mendel for his acceptance to be involved in the thesis committee.

My sincere thanks go to Dr. Björg Pauling for being a good friend, organizing the IGC, and for helping me with my thesis. Many thanks to Mrs. Eva Saxinger for the techincal assistance and good conversations.

I thank PD. Dr. Susanne Illenberger and Dr. Martin Rothkegel for the useful discussions and support. I thank Kai Murk, Berenike Kleinhenz for the good chat and fun in the lab.

I am very thankful to my dear friend Jose´ Santamaria for being a good moral support and for influencing my personality in many good ways, especially by introducing me to the "western culture" and by guiding me throughout.

Many thanks to dear Maryam for being a caring friend. I thank the "sweet girl" Anika Steffen for her guidance, love and care.

My sincere thanks to all my good friends, Bhavani, Senthil, Rajesh, Harold Stiege, Gomathi for their love and care and for many special moments.

I am grateful to my parents, especially my mother for her constant encouragement, support, love and trust on me which helped me to get to this stage. Thanks to my dear brother for his love.

I am very happy to have Kamesh in my life; I thank him for his unconditional love, encouragement and support.